

NET ELECTRICAL LOAD FORECASTING IN THE PRESENCE
OF NEW GENERATION TECHNOLOGIES

By

ALIRAHM SAIDIAN

Bachelor of Science
Jundi Shapour University
Ahwaz, Iran
1971

Master of Science
University of Oklahoma
Norman, Oklahoma
1980

Submitted to the Faculty of the Graduate College
of the Oklahoma State University
in partial fulfillment of the requirements
for the Degree of
DOCTOR OF PHILOSOPHY
December, 1986

Thesis
1986D
S. 1325n
Cop 2



NET ELECTRICAL LOAD FORECASTING IN THE PRESENCE
OF NEW GENERATION TECHNOLOGIES

Thesis Approved

R. Ramakumar

Thesis Adviser

W. W. Grace

Wm. S. Hughes

W. E. Liguette

Norman N. Durham

Dean of the Graduate College

ACKNOWLEDGMENT

In the name of God the most merciful and most compassionate. I would like to express my appreciation to my adviser, this kind and energetic scholar, Dr. R Ramakumar, for his guidance and assistance throughout this study

The interest and comments offered by, Dr W. L. Hughes, the time spent by my other thesis committee members, Dr D D Lingelbach, and Dr D. W Grace, are sincerely appreciated

I wish to thank Dr T Ireland, Management Department, Dr V Marco, Statistics Department, Dr M R. Sayeh, and Mr M. H. Ramazani, Mr K Ashenayi, Mr M. Malakoti, and Mr. W. Jewell, Electrical Engineering Department, Oklahoma State University, and Mr L Karimi, Senior Engineer from N.I O C. for their valuable discussions

I wish to thank Mr Stan Hill from Public Service Company of Oklahoma (PSO) for providing the load and temperature data used in this thesis.

I would like to acknowledge the financial support received from the Shahid Chamran University, Ahawaz, Iran. Also, the support received from the School of Electrical Engineering, Oklahoma State University as graduate teaching assistant is appreciated My parents Mr and Mrs Saidian, my wife, Sara, and my children, Soheil, Sasan, Saideh, Said, and Maryam, my sisters and brothers and relatives deserve a medal for the tolerance and support provided over a long period in graduate school and in this country They are all appreciated

I am grateful to Ms. Barbara Caldwell for typing this thesis

Finally, I dedicate this thesis to those who are working for the truth.

TABLE OF CONTENTS

Chapter		Page
I	INTRODUCTION	1
	1.1 Photovoltaic (PV) and Electric Utilities . . .	1
	1.1.1 History	2
	1.1.2 Recent Developments	3
	1.1.3 Promises and Prospects	8
	1.2 Wind Electric Conversion Systems and Electric Utilities	9
	1.2.1 History	9
	1.2.2 Recent Developments	10
	1.2.3 Promises and Prospects	14
	1.3 Forecasting Concepts Applied to Power Systems	15
	1.3.1 Role of Forecasting	16
	1.3.2 Types of Forecasts	17
	1.4 Literature Survey	18
	1.4.1 Alternative Power Generation Technologies	18
	1.4.2 Load Forecasting	19
	1.4.3 Load Forecasting in the Presence of Alternative Power Generation Technologies	20
	1.5 Problem Statement	21
	1.6 Method of Analysis	22
	1.7 Organization of the Thesis	23
II	THE IMPACT OF ALTERNATIVE ELECTRIC POWER GENERATION TECHNOLOGIES ON A UTILITY SYSTEM	25
	2.1 Distinguishing Features of Alternative Power Generation Technologies	25
	2.2 Utility Concerns - Related Issues	32
	2.3 Barriers to Load Modeling and Load Forecasting	36
III	MODELING THE OUTPUT OF AN ALTERNATIVE ELECTRIC POWER GENERATION SYSTEM	39
	3.1 Introduction	39
	3.2 Time Series Model for the Output of Photovoltaic System	40
	3.3 Wind System Output	50
	3.4 Discussion	57

Chapter	Page
IV DEVELOPMENT OF MODELS AND LOAD FORECASTING IN THE PRESENCE OF NEW GENERATION	61
4.1 Introduction	61
4.2 Univariate Time Series Analyses	62
4.2.1 Net Demand Forecasting in the Presence of PV (Approach A)	65
4.2.1a Two-axis Tracking Flat-plate PV Systems	65
4.2.1b Two-axis Tracking Concentrator PV Systems	74
4.2.2 Net Demand Forecasting in the Presence of PV (Approach B)	78
4.2.2a Two-axis Tracking Flat-plate PV Systems	78
4.2.2b Two-axis Tracking Concentrator PV Systems	86
4.2.3 Models for Net Demand with PV Present (Approach C)	86
4.2.3a Two-axis Tracking Flat-plate PV Systems	90
4.2.3b Two-axis Tracking Concentrator PV Systems	95
4.2.4 Net Demand Forecasting in the Presence of PV and Wind Electric Systems (Approach D)	99
4.2.4a Two-axis Tracking Flat-plate PV Systems	99
4.2.4b Two-axis Tracking Concentrator PV Systems	108
4.2.5 Models for Net Demand with PV and WECS Present (Approach D continued)	113
4.2.5a Two-axis Tracking Flat-plate PV Systems	113
4.2.5b Two-axis Tracking Concentrator PV Systems	118
4.3 Multiple Time Series Analysis	118
4.4 Discussion of Results	132
V SUMMARY AND CONCLUSIONS	139
5.1 Summary and Concluding Remarks	139
5.2 Scope for Suggested Further Work	146
REFERENCES	150
APPENDIX	156

LIST OF TABLES

Table	Page
I Categorization of New Technologies	38
II Typical Photovoltaic Module Output at Different Times During a Day	52
III. Typical WECS Output at Different Times During a Day	60
IV Summary of the Estimated Parameter Values for Model of Equation 4 2	68
V Summary of the Estimated Parameter Values for Model of Equation 4 3	70
VI Summary of the Estimated Parameter Values for Model of Equation 4 4	72
VII Summary of the Estimated Parameter Values for Model of Equation 4.5	73
VIII Summary of the Estimated Parameter Values for Model of Equation 4 6	77
IX Summary of the Estimated Parameter Values for Model of Equation 4 7	83
X Summary of the Estimated Parameter Values for Model of Equation 4 8	87
XI Summary of the Estimated Parameter Values for Model of Equation 4 9	92
XII Summary of the Estimated Parameter Values for Model of Equation 4 10	98
XIII Summary of the Estimated Parameter Values for Model of Equation 4 11	105
XIV Summary of the Estimated Parameter Values for Model of Equation 4 12	115
XV Summary of the Estimated Parameter Values for Model of Equation 4 13	119

Table		Page
XVI.	Summary of the Estimated Parameter Values for Model of Equation 4.19	127
XVII	Summary of the Estimated Parameter Values for Model of Equation 4.23	129

LIST OF FIGURES

Figure	Page
1. Typical Current-Voltage Characteristic for a Solar/Cell/module	41
2. Equivalent Circuit for a PV Cell/Module	42
3. Simplified Equivalent Circuit for a PV Cell/Module	43
4. Block Diagram of a Utility-Interactive Photovoltaic System	45
5. Algorithm "PVTALGO" Flowchart	51
6. Typical PV Module Output (W) at Different Times During a Day (6 am - 7 pm)	53
7. Typical insolation data (W/m^2) at Different Times During a Day (6 am - 7 pm)	54
8. Typical Electrical Output Characteristics of a Large WECS	56
9. Typical WECS (MOD-2) Output (MW) and the Corresponding Wind Data (m/sec) at Different Times During a Day (6 am - 7 pm)	59
10. Forecast Flowchart (Approach A)	66
11. Forecasts of Hourly Net Demand (MW) in the Presence of Two-Axis Tracking Flat-Plate PV Systems with 5% Penetration for June 30, 1975 (Approach A)	75
12. Forecasts of Hourly Net Demand (MW) in the Presence of Two-Axis Tracking Flat-Plate PV Systems with 5% Penetration for July 1, 1975 (Approach A)	76
13. Forecasts of Hourly Net Demand (MW) in the Presence of Two-Axis Tracking Concentrator PV Systems with 5% Penetration for June 30, 1975 (Approach A)	79
14. Forecasts of Hourly Net Demand (MW) in the Presence of Two-Axis Tracking Concentrator PV Systems with 5% Penetration for July 1, 1975 (Approach A)	80

Figure	Page
15 Forecast Flowchart (Approach B)	81
16 Forecasts of Hourly Net Demand (MW) in the Presence of Two-Axis Tracking Flat-Plate PV Systems with 5% Penetration for June 30, 1975 (Approach B)	84
17 Forecasts of Hourly Net Demand (MW) in the Presence of Two-Axis Tracking Flat-Plate PV Systems with 5% Penetration for July 1, 1975 (Approach B)	85
18 Forecasts of Hourly Net Demand (MW) in the Presence of Two-Axis Tracking Concentrator PV Systems with 5% Penetration for June 30, 1975 (Approach B)	88
19 Forecasts of Hourly Net Demand (MW) in the Presence of Two-Axis Tracking Concentrator with 5% Penetration for July 1, 1975 (Approach B)	89
20 Forecast Flowchart (Approach C)	91
21. Forecasts of Hourly Net Demand (MW) in the Presence of Two-Axis Tracking Flat-Plate PV Systems with 5% Penetration for June 30, 1975 (Approach C)	93
22 Forecasts of Hourly Net Demand (MW) in the Presence of Two-Axis Tracking Flat-Plate PV Systems with 5% Penetration for July 1, 1975 (Approach C)	94
23. Forecasts of Hourly Net Demand (MW) in the Presence of Two-Axis Tracking Concentrator PV Systems with 5% Penetration for June 30, 1975 (Approach C)	97
24 Forecasts of Hourly Net Demand (MW) in the Presence of Two-Axis Tracking Concentrator PV Systems with 5% Penetration for July 1, 1975 (Approach C)	98
25 Forecasts Flowchart (Approach D corresponds to Approach A)	100
26 Forecast Flowchart (Approach D corresponds to Approach B)	101
27 Forecasts of Hourly Net Demand (MW) in the Presence of Two-Axis Tracking Flat-Plate PV and WECS with 5% Penetration each for June 30, 1975 (Approach D corresponds to Approach A)	102
28 Forecasts of Hourly Net Demand (MW) in the Presence of Two-Axis Tracking Flat-Plate PV and WECS with 5% Penetration each for July 1, 1975 (Approach D corresponds to Approach A)	103

Figure	Page
29. Forecasts of Hourly Net Demand (MW) in the Presence of Two-Axis Tracking Flat-Plate PV and WECS with 5% Penetration each for June 30, 1975 (Approach D corresponds to Approach B)	106
30. Forecasts of Hourly Net Demand (MW) in the Presence of Two-Axis Tracking Flat-Plate PV and WECS with 5% Penetration each for July 1, 1975 (Approach D corresponds to Approach A)	107
31. Forecasts of Hourly Net Demand (MW) in the Presence of Two-Axis Tracking Concentrator PV and WECS with 5% Penetration each for June 30, 1975 (Approach D corresponds to Approach A)	109
32. Forecasts of Hourly Net Demand (MW) in the Presence of Two-Axis Tracking Concentrator PV and WECS with 5% Penetration each for July 1, 1975 (Approach D corresponds to Approach A)	110
33. Forecasts of Hourly Net Demand (MW) in the Presence of Two-Axis Tracking Concentrator PV and WECS with 5% Penetration each for June 30, 1975 (Approach D corresponds to Approach B)	111
34. Forecasts of Hourly Net Demand (MW) in the Presence of Two-Axis Tracking Concentrator PV and WECS with 5% Penetration each for July 1, 1975 (Approach D corresponds to Approach B)	112
35. Forecast Flowchart (Approach D corresponds to Approach C)	114
36. Forecasts of Hourly Net Demand (MW) in the Presence of Two-Axis Tracking Flat-Plate PV and WECS with 5% Penetration each for June 30, 1975 (Approach D continued)	116
37. Forecasts of Hourly Net Demand (MW) in the Presence of Two-Axis Tracking Flat-Plate PV and WECS with 5% Penetration each for July 1, 1975 (Approach D continued)	117
38. Forecasts of Hourly Net Demand (MW) in the Presence of Two-Axis Tracking Concentrator PV and WECS with 5% Penetration each for June 30, 1975 (Approach D continued)	120
39. Forecasts of Hourly Net Demand (MW) in the Presence of Two-Axis Tracking Concentrator PV and WECS with 5% Penetration each for July 1, 1975 (Approach D continued)	121

Figure	Page
40 Forecasts of Hourly Load (MW) for June 30, 1975 (Univariate Time Series Process)	125
41 Forecasts of Hourly Load (MW) for July 1, 1975 (Univariate Time Series Process)	126
42. Forecasts of Hourly Load (MW) for June 30, 1975 (Bivariate Time Series Process)	130
43 Forecasts of Hourly Load (MW) for July 1, 1975 (Bivariate Time Series Process)	131
44 Forecasts of Hourly Load (MW) Over Each 3 Hour Period for June 30, 1975 (Univariate Time Series Process)	136
45 Forecasts of Hourly Load (MW) Over Each 3 Hour Period for June 30, 1975 (Bivariate Time Series Process)	137

LIST OF SYMBOLS

A	- constant which depends on the cell's material and it's area ($326.7264 \times 10^{-3} \text{ amp./} \theta_K^{1/2}$)
AR(P)	- autoregressive model with order of P (P=1,2, ...)
ARMA(P,q)	- autoregressive and moving average with orders of P and q (q = 1,2, ...)
ARIMA	- integrated autoregressive and moving average
B	- back shift operator ($B^m Z_t = Z_{t-m}, m=1,2,\dots$)
b	- a delay parameter
\hat{a}_t	- estimated residual
B	- constant which depends on the cell's material ($12881 \text{ } 81227 \theta_K$)
θ_C	- celsius degree
cm^2	- square centimeter
D	- order of seasonal (periodic) differencing (12,24, ...) -- $(1-B^{12})Z_t = Z_t - Z_{t-12}$
d	- order of regular differencing -- $(1-B^1)Z_t = Z_t - Z_{t-1}$
$\frac{d}{dv}_{pu}$	- mathematical operator (derivative)
e	- electronic charge (1.6021×10^{-19} coulomb)
h_t	- $6.4 \times 10^{-4} \text{ K}^{-1}$ for silicon
I	- current
I_j	- junction current
I_0	- dark current
I_{pu}	- normalized (per unit) current
$I_{\max}(\phi_e, T_c)$	- output current corresponds to maximum power output
I_{s0}	- short circuit current under standard conditions

I_s	- short circuit current
o_K	- Kelvin degree
K	- Boltzman constant (8.6168×10^{-5} eV/ o_K)
l_n	- natural logarithm
N_t	- noise function
n	- number of cells in the module (35)
n_t	- the transformed and difference value of N_t
P	- order of autoregressive models (1,2,..)
P_e	- electrical power output in (kW)
PV	- photovoltaic
P_{pu}	- per unit power
P_{max}	- module's maximum power under standard conditions (40 watts)
$P_{max}(\phi_e, T_c)$	- maximum output power
q	- order of moving average models (1,2,..)
R_s	- series resistance
R_{sh}	- shunt resistance
$\hat{r}_{\hat{a}\hat{a}}$	- autocorrelation functions of the estimated residuals
$\hat{r}_{\alpha\hat{a}}$	- cross-correlation functions between prewhitened input and estimated residuals
$\hat{v}_{\alpha\beta}$	- cross-correlation functions between prewhitened input, and filtered output
T_a	- ambient temperature
T_{C0}	- operating cell temperature under standard conditions ($25^{\circ}C$ or $298^{\circ}K \pm 5^{\circ}C$)
T_c	- operating cell temperature
u_{t-1}	- a sequence of independent random disturbances with zero mean and a variance σ_u^2 , when white noise is considered
V	- voltage
v	- hourly wind speed

$V_{\max}(\phi_e, T_c)$	- output voltage corresponds to maximum power
V_{OC0}	- open circuit voltage under standard conditions
V_{OC}	- open circuit voltage
V_{pu}	- per unit voltage
W	- watt
WECS	- wind electric energy conversion
X_t	- input series (temperature data)
x_t	- the transformed and difference value of X_t
Y_t	- output series (load data)
y_t	- the transformed and difference value of Y_t
Z_t	- time series under consideration
α	- constant which depend on the module which as been used
β	- constant which depend on the module which as been used
ν	- constant which depend on the module which as been used
α_t	- prewhitened value of x_t
β_t	- prewhitened value of y_t
ϵ_t	- prewhitened value of n_t
ϕ_{e0}	- solar insolation at standard conditions (1000 w/m ²)
ϕ_e	- solar insolation
$\phi_p(B)$	- autoregressive models parameters ($\phi_p(B)=1-\phi_1B^1-\phi_2B^2, \dots, \phi_pB^p, p = 1,2, \dots$)
$\phi_{pn}(B)$	- autoregressive models parameters for noise function
$\theta_q(B)$	- moving average models parameters ($\theta_q(B)=1-\theta_1B^1-\theta_2B^2-\dots-\theta_qB^q, q = 1,2, \dots$)
$\theta_{qn}(B)$	- moving average parameters for noise function
$\psi(B)$	- linear operator or the transfer function of the filter $\psi(B) = \psi_0 + \psi_1B^1 + \psi_2B^2 + \dots$
∇^d	- regular differencing operator - $(1-B^1)Z_t = Z_t - Z_{t-1}$
∇^D	- seasonal differencing operator -- $(1-B^{24})Z_t = Z_t - Z_{t-24}$

- $\delta_r(B)$ - corresponds to rth order AR -- $(1 - \delta_1 B^1 - \dots - \delta_r B^r, r=1,2,\dots)$
- $\omega_s(B)$ - corresponds to sth order MA -- $(\omega_0 + \omega_1 B^1 + \dots + \omega_s B^s, s = 1,2,\dots)$
- μ - expected value of Z_t
- η_{CS} - module's efficiency under standard conditions (10.76%)
- η_l - power losses efficiency (0.9)
- $\eta_{\max}(\phi_e, T)$ - maximum efficiency of cell
- η_{pc}, η_{pt} - efficiencies of the power converter and power tracker, respectively (0.9)
- η - overall efficiency of module
- $\nu(B)$ - impulse response function -- $(\nu_0 + \nu_1 B^1 + \nu_2 B^2, \dots)$
- $\hat{\nu}_k$ - estimated impulse response function ($k = 1,2,\dots$)
- χ^2 - statistical operator (chi-square)

CHAPTER I

INTRODUCTION

1.1 Photovoltaics (PV) and Electric Utilities

Semiconductors truly brought about a revolution in the technology for communicating and processing information a few decades ago. But the age of silicon still remains in full swing and its technological surprises are still emerging. One of them is the photovoltaic cell, which is made of very thin layers of suitably doped silicon or other semiconductor materials to convert sunlight directly into electricity. Researchers believe that this device can contribute a significant portion of the electric power supply in U.S., and in other parts of the world as well, by the end of this century [1].

Photovoltaics (PV) continues to be the most promising renewable energy technology with a potential to make a significant impact on the future electric power generation mix. Aggressive research and development have led to the growth of world-wide remote and consumer electronics markets for PV. The awareness of the public and technical communities has been sharpened in spite of the recent happenings in the global energy scene. Utility interest in photovoltaics is at a high level and the experience being gained from the three MW-scale central-station PV plants in California has been very encouraging and has built up the confidence in PV as a technically viable generation option [2].

Many specific technologies are still competing and no clear winner has emerged yet because of the wide variety of markets and their special requirements. The world-wide accumulated production of PV approached the 100 MW level towards the end of 1985 and it is expected to soar to 10,000 MW sometime during the 1990-1995 time period [2].

1.1.1 History

PV is not just a current fad, in fact it has a history older than that of the space age. The knowledge of the fundamental principles involved in the operation of PV cells predates Edison's incandescent lamp by about forty years. Edmund Becquerel, a French physicist observed in 1839 that "a small voltage was created when one of two metal electrodes was placed in a weak conducting solution and the apparatus was exposed to light". Nothing much was added to the knowledge of PV effect until the 1870's when it began to be studied in solids, specifically selenium (see reference 1)

The first selenium devices were demonstrating efficiencies of 1-2% in the 1880s. Selenium cells were used to photometric devices because of their sensitivity to the visible light spectrum and they are still used in today's light meters. Early inventors had visions that selenium cells would someday compete with the electric dynamo as a means of generating large amounts of power. The arrival of quantum mechanics in the 1930s and, later, the field of solid-state physics which explained how the cells converted sunlight directly into electricity, speeded up the development of practical PV cells with higher efficiencies.

In the 1950s, researchers at Bell Telephone Laboratories stumbled on to the silicon solar cell almost accidentally. One group was working

to increase the efficiency of selenium cells when they were developing a remote power source for communications equipment. Another, in pursuit of a better rectifier, found that injecting impurities into silicon improved its electrical efficiency. A marvelously strong current was generated, when the silicon rectifier was exposed to light. Soon Bell researchers were demonstrating solar cells with 4% efficiency (see reference 1)

The quest for improved silicon solar cells began in earnest and the efficiency of experimental cells reached 6% by 1954. The world was surprised at the news about Bell Telephone System's solar battery and its fantastic possibilities for telephone service as well as for other uses. In spite of the achievement of 15% efficiencies in experimental devices, the solar cell remained nothing more than a scientific curiosity because it was very expensive and had to be handmade from very high purity silicon.

Almost immediately after the Soviet satellite Sputnik was launched in October 1957, the silicon cell was recognized as the best hope to provide a few watts of on-board power for satellites with very light weight, cost was of little concern. In 1958 when the American satellite Vanguard went into orbit, it carried PV cells. "The space age and the silicon era had begun in tandem"

1 2 2 Recent Developments

Research and development work around the world is pushing the technology of solar cells closer and closer to its limit. Single-junction silicon cell efficiencies are approaching 21% in the laboratory. Amorphous cell efficiencies have crossed the 10% mark.

Significant progress is being reported in the fabrication and performance of multi-junction and heterojunction cells.

Design procedures for large and small PV systems to achieve fault-tolerant and reliable operation have made strides. Encapsulation and packaging have advanced to the level that it is now possible to expect 30 year lifetimes and performance goals in the near future.

Generation costs are being reduced by increasing efficiencies, decreasing balance-of-system costs, and by decreasing cell and module fabrication costs through mechanization. This multi-pronged attack on the most crucial aspect of PV is producing tangible results and is making the realization of the cost targets a near-reality. Utilities have begun to look at PV from its best angle -- its ability to supply energy during peak (or within 90% of peak) hours, unattended operation, low maintenance, modular design, rapid construction and commissioning, lack of harmful emissions, and absence of water requirements [2].

The world shipments of PV modules was 25 MW (peak) during 1984, of which one-third (8.4 MW) was manufactured in the United States. During 1985, nearly 18 MW of PV were installed in major electric plants in the U.S. They ranged in size from a few kW up to the 6.5 MW Carrisa Plains plant in California. By the end of 1985, world-wide accumulated production of PV was approaching the 100 MW level. This figure is expected to increase to about 10,000 MW sometime during the 1990-1995 time period [2].

Recently, private industries, most notably ARCO Solar, have played a significant role in the design, installation, and operation of MW-scale terrestrial PV central-station systems. The experience of California utilities, Southern California Edison Company (SCE) and

Pacific Gas and Electric Company (PG&E), which have MW-size PV systems on their grids has been very good and it has increased the confidence that PV could be a viable generation option for utilities in the southwestern part of the United States in the next decade [3]

The performance of the Lugo plant has been monitored continuously since it first went on line in November 1982. It has provided an opportunity to examine the diurnal source of energy of a PV plant from the utility view point [4]

Construction of Phase 1 of the Sacramento Municipal Utility District (SMUD) plant has been completed and the system went on line in July 1984. It is the first large central-station PV plant to be designed for and owned by an electric utility. As such, it was specially designed to maximize the plant value to SMUD. The array field is rated at 1.19 MW (dc) under standard test conditions. One line-commutated inverter converts the dc output into ac for delivery to the SMUD 12.47 kV distribution grid [5].

Several innovative design features have been incorporated in SMUDPVI resulting in cost reduction, improved electrical design, and high performance from the power conditioner. Initial operating experience indicates compliance with design requirements and expectations. In particular, the power conditioning unit exhibited a net efficiency of 96 to 96.5% over most of the operating range, operating at a power factor greater than 0.9. Total harmonic voltage distortion at the 12 kV interface was in the range of 2 to 3%. Detailed data on its operation have been collected since September 1984 but the information has not yet been made available. Meanwhile, the next 1 MW increment is nearing completion at the same location [5].

Carrisa Plains Plant, constructed by Arco Solar on PG&E land, now has an aggregate capacity of 6.5 MW and it was connected to the PG&E grid on November 14, 1983. A novel technique employed in the construction of this plant enabled its completion in about the same time as it took for the Lugo plant [6]. Quantitative data on plant performance and cost have not yet been released by Arco Solar.

Skyharbor concentrating PV plant, which is a 225 kWdc (nominal) Fresnel-lens point-focus (33x) concentrator design went on line in May 1982, interconnected with the Arizona Public Service (APS) grid. By necessity, it is a two-axis tracking system. During the first year of operation, there were many hardware and computer related problems and as such its performance to date is not representative of its potential. Energy production during the first year was about 60% of the expected value of 440 MWh (ac), with a net capacity factor of only 13.5%. A 20 to 30% improvement in the annual performance is expected during the next few years [7]. APS experience indicates that there are no major technical problems with PV plants in the area of grid-connected operation.

There are several intermediate (medium-size) PV experiments scattered throughout the U.S. as well as Europe and the numbers are growing rapidly (see reference 3). The purpose of these experiments is to validate the technical viability of PV as a generation supplement under a variety of operational and climatic conditions. Data from these systems are providing valuable information and feedback for improving the installation, design, planning, and operation of PV systems in conjunction with existing utility grids. A selected list of medium-size experiments in the U.S. is given below.

Agricultural water pumping system in Mead, Nebraska 29.3 kW system, became operational in July 1977

Mt. Laguna radar site, California 49.6 kW system, became operational in August 1979.

Natural Bridges Monument in Utah 105.6 kW system, became operational in June 1980

Lovington Square Shopping Center in Lovington, New Mexico 90.4 kW system, came operational in March 1981.

Beverly High School in Beverly, Massachusetts 90.4 kW system, became operational in April 1981

Mississippi County Community College in Clytheville, Arkansas 240 kW (electrical) and 625 kW (thermal) system, became operational in September 1981

Wilcox Hospital in Kauai, Hawaii 35 kW (electrical) and 230 kW (thermal) system, became operational in January 1982

Oklahoma City Science and Art Center (Omniplex) 135 kW system, tied to the Oklahoma Gas and Electric grid, became operational in March 1982

BDM Building in Albuquerque, New Mexico 47 kW (electrical) and 280 kW (thermal) on rooftop became operational in July 1982

DFW Airport Solar Power System combined photovoltaic and photo-thermal system, 27 kW (electrical) and 140 kW (thermal as 57°C water), operating continuously from September 1982, to date No significant performance degradation has been detected yet [8]

Georgetown University in Washington, D C PHENEF (Photovoltaic Higher Education National Exemplar Facility) program to provide

utility-interactive PV power for the Intercultural Center, completed in Fall 1984

The commission of the European Communities has implemented a series of 15 PV pilot projects ranging in size from 30 to 300 kW, with an aggregate installed capacity of 1 MWp [9]. The systems are installed in 8 different countries, but with the same monitoring system. The projects were completed in the 1983-84 time frame and data are being gathered to accumulate detailed information on cost, performance, operation, reliability, and maintenance. All the data are transmitted to Joint Research Center at Ispra for analysis.

1.1.3 Promises and Prospects

Fossil fuels, nuclear fission, and hydroelectric generating plants are expected to supply the bulk of the electricity needs of the United States through the year 2000. However, sustained research and development have resulted in steady increases in the efficiencies of solar cells and in substantial decreases in photovoltaic (PV) module costs in the recent past, pointing to a bright future for utility-scale applications of photovoltaics (see references 1, 7, and 10)

Utility interest in photovoltaic technology is steadily increasing [11,12] and most of the future shipment of PV modules is expected to be to utilities. The emphasis of Federal support has shifted towards basic research and away from large proof-of-concept experiments. But the Federal government continues to be one of the major players in determining the rate of growth of PV technology and use by its plans to extend, modify, or eliminate residential and business solar tax credits.

The future of PV for terrestrial applications looks very bright. Single crystal and polycrystalline cells with cell efficiencies of 20% and array efficiencies of 17 to 18% are expected to be commercially available [13]. Sheet grown silicon arrays at \$1/Wp and amorphous silicon modules (operating at 9% efficiency) at less than \$1/Wp are also predicted to make their way into the PV scene. The coming years will see many more of what EPRI calls "solid-state power plants" interconnected with utility grids in the Southwestern part of the U S first and elsewhere later.

1.2 Wind Electric Conversion Systems and Electric Utilities

1.2.1 History

For centuries, human beings have been fascinated by the winds sweeping across the earth. They have harnessed wind for useful purposes for almost the same length of time. Windmills and watermills were the first engines devised by humans [14]. First windmills were used for the generation of electricity during the 19th century. Early developments in this field took place most likely in European countries, notably in Denmark, France, Germany, and Holland. In Denmark, generation of power from wind became a necessity due to a cutoff of 95% of their fuel supply during the first and the second world wars. Because of the early successes, the neighboring countries -- England, France and Germany, developed small and large wind systems for the generation of electricity. Almost all of the projects had to be abandoned because of frequent technical problems and the high cost involved in their repair [15].

The 200 kW Gedser mill in Denmark (1956-1957), [16], the Best Roman (800 kW) near Paris (1958-1963), [17], the 100 kW unit in Orkney, U.K. 1952-1956, [18,19], and 100 kW Hutter's system in Germany (1958), [20,21] are among the large windmills built and successfully operated in Europe.

In the United States, early significant works in this area were initiated by Palmer Putnam in 1934 [22]. The Smith-Putnam's 1250 kW wind plant was commissioned and built on October 19, 1941. The project was abandoned just after one of its blades broke off in March, 1945 and it was not repaired due to the subsequent preoccupation of the country with World War II [23].

The oil embargo of 1973, increasing consumption of energy during the decade of the seventies, realization of the limitations of fossil fuels, large increases in fuel costs, and public awareness of the environmental impacts of unrestricted consumption of fossil fuels have encouraged the interest in wind power in the United States. A number of parallel activities under 45 different projects on wind energy conversion systems research development and design were initiated by Energy Research and Development Administration (now the Department of Energy) along with NASA

1 2 2 Recent Developments

A recent EPRI survey (1979) indicated that 83 wind energy projects were being conducted by 51 electric utilities in the United States [24]

For instance, Pacific Gas and Electric Co and Southern California Edison Co have included wind electric capacities of 82.5 and 43 MW (in terms of machine ratings) respectively in their generation expansion

plans for 1990. An agreement has been signed by Hawaiian Electric Co., Inc. to buy up to 80 MW (machine ratings) of wind-generated power by 1985 from a private firm which will retain ownership of the wind machines.

Federal wind energy program activity under DOE direction was designed to be broadly based. Small wind machines with rated output less than 100 kW still represent an important area of attention for the Federal program [24]. The primary focus is to learn about the performance, efficiency, dynamics, and other technical issues associated with the many small commercial machines that have been developed without government funding.

Several megawatt-scale wind turbines which are generally the product of aerospace technology are in operation today. They are producing energy as well as valuable data on their long-term performance and economics [25].

Over 100 active companies and 85 operating wind power stations were reported by an EPRI-sponsored survey in 1983. According to the state energy commission, in California, home to most of the wind turbines, an estimated 500 MW would be on line by the end of 1984.

Over 3,600 wind systems with a combined capacity of 239 MW (installed) were in the U.S. by the end of 1983. About 8,200 wind turbines having a total capacity of over 613 MW were installed in the U.S. at the end of 1984. Over 4,500 additional turbines with total capacity of over 374 MW, were installed by the developers in California and other states, by the end of 1984 [26].

Southern California Edison Co., PG&E, and San Diego Gas & Electric Co. are the major utilities in the U.S. gaining experience in

integrating wind energy from independent producers with their transmission and distribution systems. In addition, PG&E and SCE are both involved in wind turbine testing programs of their own. SCE is testing four different machines at San Geronimo Pass, including a 500-kW vertical axis eggbeater-type turbine made by DAF Indal Ltd of Canada. PG&E is involved with a MOD-2 near the Carquinez Straits northeast of San Francisco (see reference 25).

The wind industry had an excellent year in 1985. About 5,000 wind turbines with a total installed capacity of 485 MW were installed in California. By the end of 1985, an estimated 13,189 wind turbines with a total capacity of 1,098 MW, had been installed on windfarms in California.

The electrical energy production by wind farms has shown a dramatic increase. The total generated electricity amounted to 632.2×10^6 kWh by the California's windfarms in 1985 alone. This amount of energy is more than triple the 183.2×10^6 kWh generated by the wind farms in the same state in 1984. According to the number of turbines installed, by the end of 1985, the total combined generated energy of the windfarms should easily exceed 10^6 kWh in 1986 [27].

PG&E is one of the largest investor owned utilities in the U.S., serving the demands of 3.5×10^6 electric customers in addition to 2.9×10^6 gas customers, set a new all-time area peak demand load of 16,507 MW, on July 9, 1985. Of this, 7% energy mix needs were expected to be supplied from alternative sources including wind and solar. This contribution is projected to increase to 27% of the utility's need in 1995 [28].

Obviously, wind-electric conversion is considered seriously as an alternative by PG&E. Conceptual design of windplant, pooling the resources of many engineering departments, namely, Engineering Research Department and Generation Planning and Siting Department has already begun by the company. It is also estimated that there were 5,503 wind turbines, with total capacity of 524 MW, installed in the PG&E's service at end of 1985 [28].

SCE is another major electric utility in U.S., which have installed about 7,686 wind turbines having a total capacity of 574.3 MW in its territory. Of these, 95% were connected to the grid, and the rest is expected to be on-line soon (see reference 27).

Several European countries and Canada also have substantial wind turbine development programs. Research and development program in Canada has focused mainly on vertical axis machines. Megawatt-scale horizontal-axis designs are main focus in Sweden and West Germany. Industrial firms for the Kernforschungsanlage Zulich (KFA), which manages the German wind program, built the Growian I (3-MW, 100-m-rotor machine near Brunsbuttel), and the Growian II, near Bremerhaven which boasts the world's largest single-blade turbine. The Growian I, boasts the world's largest-diameter rotor and features a variable-speed generator.

Several hundred machines in the 50-kw range were operating throughout Denmark by 1983. Two 630-kW wind turbines at Nibe, are being operated by the Danish utility Elsam. Although Denmark was frontrunner in wind turbine technology, at present it is involved only with smaller designs compared to Sweden's and Germany's megawatt-scale machines.

A multiturbine development on the isolated Orkney Island power system has been planned by the United Kingdom as a major step in developing wind resources. A 250-kW, 20-m-rotor turbine has already been placed in operation by an industrial group of aerospace, energy, and construction firms, and a 3-MW, 60-m design was scheduled for completion in 1985. Two other large turbines are planned at the site for future.

Other nations, notably Australia, Brazil, France, Japan, the Netherlands, and Norway have significant, but more-modest and less-advanced, wind energy programs.

1.2.3 Promises and Prospects

A combination of economic, technical, and political factors has pushed further into the future the time when large, megawatt-scale wind turbines may be considered as a viable commercial electric power generation technology until the achievement of technical advances in the technology of large turbines. Current test and refinement programs on existing large turbines are necessary not only to improve them but also to achieve the insights which can be helpful to advance the technology of smaller turbines [25].

The aim of the Federal program is to reduce wind generation costs down to competitive levels. Focussing on simple machines with improved performance, inexpensive flexible towers and cheaper rotor blades and, eventually, mass production is the major thrust to reduce capital costs.

Although in some parts of the U.S. wind-electric generation is used to generate valuable energy and experience as well, the technology should still be considered as in the R&D stage. Almost all wind turbines have experienced some mechanical problems, and maintenance as well.

as operation costs have been high. In spite of all of the problems with some wind systems and other disappointments, there remains cause for optimism that wind generated electricity could be competitive in certain selected regions of the world with good wind regions.

1.3 Forecasting Concepts Applied to Power Systems

Electric utilities have been interested in power system load forecasting for many years. Recently it has become one of the major requirements in effective and efficient power system planning. The reasons for this are as follows:

1. The growing complexity of power systems.
2. Increasing consumer demands.
3. Rapid increases in the cost of oil as well as other fuels.

An appropriate load forecast is the basis of all utility planning. In fact, load forecasts are the starting points of most operating and planning decisions such as generation expansion, including the integration of alternative power generation schemes such as photovoltaics and wind-power generation in electric utilities.

Unconventional power generation systems differ significantly from conventional utility equipment. Consequently, under high penetrations, they may cause inadequacies in the existing load forecasting techniques normally employed in traditional utility systems work. Such inadequacies may cause severe problems in the planning and operation of the system from the view points of economics and reliability [29].

The necessity of prior knowledge of the load is critical from the design, operation and control points of view for the utility system.

since they are responsible to meet the power demanded by their consumers in a reliable manner.

1.3.1 Role of Forecasting

The usefulness of any load forecasting technique depends on its ability to supply information for the following tasks [29,30].

1. System and generation planning.
2. Transmission and distribution planning.
3. System operation and revenue forecasting.
4. Unit commitment and economic dispatch.
5. System security.

Many diverse issues, including load forecasts, must be considered in making generation planning decisions. Determination of generation additions based on the required reserve margin (difference between net system capability and system peak load) is frequently done by using estimated future peak loads.

In making assessments in the areas of transmission planning, load flow, transient and dynamic stabilities, short circuit calculations as well as reliability analyses, the importance of the role of load forecasts should be kept in mind (see reference 29). For these, loads have to be specified in more detail. For instance, the specification of real and reactive load components simultaneously at a number of bus locations are required for load flow studies [31], and the necessity of the characterization of the voltage and frequency dependence of loads are obvious in transient stability analyses [32].

Both energy and maximum-demand forecasts are necessary for planning from an economic point of view and for determining schedules for

investments in additional generation and transmission to provide quality service to customers [33].

Forecasts of future sales play an important role in the financial health of a utility. They allow the establishment of consumer rates which provide a feasible return on the utility's investment and to permit the financing of further construction and development of its system.

It should be emphasized that distribution load forecasting is more difficult than overall system load forecasting due to the following reasons [34].

1. Distribution forecasts have to consider the timing of load growth, and the specific location and size of areas.

2. Much more data are necessary for distribution forecasts because small geographical areas and individual large consumers should be considered separately due to the great amount of fluctuation in load growth patterns.

1.3.2 Types of Load Forecasts Based on the Time

Periods Considered

Forecast should be accurate and comprehensive as well. Typically, the accuracy of a forecast decreases with increasing time lead.

Load forecasts over a few minutes to a few days ahead are helpful in addressing maintenance scheduling problems for handling unit commitment and economic dispatch as well as security analysis such as on-line load flow solution [34,35].

Energy forecasts over a period of a few weeks to several years or more contribute to the study of revenue forecasting.

The majority of load forecasting is done over a period of one or two years, with the establishment of budgets for distribution construction on an annual basis. In order to determine a preliminary basis for allocating resources and to meet the system load projections, a forecast over a five-year period is required. Establishing an overall expansion plan and early purchase of substation sites and right-of-ways are dependent upon long-term distribution forecasts covering a period of ten to fifteen years [36]

1.4 Literature Survey

The purpose of this section is to summarize and present a brief review of some of the recent literature on the latest technical and economic developments, particularly in photovoltaics, with special emphasis on the topics of potential interest to the electric utility companies, especially on load forecasting in the presence of alternative power generation technologies, and to put the problem under study in proper perspective.

1.4.1 Alternative Power Generation Technologies

Despite the potential of alternative energy sources to supply a part of the global energy needs, historically, interest in such sources and systems has been only minimal and sporadic until recently.

The term alternative energy sources include different manifestations of solar energy (solar radiation, solar heat, biomass, and falling water), geothermal, and sometimes even nuclear (fission as well as fusion). However, this dissertation considers only photovoltaics and wind energy conversion in the context of how they influence utility load

forecasting. The reason for this focus is that the power generated by these two means is highly variable and could adversely affect utility planning based on load forecasting under high penetrations. In contrast, the outputs of cogeneration plants utilizing biomass and other resources are "schedulable".

The background, status, and prospects of photovoltaics and wind energy conversion have already been discussed in earlier sections of this chapter.

1.4.2 Load Forecasting

Power demand (load) forecasting is a very difficult task because of the sensitivity of load to environmental phenomena (e.g. weather, temperature) as well as to fluctuations in the economy. Many approaches have been used in electrical load forecasting, each with its own limitations, advantages and disadvantages that determine their applicability [37-39].

Reyneau [40] was the first to realize the necessity of considering demand (load) forecasting in a power utility at a time (1918) when most utilities were oil or coal fired with quite low load densities.

Christiaanse [41] used exponential smoothing by emphasizing the analysis of load data and developed an algorithm for short-term hourly load forecasting. Several other researchers, notably Gupta (see reference 33), Keyhani [42], Vemuri, et al [43], and Meslier [44], used time series analysis and Box-Jenkins methods to forecast future load [45,46]. Sensitivity of the load demand to weather has been considered by Thompson [47], and Keyhani and Miri [48].

Recently, Willis [49] used two-dimensional spatial frequency analysis to the power system configuration. In this approach, both the load forecast and its error are treated as images, or two dimensional signals. He also employed the trending method and used clustering of historical load at the small area level in the forecast algorithm to get better results over normal curve fit method [50]. In addition, he extrapolated load growth for distribution planning [51].

The most recent load forecasting research has been done by Willis and Tram [52] for use in transmission planning. They have investigated two aspects: (i) the effect of forecasting error on transmission system planning, the (ii) procedures required to generate forecasts. Their major conclusions are reproduced below.

Future substation loads are a function of both decisions in future distribution planning and also of the changing nonuniform geographic distribution of load. Spatial correlation of error is as important in determining impact as in the average magnitude of the errors. The transmission system planned from an incorrect forecast may function but fail to meet contingency criteria.

1.4.3 Load Forecasting in the Presence of Alternative Power Generation Technologies

Considerable work has been done in recent years on the problem of utility electrical load (demand) forecasting. All these methods assume that only conventional generation sources are present. So far, not much attention has been given to the effects of the presence of alternative electric power generation such as photovoltaics and wind power generation, on utility load forecasting.

The application of classical forecasting techniques to load forecasting including the integration of new energy technologies, problems

arising due to the presence of new energy technologies, and the necessity of modifying demand load forecasting models have been brought up by the most recent works of Camerford and Gellings (see reference 37), Fink and Feero [53], Ruane and Finger (see reference 29), Bose and Anderson [54], and Chalmers, et al [55]. Time series analyses have been used to simulate hourly global radiation sequences [56], and to suggest a model to forecast solar radiation data [57]. Time series models have also been used to simulate and forecast wind speed and power output of wind-electric conversion system [58], to determine a model for wind speed [59], and to analyze wind stream and turbine power [60]. These topics will be discussed further in the forthcoming chapters because of their relevance to the present effort.

1.5 Problem Statement

Several new electric generation technologies are being introduced at present by homeowner and businesses under encouragement from PURPA (Public Utility Regulatory Policies Act) and the number of systems coming on line is growing very fast.

As the penetration of new generation technologies increases, their presence will have to be considered in load forecasting. This is the problem studied in this work.

Photovoltaics and wind-electric systems depend on renewable resources (solar radiation and wind) which have inherent short-term variations. They violate almost all the assumptions made in analyzing conventional generation systems. Their power outputs are highly variable because they depend on meteorological factors, it is difficult to control power quality, output and demand are weather dependent and so

they both are correlated to some extent, and systems can be built in small units colocated with the load and therefore distributed throughout the grid. Finally, they can be installed by customers as well as by utilities.

These two technologies (PV and wind-electric) have the highest load forecasting barriers among all the new generation technologies being considered at the present time.

From the PV system point of view, the first step is to derive an algorithm to calculate PV output under variable insolation, temperature and wind speed conditions in the form of a time series designated as "PVTSALGO".

The output of this algorithm, along with the output of wind electric systems are used to forecast the "net" demand of a utility in the presence of photovoltaic and wind electric systems.

1.6 Method of Analysis

To reach the goal of assessing the impact of grid-connect PV and wind electric conversion systems from the load forecasting point of view, the following step-by-step procedure will be followed.

(1) Develop an algorithm to calculate PV system output under variable insolation, temperature, and wind speed conditions. Also review and formalize the method to calculate wind electric conversion system (WECS) output.

(11) Employ the algorithm developed in (1) in conjunction with univariate time series analyses to forecast the insolation, ambient temperature, and wind speed to calculate (forecast) PV system output for both two-axis flat-plate and concentrator systems. The final forecasts

of "net" demand are obtained by subtracting the calculated PV system output from the load forecast.

(111) Calculate PV system output for both two-axis flat-plate and concentrator systems from raw historical data first and then forecast these outputs using suitable models. Once again, forecasts of the final "net" demand are obtained by subtracting the sum of the calculated PV output from the load forecast.

(1v) The historical "net" demand which is equal to the actual demand minus the PV output is calculated and will be used as final data to forecast the future "effective" demand.

(v) The steps outlined in (11) through (1v) will be repeated for the case of grid-connected PV and wind electric conversion systems to calculate (forecast) final "net" demand on the utility.

(vi) Study the impact of temperature on load and its effect on the forecasting modeling procedures by using multiple time series analyses.

The hourly load and temperature data used in this study were provided by the Public Service Company of Oklahoma (PSO) and the rest of the data were obtained from Solmet tape [61].

The results will be tabulated and presented in the form of families of curves. Moreover, these tables and curves should be discussed and some useful conclusions will be drawn which may be helpful in planning studies. Further, this study will also form a good background for further research work and refinements that are yet to come.

1.7 Organization of the Thesis

Chapter II summarizes the impacts of alternative electric power generation on the utility system, brought about by the significant

differences between conventional and unconventional technologies. Utility-related issues, impacts and concerns as well as barriers to load modeling and load forecasting are also discussed.

Chapter III presents an approach and develops an algorithm to calculate PV system output under variable insolation, temperature, and wind speed conditions in the form of a time series, designated "PVTSALGO". This algorithm has been tested and used to calculate the PV output for different sets of selected data. Calculation of the power output of a wind electric conversion system is also discussed in this chapter.

Chapter IV develops models to calculate and forecast the net-demand by using univariate time series analyses in the presence of PV for two-axis tracking flat-plate and concentrator systems. Next the case of PV and wind existing together is considered. The inclusion of the impact of temperature on load by using multiple time series analyses is also discussed.

Concluding remarks and suggestions for further work are given in Chapter IV, followed by a list of references and appendix.

CHAPTER II

THE IMPACT OF ALTERNATIVE ELECTRIC POWER GENERATION TECHNOLOGIES ON A UTILITY SYSTEM

2.1 Distinguishing Features of Alternative Power Generation Technologies

Since the early seventies when the price and limitations of fossil fuels as well as the quality of the environment became public issues, alternative electric power generation has become a topic of world-wide interest. Until economical and reliable energy storage and reconversion systems are available, large-scale use of most of the alternative energy sources will be in the form of conversion to electrical energy, to be pumped into an existing utility system. The impacts of such grid-connected operation on the electric utility are discussed in this chapter.

The new (alternative) technologies are substantially different from conventional generators used by electric utilities. Many of the assumptions made about electric power generators and loads in traditional models of electric power systems may be violated by one or more aspects of unconventional generating systems. Examples of the assumptions involved are enumerated below.

1. Electric power generators are not intermittent, they are dispatchable when they are not on maintenance.

2 High quality (utility-grade) three-phase power with a controllable power factor is produced by conventional generators.

3 The power generated is essentially independent of the weather conditions and demand.

4 Conventional generators are built in large units (100 to 1500 MW) and they operate very efficiently (> 95%). They are typically located at some distance from the load.

5. All new capacity is planned and constructed by the utilities themselves.

6 The utility controls all the electric power generated

Unconventional generation systems greatly differ in their attributes as compared to conventional electric power generators. Such attributes can present special design and analysis difficulties for utilities whose existing planning and operation methods have been designed based on conventional generation. Every new technology with potential load modeling and forecasting barriers differs from conventional generation in one or more of the following aspects: scales of units, intermittent operation, correlation with load, ownership, dispatchability, power quality, and load shifting (see reference 29)

2.1.1 Small Scale

In contrast to conventional systems (which have exhibited economies of size with a minimum of about 100 MW), the new technologies, such as wind, photovoltaics, fuel cells, and batteries have no clearly defined minimum economic size. The small scale of the alternative technologies has several implications. First, the units do not need to be located at a central location far from the load, they could be co-located with the

load in many small units. Second, in contrast to the all-or-nothing capacity additions associated with large thermal units, alternative generation capacity might be constructed in small increments in response to increases in the load.

2 1.2 Intermittent Output

Two basic assumptions (introduced earlier) are made in the modeling and operation of electric power systems. The first one is that system operators can increase the power output of a conventional generator up to its rated capacity at any time. Another assumption is that a conventional generator can generate power at any time except when it is out on maintenance or repair. These two assumptions could be violated by the intermittent power output from some of the alternative generations, specifically solar and wind. Both wind and insolation have short-term variations and strong daily as well as seasonal variations, in addition to being dependent on weather conditions. Consequently, they are uncertain and uncontrollable.

2 1.3 Correlation of Generation with Demand

The main advantage of solar and wind systems is that their incremental energy cost is essentially zero. As such, the output of solar and wind systems is used whenever it is available. Consequently, the original demand minus the new generation would be the net demand on conventional generators.

Unlike the assumption that load forecasting and power generation studies can be undertaken independently in the case of traditional systems, in the case of unconventional systems, power generation is

dependent on meteorological effects. Unconventional power generation is correlated with components of the load.

Load frequency control (LFC) raises and lowers conventional generation to make it follow the load by sending control signals once every few seconds. The necessity of having generation under control is obvious and conventional generators have adequate response rates to follow the load (see reference 54).

If the outputs of alternative energy systems are not controlled or monitored, their effect will be seen by the LFC as negative load. As mentioned earlier, the effective or net load is the actual load minus the new generation. While the actual load could be followed adequately by the response rates of conventional generators, it may not be possible to follow the effective or net load when sufficient alternative generation is present.

The output variations (and response rates) of some of the unconventional generators could be much faster than those of conventional generators and in high penetrations the random effects of the outputs of alternative energy systems cannot be followed by conventional generators.

This points to the desirability of putting the new technologies under control. An added advantage is that the high response rates, which is a disadvantage when not controlled, can then be used to obtain better following of the actual load. This is a benefit for systems that have mainly thermal generation today as they have difficulty in providing good regulation (see reference 54).

To consider the control of the new technologies, two different characteristics must be taken into account. First the unit size of some of these sources is very small (in the kW range). Second, their

response can be considered instantaneous. These issues point to the use of block control where many of these generators are switched together. Such a control could be installed easily in a central plant, but is not easy when the sources are highly dispersed.

The availability of power from the new technologies is the main problem hindering their control. For instance, it is not possible to count on solar and wind energy resources for a significant amount of regulation. Therefore, sufficient response must be available from other sources during nighttime, cloudy, or calm periods. In this case the control of alternative energy sources provides no advantage. The installation of adequate amounts of storage devices such as batteries with fast response is one possible solution to this problem, but the cost is prohibitive at present. However, storage devices could be used for control when the new generation sources cannot generate power.

Although the regulation of a thermal generation system can be improved by using the instantaneous response of some of the unconventional technologies, it must be mentioned that the LFC cycle is a slow one, specially if long communication delays are involved. At present, power systems utilize the stored energy in the inertias of the rotors for immediate regulation in the case of major disturbances. Because most of the alternative technologies do not have this inertia and the associated reserve energy, the result might be poor regulation for changes that exceed this storage reserve. The traditional stored energy will be reduced relative to system size in the case of high penetrations of the new technologies.

2.1.4 Ownership

The ownership is the one of the factors which affects the controllability of the new technologies. The Public Utility Regulatory Policies Act (PURPA) encourages dispersed ownership to generate power and to sell the excess to the utility. But the question of the relationship between the utility and the owner is left open. Some of the new generation methods do exhibit economies of scale that make power generation with small capacities economically viable.

The above issues allow decisions of how much capacity to construct and when to construct under the control of both the consumers and the utility. The decisions made by the consumers present increased load variability on the utility. It is necessary for the electric utilities to predict the actions of the consumers and also to influence their action to design and operate the system efficiently.

2.1.5 Economic Dispatch

At present, almost all generators are controlled from a central dispatch control center to match the power generation with the demand. But it is not clear that this will be the case for the alternative energy technologies. Depending on the technology and the configuration, new technologies may or may not be dispatchable.

Since dispatching boils down to dividing up the new load among the traditional generation sources, those new technologies which are not under utility control do not affect economic dispatch.

Several different factors have to be considered if the new energy sources are under utility control. Since the incremental generation cost is zero for new technologies utilizing renewable energy sources,

they should be dispatched completely. The exception among those are the units being utilized for regulation.

Other technologies such as fusion, MHD, biomass, and OTEC, are indistinguishable from traditional technologies from the dispatchability point of view.

Small-scale electric generators such as hydro and cogeneration may or may not be dispatchable depending on their ownership and the agreements (if any) between utility and owners. Although the utility does have indirect control through purchase agreements and/or through time-of-day and buy-back rates, the ultimate decision to generate or not lies with the owner and not with the utility.

2.1.6 Quality of Power

Three-phase, 60 Hz, alternating current at standard voltage with controllable real and reactive powers is generated by conventional generators. Some of the new technologies such as photovoltaics and fuel cells generate direct current.

In order to be interconnected with the grid, the dc output must be inverted and synchronized with the utility grid. Utilities have been able to set safety and quality standards for the power sold to them by owners via PURPA. The potential effects of a large number of small generators on distribution feeders are yet to be fully investigated. Wind energy systems employing induction generators or line-commutated inverters in particular pose a special problem due to their reactive power requirements.

2.1.7 Load Shifting

A customer may shift his or her demand to match the output of the user-owned new generating unit. If a buy-back agreement exists with the utility and if the customer receives a fair rate for the power, load shifting is unlikely to occur because the user will be indifferent between generating and buying power.

2.2 Utility Concerns and Related Issues

The introduction of a new power generation technology such as photovoltaics and wind electric generation into an existing electric utility system requires the consideration and resolution of several issues. They are categorized and listed below (see reference 7).

1. Planning issues
 - a. Capacity displacement
 - b. Energy displacement
 - c. Influence on load forecasting
 - d. Generation mix optimization
 - e. T&D system design
2. Operational issues
 - a. Impact on overall system reliability
 - b. Influence on reserve margin required
 - c. Maintenance and repair
 - d. Dispatch
 - e. Weather forecasting and its use
3. Institutional issues
 - a. Siting
 - b. Safety

- c. Ownership
 - d. Environmental impact
 - e. Financing
 - f. Rate structure
 - g. Incentives -- tax, depreciation, etc.
4. Hardware issues
- a. Performance characteristics of, as an example,
 - (i) PV modules and panels
 - (ii) Aeroturbines
 - (iii) Power conditioning and interface components
 - (iv) Trackers (if any) and other ancillaries
 - (v) Existing system as seen at the interface point
 - b. Cost
 - c. Lifetime and survivability under severe weather conditions
 - d. Plant construction
 - e. T & D construction

It is difficult to address all the utility-related issues in one subsection. Therefore, certain key issues are identified and progress made in these areas are discussed in some detail. For example the usefulness of central-station PV plants to a utility primarily depends on the following factors

1. Generation cost as compared to the alternatives,
2. Match between PV plant output and the system peak demand and
3. Ability to integrate with the rest of the system without any deleterious effects.

Generation costs can be decreased by lowering module costs and by increasing efficiencies. PV module costs have been steadily coming down

and cell efficiencies are being increased by pushing the technology closer and closer to its physical limit

Pacific Gas and Electric Company (PG&E) has been conducting a series of experiments in its San Ramon and Davis test facilities in California on the performance of different types of PV modules [62,63] and on the influence of different tilts and azimuthal orientations (see reference 6) on the power output profile. One of the important conclusions was that the output of an array oriented 60 degrees west-of-south with a 30 degree tilt is a good match to PG&E's peak demand period, with a distribution close to global tracking and better than direct normal. In addition, the gain in energy in summer months (when it is most needed and valuable to the utility) is greater for a 30 degree tilt 60 degrees west-of-south orientation than for a 30 degree tilt with due south orientation.

The capacity factor of a photovoltaic system computed on an annual basis is not a very good indicator of the match to the system load, especially in the case of summer-peaking utilities. A better indicator can be estimated by calculating the capacity factor of the PV system during the periods when the load is within 90% of the daily system peak and considering only weekdays. Such a calculation for the 1MW Lugo plant connected to the Southern California Edison (SCE) grid in California gives a value of 72% during the months of May and June, considering only the weekday time periods between 11 am and 5:30 pm.

The experience of California utilities, SCE and PG&E, which have MW-size PV systems on their grids has been very good and it has increased the confidence that PV could be a viable generation option for utilities in the southwestern part of the United States in the next

decade. These plants have essentially zero operation and maintenance costs, are operated largely unattended, and generate significant amounts of electrical energy, close to the predicted values. The absence of surprises bodes well for the future of central-station PV systems as a source of utility-scale bulk electric power generation. The performance of existing central-station PV projects in California and related issues were discussed earlier in section 1.1.

Ongoing activity in windpower indicates its feasibility in parts of the world endowed with good wind regimes. The results of several major research efforts to evaluate the value of wind energy conversion systems to about 14 electric utilities indicate that the WECS breakeven cost value is highly dependent on several factors wind resource, utility generation mix, assumed WECS penetration, and time of WECS installation [64].

Operation of MW-size windfarms in California, with SCE and PG&E in particular, has been a very positive experience and it has increased the confidence that wind could also be a good alternative source of electric power generation for utilities in the United States. However, many of the utility concerns discussed in the context of photovoltaics are applicable for wind electric systems also. Important examples of such concerns include the ramp rates required of conventional generators, effect on reliability, capacity credit, impact on system stability in the case of sudden large variations in their output power, reactive power consumption in the case of induction generators, safety, islanding, and a host of economic concerns.

2.3 Barriers to Load Modeling and Load Forecasting

The technologies and their attributes that create the highest potential for causing load modeling and load forecasting difficulties have been presented in detail in the previous sections. Table 2.1 categorizes the new technologies based on the relative levels of anticipated carriers.

Fusion, MHD, geothermal, fuel cells, solar power satellite systems (SPSS), and ocean thermal energy conversion (OTEC), rely on traditional fuels or energy sources which are renewable on long time-scales or available at all times and therefore do not show any serious short-term variations. Large centralized plants are required for these technologies and they are expected to be utility owned, and dispatched. These technologies are similar to conventional generation from the view points of load modeling and forecasting.

Other technologies such as compressed air storage and underground pumped storage operate like pumped hydro systems. Storage has been studied for many years and presents no new load modeling and forecasting barriers.

One new technology, customer thermal energy storage, affects loads by shifting thermal and electrical demands in time. It is not intermittent, does not generate any power and can only be influenced by rates or connection agreements.

Small-scale hydro and biomass conversion systems depend upon resources that are renewed seasonally and therefore are similar to the hydro-electric technology which is widely used and well-integrated into many electric utilities. The main difference is in the ownership and in

the scale of units. Cogeneration systems using fossil fuels also come under small-scale non-intermittent privately-owned technologies.

The last category of alternative energy technologies depend on short time scale renewable resources such as wind and solar. They violate almost all the assumptions made in traditional models. Power output is not consistently available because it is dependent on meteorological factors, it is hard to control power quality, output and demand are weather dependent and so are both correlated to some extent, and they can be built in small units co-located with the load. Finally, they can be installed by customers as well as by utilities. Customer-owned intermittent small-scale devices can satisfy local load as well as producing power for the utility. Such generation systems present the highest barriers for load modeling and load forecasting. This dissertation focuses on these technologies in the context of short term load forecasting.

TABLE I
CATEGORIZATION OF NEW TECHNOLOGIES

No Load Modeling Barriers

MHD

Fusion

Fuel Cell

Ocean thermal energy conversion

Geothermal

Solar Power Satellite

Low Load Modeling Barriers

Battery

Compressed air

Underground pumped storage

Small-scale and run-of-river hydro

Biomass

Cogeneration

High Load Modeling Barriers

Wind

Photovoltaic

Solar thermal power

Solar heating and cooling

Customer thermal storage

Source Kuliasha, M A and Reddock, T W Editors "Research Needs for the Effective Integration of New Technologies into the Electric Utility," Oak Ridge National Laboratory, Report No CONF-820772, July 1982

CHAPTER III

MODELING THE OUTPUT OF AN ALTERNATIVE ELECTRIC POWER GENERATION SYSTEM

3.1 INTRODUCTION

Over the past decade, many researchers have contributed to the analysis of the effects of penetration of new electric power generation technologies (PV and WECS) into electric utilities and to the development of models in the context of performance prediction and forecasting (see reference 29, 37, and 53-60). However, very little work has been done on the use of these results to study the impact of the penetration of new generation technologies on electric load forecasting.

One approach to find a solution to the problem under consideration is to develop a time-series model for each of the significant variables involved and use them in the forecasting process. Therefore, the necessity of deriving an algorithm to calculate PV system output under variable insolation, temperature and wind speed conditions in the form of time series is the first step in the study of load forecasting in the presence of PV. Similar statements apply when wind electric systems are present either alone or alongside of PV.

The next section develops an algorithm, called "PVTSALGO", for the output of a PV system in a time series form. This is followed by the development of a time series for the output of a wind electric system from known wind speed and performance characteristics. These series are

used in the next chapter to forecast the load on the electric utility under study in the presence of these new electric power generation technologies.

3.2 Time Series Model for the Output of a Photovoltaic System

In this research, central-station PV systems connected to an electric utility grid via power trackers and power conditioners without any intermediate energy storage and reconversion are considered.

In contrast to conventional generation systems in which the input depends on the output, the input to a PV system is fixed by external factors such as cloud cover, location, time of day, etc. Consequently, to minimize generation cost, PV systems are operated at or near their maximum power output as far as possible.

The typical current-voltage characteristic of a solar cell/module is shown in Figure 1 and the corresponding equivalent circuit is shown in Figure 2. Under the idealization assumptions, (i) negligible series resistance, $R_s = 0$ and (ii) very large shunt resistance, $R_{sh} \approx \infty$, the equivalent circuit can be simplified to the one shown in Figure 3 [65] and this is considered to be adequate for load forecasting because of the penetration levels expected and also because of the very nature of the forecasting process and the way in which the results will be used by utility planners.

When a constant resistance load is connected across the output terminals of a PV system, the corresponding operating point is given by the intersection of the I-V curve and the constant resistance line as shown in Figure 1. As the load resistance changes, the operating point

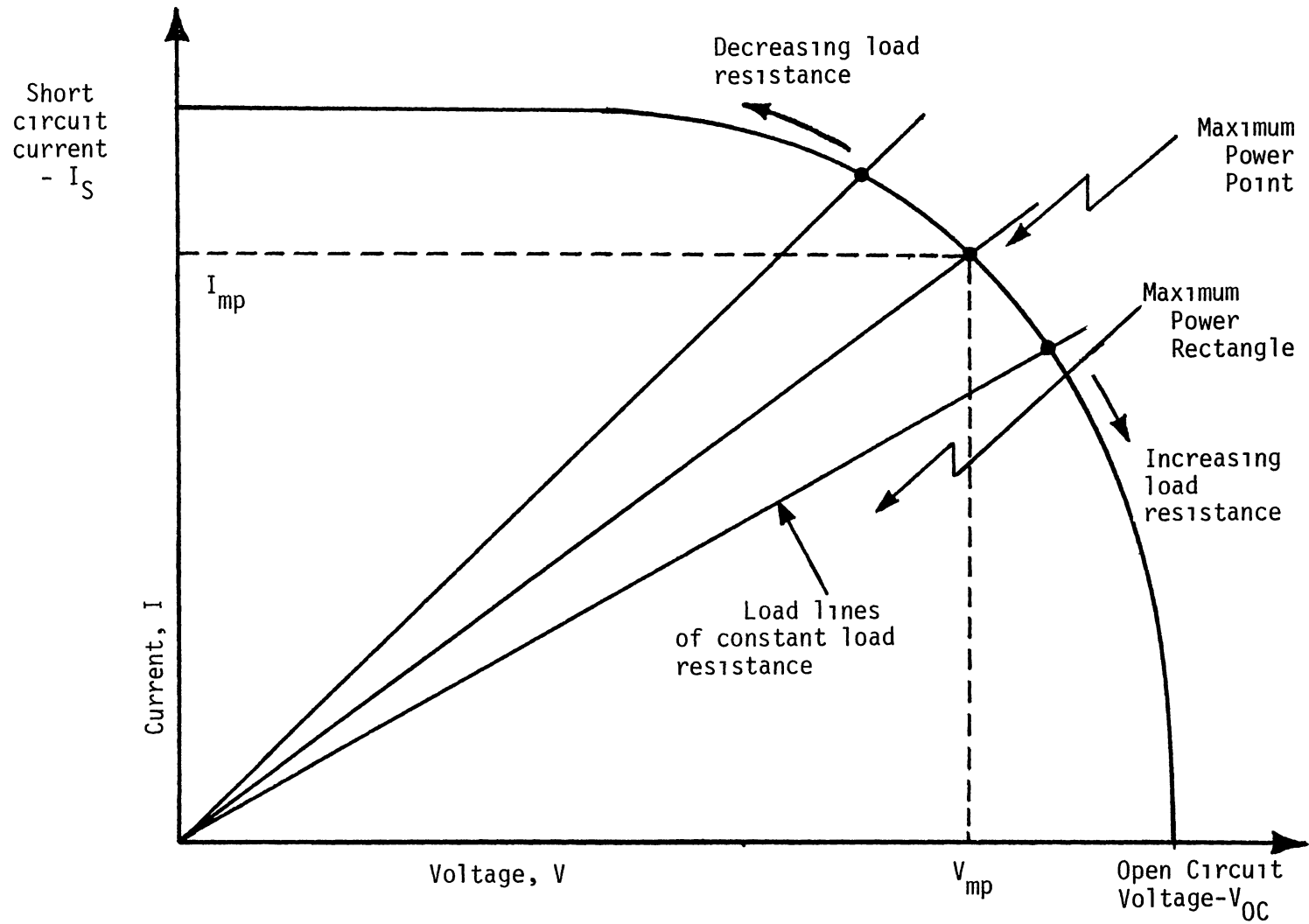


Figure 1 Typical current-voltage characteristic for a solar cell/module

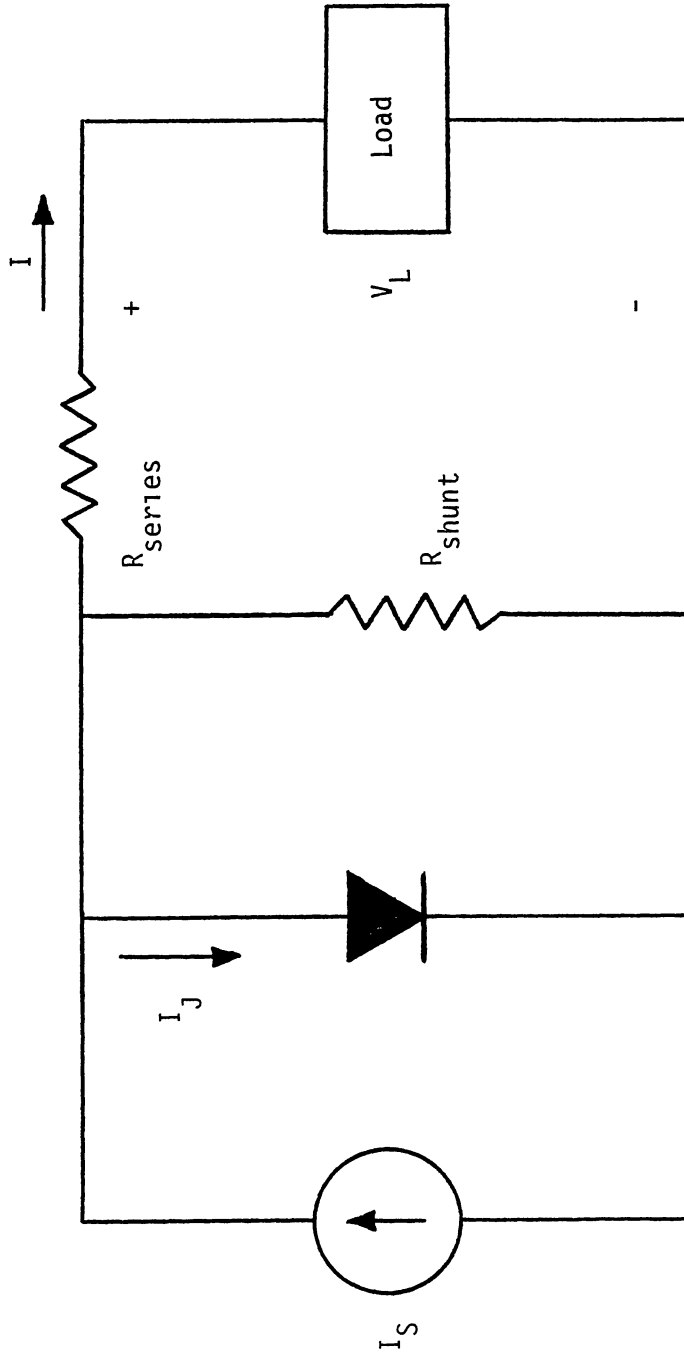


Figure 2 Equivalent circuit for a PV cell/module

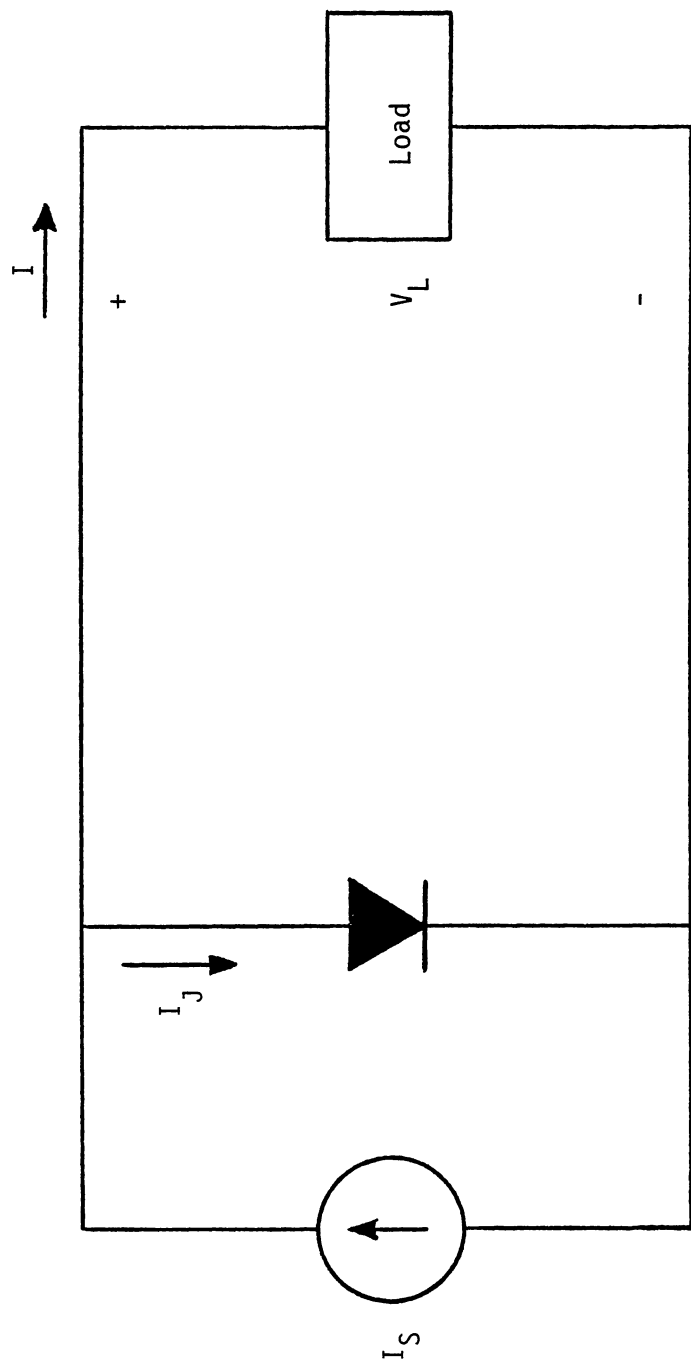


Figure 3 Simplified equivalent circuit for a PV cell/module

moves along the curve (right or left depending on whether the load resistance increases or decreases).

It is desirable to make the operating point always coincide with the maximum power point, which is not difficult in a static world. However, problems arise due to the insolation varying at different times during a day. The operating and maximum power points may be aligned at noon, but will be separated in the morning and late afternoon. The load may be adjusted to optimize the power output of the PV system at some-time during a day (say, morning), but it could be miserably out of tune at other times unless a maximum power tracker is employed.

In the present case the PV system is feeding power to the utility grid whenever adequate insolation is present. Therefore, it is reasonable to assume that the power conditioner is controlled in such a way as to adjust the output of the PV system to be optimal, in other words the operating point is assumed to coincide with the maximum power point whenever the PV system is operating. Such an operation will also minimize generation cost and tend to make the PV system cost-effective. However, the output power will still be varying and intermittent because of changes in insolation, ambient temperature, and wind speed because of its effect on cooling. Figure 4 shows a simplified block diagram of a utility-interactive PV system employing a power tracker and a power conditioner.

A PV module consists of a number of PV cells which are usually connected in series. All the rules that pertain to one solar cell apply to a module as well, except that a module has a higher voltage rating and a higher power output [66]. Similar statements are applicable to a panel which consists of several modules, an array which consists of

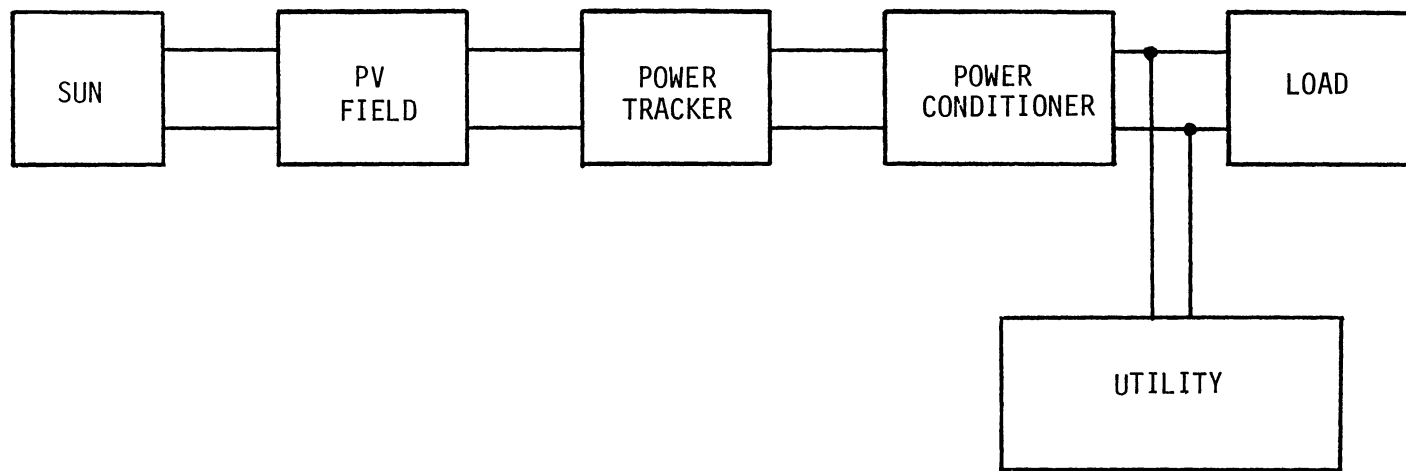


Figure 4 Block Diagram of a utility - interactive photovoltaic system

several panels, a subgroup consisting of many arrays, a group consisting of several subgroups and ultimately to the entire PV system itself.

In this study a typical PV module with 35 cells, each having 81.29 cm^2 area, connected in series is chosen (ARCO, solar M51 40 Watt solar module). This module has the following specifications under standard conditions ($\phi_{e0} = 1000 \text{ W/m}^2$, $T_{C0} = 25 \text{ C}^0 \pm 0.5 \text{ C}^0$ cell temperature)

$$V_{OC0} = 21.0 \text{ volts}$$

$$I_{S0} = 2.6 \text{ amps}$$

$$\eta_{CS} = 10.76\%$$

$$P_{max} = 40.0 \text{ Watts}$$

In order to develop a time series model for a PV system output, insolation, wind speed, and ambient temperature data are required in time series form (hourly data are preferred for this study). In addition, mean values of power tracker and power conditioner efficiencies must be estimated. The power losses in the connections should also be considered. Power tracker and power conditioner efficiencies (η_{pt} , η_{pc}) can be assumed to be approximately constant and they are normally high, typically higher than 90% [67].

The maximum efficiency of a PV cell or module is primarily dependent on the properties of the semiconductor material and cell operating temperature. The cell operating temperature in turn depends on ambient temperature, insolation, and wind speed as it influences cooling. Since the PV system is assumed to be operating at maximum output conditions, the overall efficiency of the PV system can be expressed as follows

$$\eta(\phi_e, T_c) = \eta_{max}(\phi_e, T_c) \cdot \eta_{pt} \cdot \eta_{pc} \quad (3.1)$$

The current-voltage characteristic of an illuminated solar cell or module operating at a temperature T_c °K with source (short-circuit) and reverse-saturation currents of I_s and I_0 respectively, can be expressed as follows [68].

$$I = I_s - I_j = I_s(\phi_e, T_c) + I_0(T_c)[1 - \exp(-\frac{eV}{kT_c})] \quad (3.2)$$

The source current I_s is linearly dependent on insolation and on cell temperature (see reference 67)

$$I_s(\phi_e, T_c) = I_s(\phi_{e0}, T_{c0}) [1 + h_t(T_c - T_{c0})] \frac{\phi_e}{\phi_{e0}} \quad (3.3)$$

The dark current I_0 is strongly dependent on the cell temperature T_c , and can be expressed by the following equation for silicon cells (see reference 65)

$$I_0(T_c) = A T_c^{7/2} \exp(-B/T_c) \quad (3.4)$$

The open circuit voltage corresponds to $I = 0$ and it can be found from (3.2) as

$$V_{OC} = \frac{kT_c}{e} \ln\left(1 + \frac{I_s}{I_0}\right) \quad (3.5)$$

Since a typical value for the ratio $\left(\frac{I_s}{I_0}\right)$ for a silicon cell under standard conditions is in the range of 10^8 to 10^{10} [69], V_{OC} can be approximated as

$$V_{OC} \approx \frac{kT_c}{e} \ln\left(\frac{I_s}{I_0}\right) \quad (3.6)$$

which clearly exhibits the dependence of V_{OC} on cell temperature T_c .

It is convenient to express the characteristics of a solar cell in normalized (per unit) form using I_{s0} and V_{OC0} as base values for current and voltage.

$$I_{pu} = \frac{I}{I_{s0}} \quad (3.7)$$

$$V_{pu} = \frac{V}{V_{OC0}} \quad (3.8)$$

As a result, the per unit (normalized) form of equation (3.2) can be written as follows

$$I_{pu} = \frac{I_s}{I_{s0}} + \frac{I_0}{I_{s0}} \left[1 - \left(1 + \frac{I_s}{I_0} \right)^{\frac{V_{pu}}{z}} \right] \quad (3.9)$$

$$\approx \frac{I_s}{I_{s0}} + \frac{I_0}{I_{s0}} \left[1 - \left(\frac{I_s}{I_0} \right)^{\frac{V_{pu}}{z}} \right] \text{ for } \frac{I_s}{I_0} \gg 1 \quad (3.10)$$

In Equations (3.9) and (3.10), z is equal V_{OC}/V_{OC0} . The normalized power output for a PV cell is defined as the ratio of the actual power output to the product ($V_{OC0}I_{s0}$).

$$P_{pu} = \frac{VI}{V_{OC0}I_{s0}} = V_{pu} I_{pu} \quad (3.11)$$

The efficiency of a cell decreases with increasing operating temperature. Since I_s is directly dependent on insolation, at any instant, with a constant input, the efficiency is maximum when the output is maximum.

The per unit output voltage V_{mpu} corresponding to maximum power output conditions can be found by equating the derivative of P_{pu} with respect to V_{pu} to zero.

$$\frac{dP_{pu}}{dV_{pu}} = 0 \quad (3.12)$$

Consequently, V_{mpu} can be found from the following implicit equation by using a trial and error procedure. It should be noted again that the ratio of source current to dark current is assumed to be very large.

$$\left(\frac{I_s}{I_0}\right)^{1 - \frac{V_{mpu}}{z}} = 1 + \frac{1}{z} V_{mpu} \ln\left(\frac{I_s}{I_0}\right) \quad (3.13)$$

The corresponding per unit output current is

$$I_{mpu} = \frac{I_s}{I_{s0}} \times \frac{V_{mpu}}{z} \left(\frac{I_s}{I_0}\right)^{\frac{V_{mpu}}{z} - 1} \ln\left(\frac{I_s}{I_0}\right) \quad (3.14)$$

The maximum power output for each cell or module can be written in the following form

$$P_{max}(\phi_e, T_c) = V_{mpu} I_{mpu} V_{OC0} I_{s0} \quad (3.15)$$

Consequently, the corresponding maximum efficiency is

$$\eta_{max}(\phi_e, T_c) = \frac{P_{max}(\phi_e, T_c)}{\phi_e} \quad (3.16)$$

Finally, the overall efficiency of a PV system including losses in the power tracker and power conditioner can be expressed as follows

$$\eta(\phi_e, T_c) = \eta_{max}(\phi_e, T_c) \times \eta_{pt} \times \eta_{pc} \times n \quad (3.17)$$

The power output of the module including the power losses due to interconnections becomes

$$P_{out}(\phi_e, T_c) = \eta(\phi_e, T_c) \times \phi_e \times \eta_\ell \quad (3.18)$$

The cell operating temperature T_c can be calculated by the following equation for double glazed modules which are cooled down twice as much as the double transparent (PMMA) modules [70].

$$T_c = T_a + \alpha(1 + \beta T_a)(1 - \nu\nu)\phi_e \quad (3.19)$$

This procedure can be summarized and illustrated like what is shown by Figure 5.

The algorithm "PVTSALGO" can now be made ready for use to compute the power output of a PV module for a known set of ϕ , T_a , and wind speed. As an example, Table II lists the calculated values of output power for the selected PV module using New Mexico data (see reference 61) for one day. These values and the corresponding insolation data are shown in Figures 6 and 7 respectively.

3.3 Wind System Output

The electrical output of a wind electric system primarily depends on the wind speed, aerodynamic efficiency of the aeroturbine, efficiency of the electric generator and the efficiency of the interface components.

The present trend is large (Megawatt scale) wind electric system design and development for operation in parallel with existing utility systems is to employ the constant or nearly constant-speed constant-frequency approach (see reference 15). The aeroturbine is operated at a constant speed and its rotary mechanical output is converted to constant-frequency utility-grade electrical output by a synchronous machine. When induction generators are used, the aeroturbines have to slip a little and consequently operate at a nearly constant speed. In

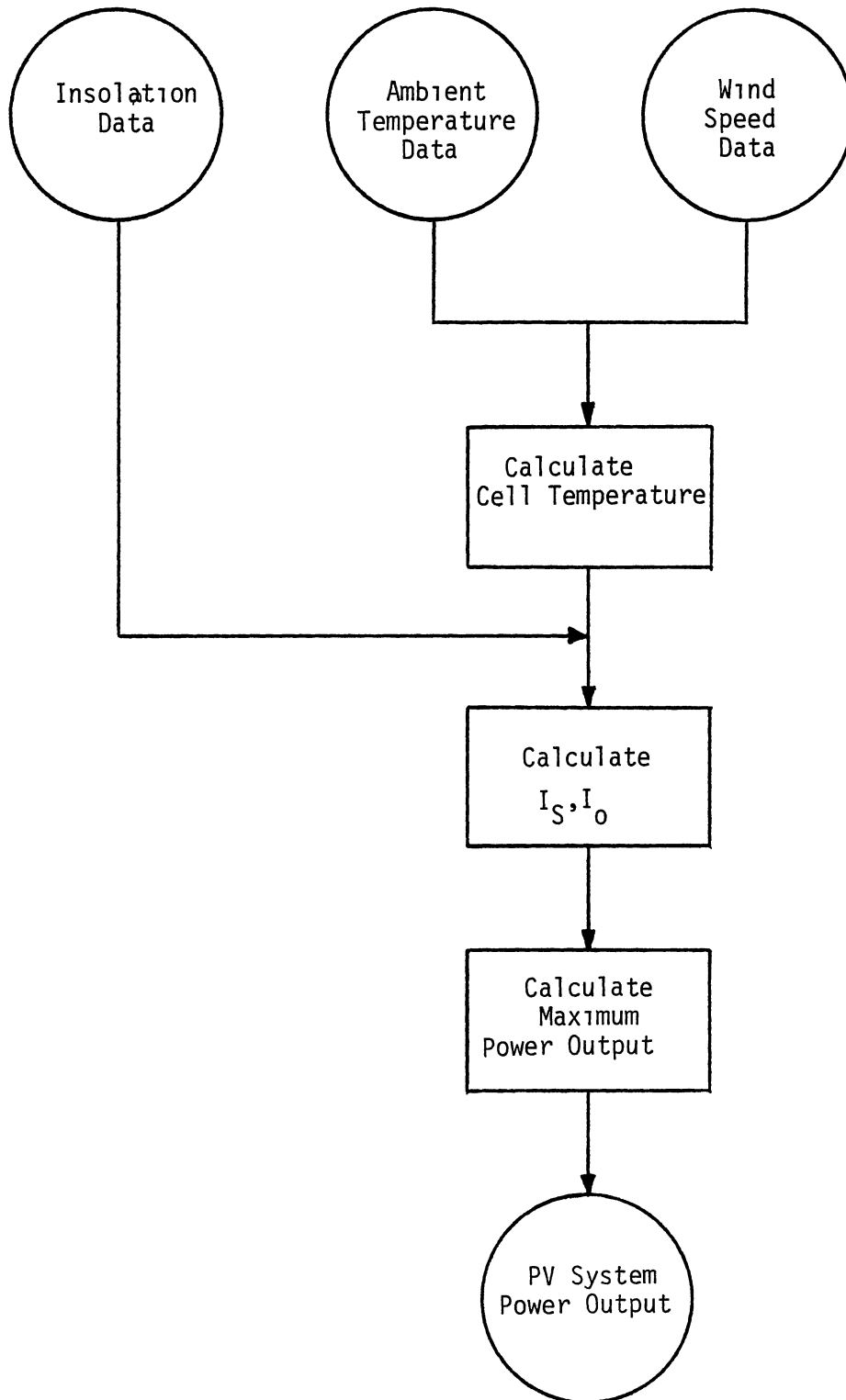


Figure 5 Algorithm "PVTALGO" flowchart

TABLE II
TYPICAL PHOTOVOLTAIC MODULE OUTPUT AT DIFFERENT
TIMES DURING A DAY

No	Year	Month July	Day 1st	Hours	Input		Ambient Temp. (°K)	Cell Temp.		Wind speed m/s	Output W
					KJ/ 2 m	W/ 2 m		°K	°C		
1	52	7	1	6 am	1314	365	290.8	298.6	17.8	1.5	14.0
2				7	2288	635.5	292.4	306.6	19.4	1.5	24.5
3				8	3015	837.5	295.2	314.7	22.2	1.5	31.7
4				9	3293	914.7	298.0	320.4	25.0	2.1	34.1
5				10	3439	955.3	299.1	322.9	26.1	3.1	35.4
6				11	3505	973.6	300.8	325.8	27.8	4.1	35.8
7				12	3535	981.9	302.4	328.3	29.4	5.1	35.8
8				1 pm	3583	995.3	304.7	331.9	31.7	2.1	35.8
9				2	3561	989.2	306.3	334.0	33.3	2.1	35.3
10				3	3490	969.4	306.9	334.3	33.9	2.1	34.6
11				4	3389	941.4	308.0	335.1	35.0	2.1	33.4
12				5	3011	836.4	308.6	332.9	35.6	3.1	29.7
13				6	1638	455.0	305.8	318.5	32.8	7.2	16.5
14				7	719	200.0	303.0	308.3	30.0	5.1	7.19

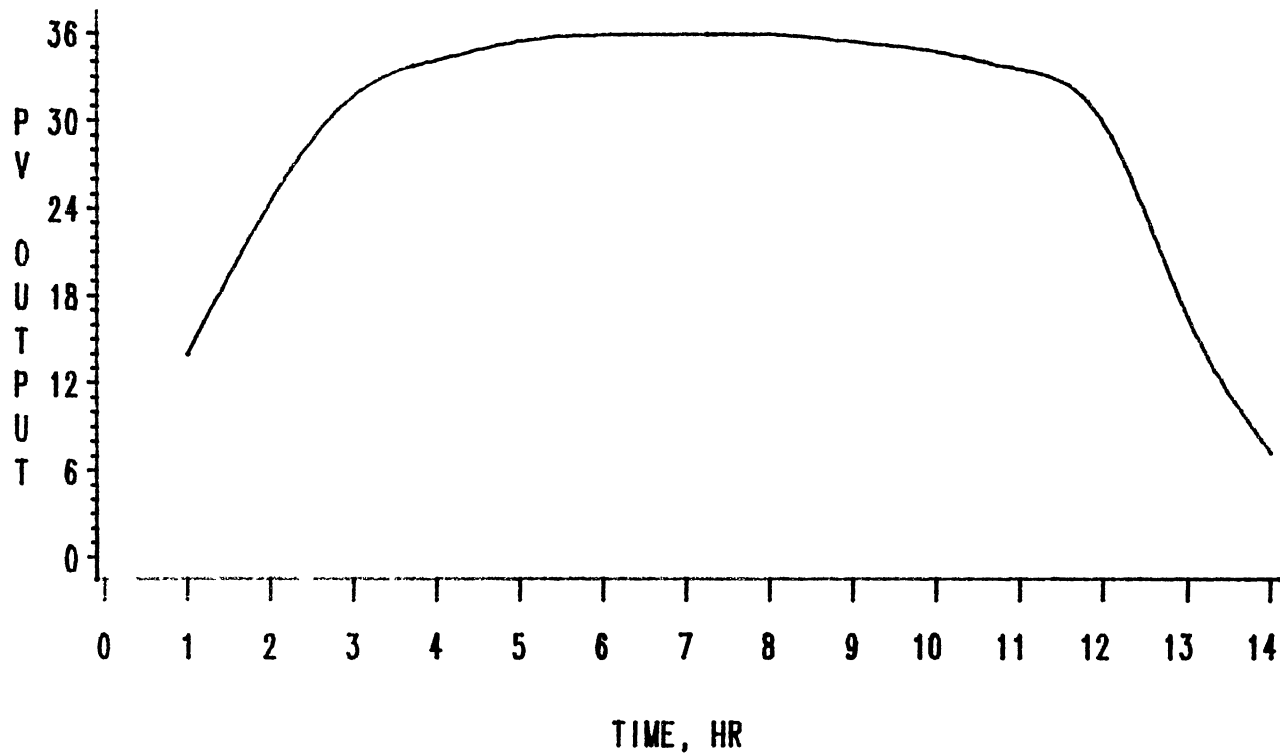


Figure 6 Typical PV module output (W) at different times during a day
(6 am - 7 pm)

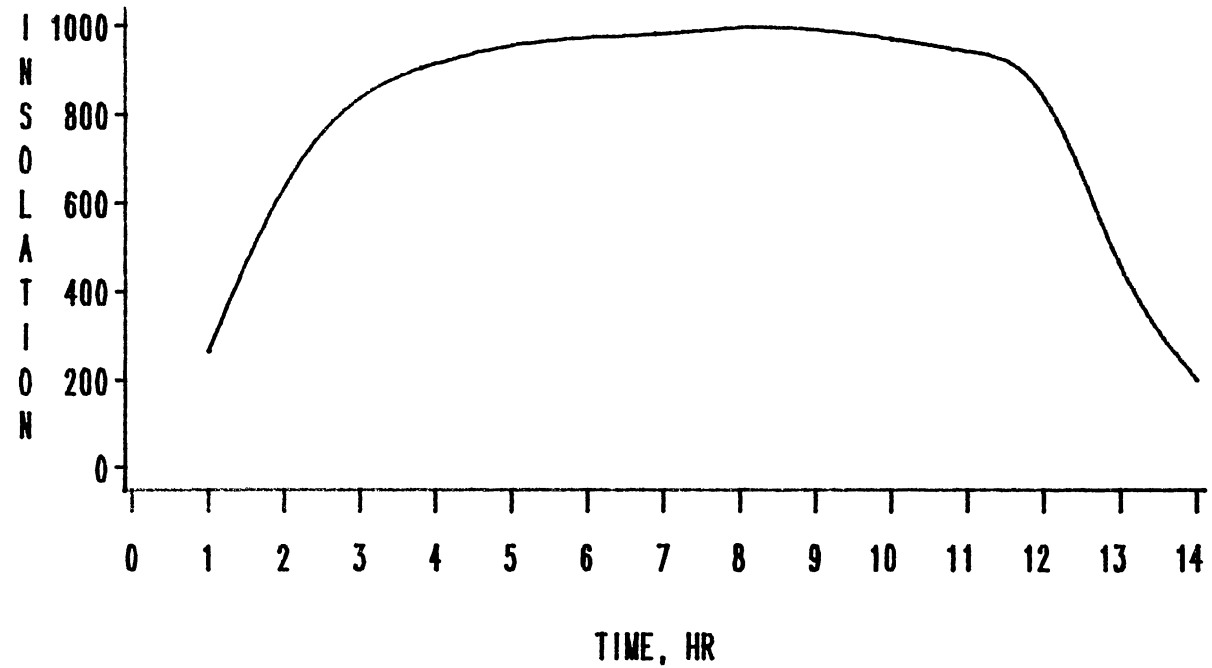


Figure 7 Typical insolation data (W/m^2) at different times during a day (6 am - 7 pm)

either case, the electrical power output starts at a wind speed which is called the cut-in speed and reaches the rated value at a wind speed which is called the rated speed. The electrical output remains constant at the rated value for further increases in wind speed (by appropriate blade pitch control) up to the cutout (furling) speed, beyond which the system is shut down because of safety reasons. Therefore, power output is zero for $v \leq v_{\text{cutin}}$ and $v \geq v_{\text{cutoff}}$. The power output characteristic of a typical large wind electric system is shown in Figure 8. As an example, for the NASA 2.5 MW MOD-2 unit, the cut-in speed is (3.8 m/sec), the rated speed is (9.8 m/sec), and the cut-out (furling) speed is (12.2 m/sec). The electrical output characteristics of the MOD-2 can be approximated by the following relations [71]

$$P(v) = \left. \begin{array}{l} 0, \quad v < v_c \\ -0.09048 - 0.17446v + 0.0515v^2, \quad v_c < v < v_R \\ P_R, \quad v_R < v < v_F \\ 0, \quad v > v_F \end{array} \right\} \quad (3.20)$$

The DOE/NASA-Lewis 100 kW MOD-0 system had a cut-in speed of (10 m/h), rated speed of (18 m/h), and a cut-out speed of (40 m/h). For the 2 MW MOD-1 design (by NASA-LeRC), the cut-in speed was (11 m/h), the rated speed was (25 m/h), and the furling speed was (35 m/h) [15].

The mean hourly wind speeds can be easily converted to corresponding power outputs by employing the power output characteristic of the wind electric conversion system. As an example, Table III lists the values of output power for the MOD-2 unit using New Mexico wind data

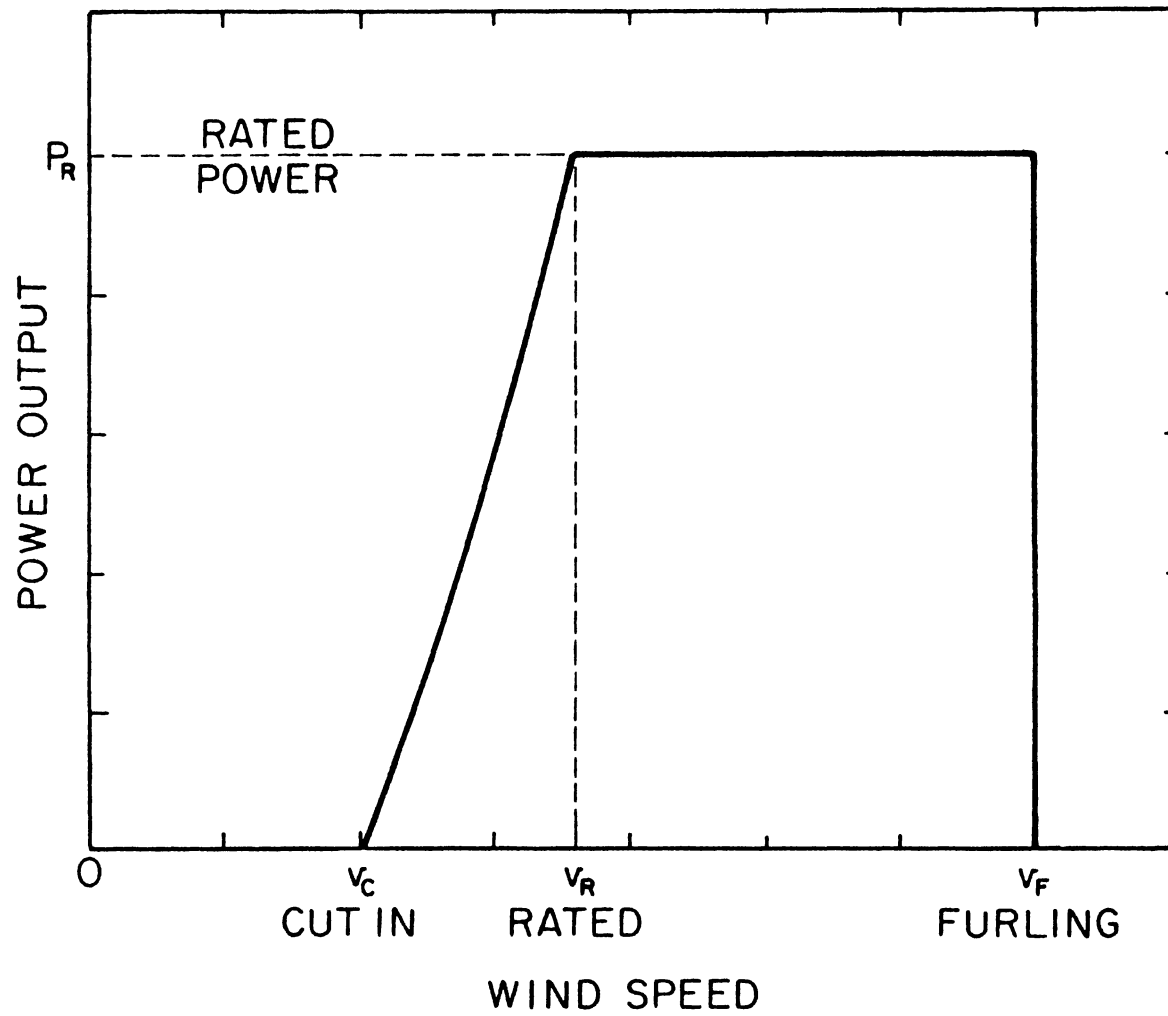


Figure 8 Typical Electrical Output Characteristics of a Large WECS

TABLE III
 TYPICAL WECS OUTPUT AT DIFFERENT
 TIMES DURING A DAY

No	Year	Month July	Day 1st	Hours	Wind speed m/s	Output kW
1	52	7	1	6 am	1.5	0.0
2				7	1.5	0.0
3				8	1.5	0.0
4				9	2.1	0.0
5				10	3.1	0.0
6				11	4.1	100.0
7				12	5.1	400.0
8				1 pm	2.1	0.0
9				2	2.1	0.0
10				3	2.1	0.0
11				4	2.1	0.0
12				5	3.1	0.0
13				6	7.2	1400.0
14				7	5.1	400.0

(see reference 61) for one day. These values and the corresponding wind data are shown in Figure 9.

Because of the combined effects of aeroturbine coefficient of performance versus tip speed ratio and generator efficiency versus power output, the relationship between the electrical output and the wind speed is slightly non-linear for wind speeds between cut-in and rated values. However, in the development of time series models for use in load forecasting, this portion of the characteristic can be assumed to be linear with very little impact on the final outcome.

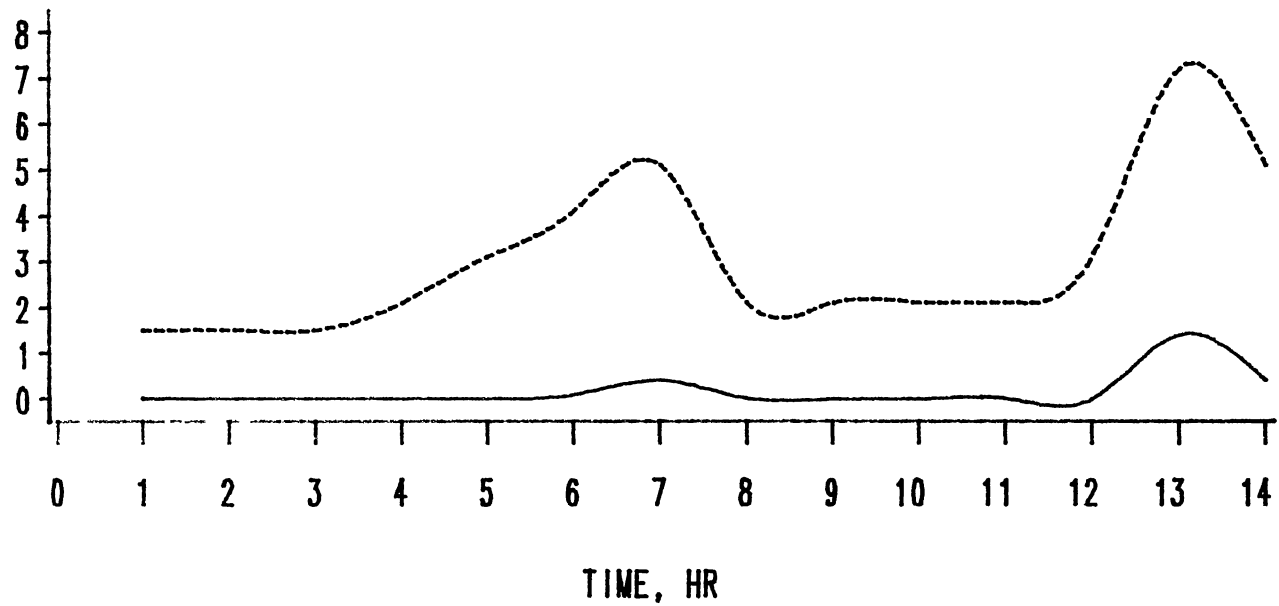
3.4 DISCUSSION

Table II and Figure 7 show that the algorithm PVTALGO works well and can be used to calculate the power output of (MW-scale) PV system. The output and efficiency of a PV system strongly depend on cell operating temperature and insolation. The fact is revealed in the data listed in Table II and plotted in Figure 7. For instance, from 11 am through 1 pm, the PV output remains the same (35.8 W) and then it starts to decrease as the cell temperature increases during afternoon hours.

Moreover, these calculations indicate the wind speed has less effect on cell temperature and therefore on the PV output.

Table III and Figure 9 indicate the wide variations that can be expected in the output of wind electric system on an hour-by-hour basis. Such variations are one of the reasons for the concerns of electric utilities. In short, the output of PV and wind electric systems are not "dispatchable" in the conventional sense.

The algorithm developed for PV and the simple procedure used to convert wind speeds into power outputs of wind electric systems enable



LEGEND - - - - - WIND SPEED ——— WIND SYST.OUTPUT

Figure 9 Typical WECS (MOD-2) output (MW) and the corresponding wind data (m/sec) at different times during a day (6 am - 7 pm)

one to obtain the hourly outputs of new generation technologies in terms of the resource variables. These are used in the next chapter to develop the time series models further and to employ them in load forecasting.

CHAPTER IV

DEVELOPMENT OF MODELS AND LOAD FORECASTING IN THE PRESENCE OF NEW GENERATION TECHNOLOGIES

4.1 INTRODUCTION

Electrical load forecasting of conventional generation systems has been under investigation for many years. Excellent papers have been published on forecasting the load on a conventional generation system. With the projected entry of large scale PV and WECS in the decades to come and their operation in parallel with existing utility grids, load forecasting in the presence of these new electric power generation technologies assumes importance.

The first and the most important aspect of forecasting is obtaining a proper mathematical model which is simple enough to work with, yet realistic and applicable to real-life situations.

The basic characteristics of solar and wind resources suggest the use of short-term (hourly or daily) load forecasting approach to consider the presence of new generation technologies-photovoltaics and wind in particular. Furthermore, because of the weather dependencies of the outputs of new generation sources (PV and wind electric systems) and the electrical loads, time series methods offer the best opportunity for developing models suitable to forecast the future demand.

Data concerning new (alternative) energy resources, say for example insolation and wind, usually take the form of consecutive hourly or

daily average values of the available resource. They are also typically highly correlated (dependent).

The Box and Jenkins methodology has been finding increasing applications in electrical load forecasting studies (see references 35-39, 43-46). Interest in the Box-Jenkins process arises from the fact that it models real life situations fairly accurately and the mathematical formulation is well developed and relatively simple. Furthermore, it is able to handle dependent data, and is the most promising approach over the other time series analysis methodologies [72] to handle the problem under study. Based on this methodology, models are developed to forecast "net" demand. The development of the models is a step-by-step procedure as mentioned earlier in section 1.6, and it is again introduced in different subsections of this chapter.

4.2 Univariate Time Series Analyses

Univariate time series properties are used in this section to derive proper stochastic models for the data used in this study and ultimately, to forecast the "net" demand on the utility under study. The procedures and the properties of each set of data under study in the form of time series are discussed step-by-step in this section.

As in many applications, the data which are analyzed and modeled in this study are dependent data. Box-Jenkins methodology can be used to handle this in time domain by building stochastic models in the form of discrete time series which can be used for obtaining forecasts of future values of the time series.

The models employed are based on the idea that a time series with highly dependent successive values can be generated from a sequence of

independent random disturbances, from a fixed distribution, usually assumed normal with zero mean and variance σ_u^2 , when white noise is considered. Consequently, a time series can be represented in the form of stochastic discrete linear processes of the form given below [73].

$$\begin{aligned} Z_t &= \mu + \psi_0 u_t + \psi_1 u_{t-1} + \psi_2 u_{t-2} + \dots + \psi_1 u_{t-1} \\ &= \mu + \psi(B) u_t \end{aligned} \quad (4-1)$$

where μ = a parameter which determines the "level" of time series $\psi(B)$ = the linear operator or the transfer function of the filter, which transforms u_t into Z_t . B = back shift operator ($B^m Z_t = Z_{t-m}$, $m = 1, 2, \dots$)

The process Z_t is said to be stationary (remains in equilibrium about a constant mean level) if the sequence ψ_1, ψ_2, \dots is finite, or infinite and convergent. The parameter μ is then the expected value (mean) of $Z_t = E(Z_t)$, about which the process varies. Otherwise, time series Z_t is non-stationary and μ does not have any specific meaning except as a reference point for the level of the time series.

The methodology employed uses low-dimensional or parsimonious models to describe time series behavior in terms of p past values (autoregressive or AR(p) models), a series q weighted "shocks" (moving average of MA(q) models), or a combined model which is called autoregressive moving average -- ARMA (p, q)

If the data which are non-stationary in real life are transformed through differencing to remove trend or seasonal effects (periodicity of the data), the model is then called autoregressive integrated moving average -- ARIMA (p, d, D, q). This model represents a wider class than the other non-stationary processes such as exponentially weighted moving

average, and it provides a family of models to adequately represent many of the time series encountered in practice [46].

Stationarity or homogeneity may also be achieved by taking a natural logarithm of the raw data. Sometimes exponential transformation is helpful also in developing models.

The development of the methodology is based on three steps or stages which can be summarized as follows:

1. Identification of the nature of the time series, its components, and the order of the components.
2. Estimation of the model parameters to completely describe Z_t .
3. Diagnostic checking of the model to detect inadequacy, to suggest proper modifications and thus, where necessary, to initiate a subsequent iterative cycle of identification, estimation and diagnostic checking. The acceptable model is then used in the forecasting process.

Autocorrelation and partial autocorrelation are two powerful statistical functions which are used as guides in the identification stage.

The unknown parameters of an identified tentative model should be estimated in such a way as to get a minimum error. To achieve such a minimum error, the use of non-linear least squares regression has been suggested [73].

Checking the adequacy of a tentative model involves examining the sample auto- and partial- autocorrelations of the residual series, a_t . The a_t s will be independently and randomly distributed close to zero for an adequate model. Moreover, auto- and partial- autocorrelation of the residuals are good guides for improving inadequate models as well as acceptable models. Chi-square test can also be used to evaluate if the

residual sample autocorrelation functions are distributed randomly. Further information on this topic is available in References (45,46,72,73).

4 2 1 Net Demand Forecasting in the Presence of PV (Approach A)

As mentioned in the previous chapter, central-station PV systems connected to an electric utility grid are considered in this research.

The latest readily available detailed insolation data for the Southwest region of the United States was for the year 1975. Consequently, all data which are used in the calculations are 1975 data in general, and for the month of June 1975 in particular.

The total capacity of the utility under study was 2244 MW in 1975. For the purposes of this study, a 5% penetration of PV is assumed. Meeting this level of penetration from PV systems will require the employment of 10957 two-axis tracking flat-plate and concentrator arrays, each array consisting of 8 panels, with 32 modules in each panel. The particular module used in this study has been discussed earlier and its specifications were introduced in Chapter III.

The major steps involved in this part of the study to forecast "net" demand in the presence of both flat-plate and concentrator systems mentioned earlier in Chapter I are shown in the flowchart of Figure 10.

4 2 1a Two-axis Tracking Flat-plate PV Systems

In this section the steps taken thus far towards the development of stochastic models to fit the selected samples of insolation, ambient temperature, hourly wind speed, and load data are summarized.

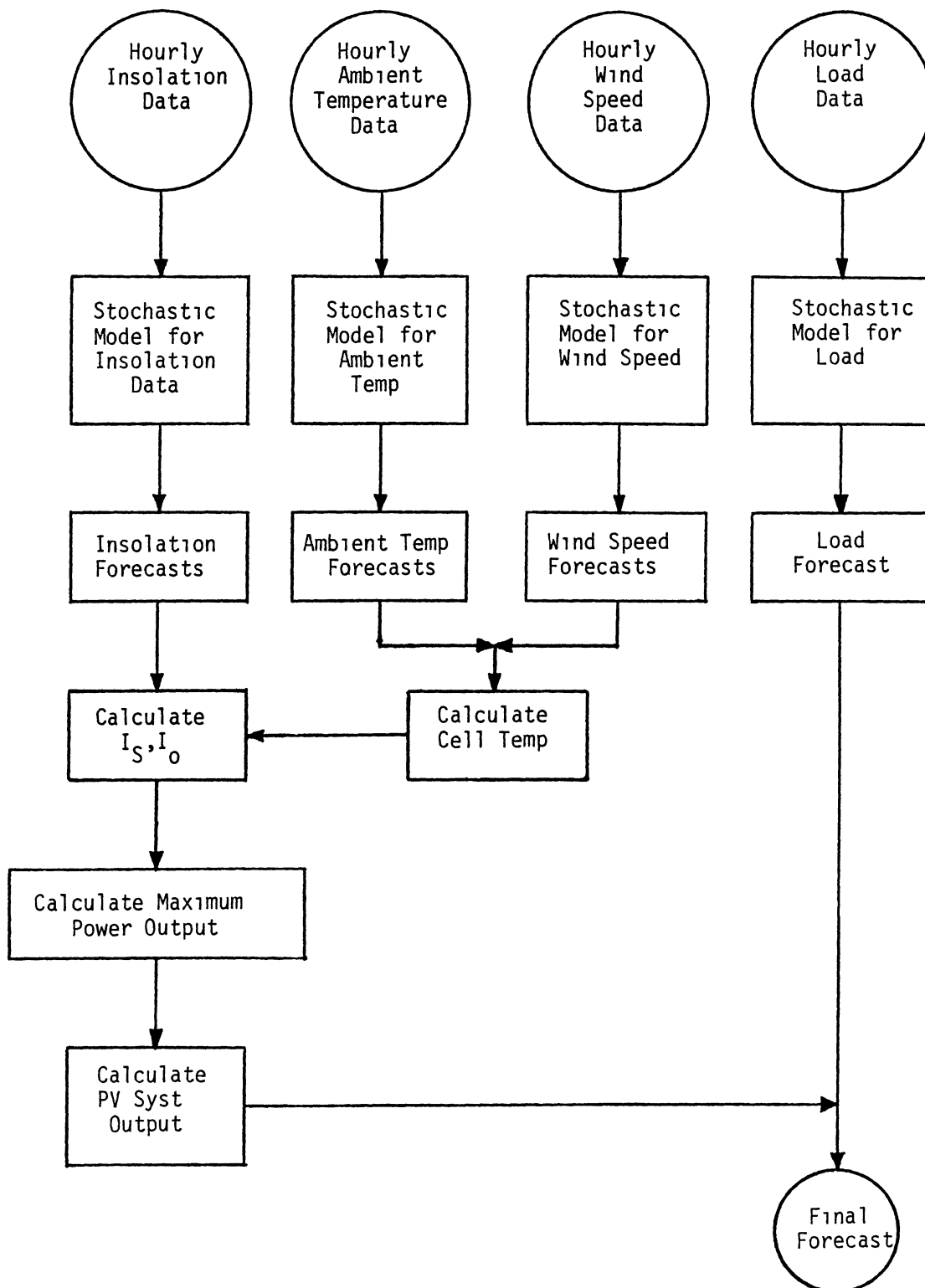


Figure 10 Forecast flowchart (Approach A)

Identification process for the total hourly insolation (direct and diffuse) data with 360 observations was undertaken. Autocorrelation of the data are characterized by a period of 12 and a failure to damp out (see Figure A1 in Appendix A), suggesting that the series is non-stationary, thus indicating the need for periodic differencing (seasonal differencing in the case of seasonal data). With the help of another differencing (regular differencing), the autocorrelation of differenced series indicate some improvements, but still there are some significant patterns (periodic non-stationary) at some lags, for example at 1 and 12 (see Figure A2). After testing several models, the following, which satisfies all the statistical tests, was selected.

$$(1 - \phi_1 B^1 - \phi_3 B^3 - \phi_4 B^4) \nabla_1 \nabla_{12} Z_t = (1 - \theta_{12} B^{12}) a_t \quad (4.2)$$

The parameters of the model given above were estimated using an iterative process. The iterative process was terminated when the relative change in the residual sum of squares was less than 1.0×10^{-4} . The estimated parameters with 95% confidence limits are summarized in Table IV.

The residuals (errors) are randomly distributed, and hence the expectation of the errors is zero, $E(e_t) = 0$. The randomness of the residuals can be seen from the residuals' autocorrelation functions which are shown in Figure A3. The calculated $\chi^2 = 42.682$ is less than χ^2 with 56 degrees of freedom and at 5% significance level from table [74]. Therefore, there is no ground for the rejection of this model.

The model (Equation 4.2) was then used to forecast insolation data. The analyses have been aided by the use of computer programs

TABLE IV
SUMMARY OF THE ESTIMATED PARAMETER VALUES
FOR MODEL OF EQUATION 4.2

Parameter type	Estimated value	95% Confidence	
		Lower limit	Upper limit
ϕ_1	-0.18082	-0.30026	-0.061378
ϕ_3	-0.16780	-0.28939	-0.046202
ϕ_4	-0.10588	-0.22988	0.018123
ϕ_{12}	0.75991	0.68120	0.83861

"Identify" and "Estimate" [75], and "Gplot" [76]. The same processes were repeated for hourly ambient temperature data.

Autocorrelation of the ambient temperature data are characterized by a period of 24 and a failure to damp out, suggesting that the series is non-stationary, thus indicating the need for periodic differencing. The autocorrelation of periodic differenced series indicate some improvements, but still there is a significant pattern (periodic non-stationary) at lag 24. After testing several models with the help of auto- and partial autocorrelation, the following model, which satisfies all the statistical tests, was arrived at.

$$(1 - \phi_3 B^3 - \phi_{24} B^{24} - \phi_{27} B^{27}) \nabla_{24} Z_t = (1 - \theta_{21} B^{21} - \theta_{24} B^{24} - \theta_{66} B^{66}) a_t \quad (4.3)$$

The parameters of the model were estimated by the same method which was used earlier in the case of insolation data. Table V lists the estimated parameters with the associated 95% confidence limits.

Autocorrelations of the residuals show that the residuals are randomly distributed (see Figure A4). The calculated $\chi^2 = 18.432$ is less than χ^2 with 66 degrees of freedom and at 5% significance level from table and once again there is no indication for further improvement.

The model (Equation 4.3) was then used to forecast ambient temperature data.

Identification process for the hourly wind speed data with 312 observations was undertaken. Autocorrelations and partial autocorrelations are characterized in such a way that the data can be modeled without using any kind of differencing transformations. After examining many models, including differenced data, the following model was selected.

TABLE V
 SUMMARY OF THE ESTIMATED PARAMETER VALUES
 FOR THE MODEL OF EQUATION 4.3

Parameter type	Estimated value	95% Confidence limits	
		Lower	Upper
ϕ_3	0.71598	0.63555	0.79640
ϕ_{24}	-0.12115	-0.23571	-0.0066028
ϕ_{27}	0.16679	0.064963	0.26862
θ_{21}	-0.16931	-0.25335	-0.085276
θ_{24}	0.71735	0.61326	0.82145
θ_{66}	-0.088916	-0.18389	0.0060555

$$(1-\phi_1 B^1) (Z-\mu) = (1-\theta_{24} B^{24}) a_t \quad (4.4)$$

The parameters of the model were estimated and the values are listed in Table VI.

The model also satisfies all the statistical test -- autocorrelations of the residuals indicate that the residuals are distributed randomly (see Figure A5). Furthermore, the calculated $\chi^2 = 57.869$ is less than χ^2 with 66 degrees of freedom and at 5% significance level from table. This model was then used to forecast wind speed data.

Identification process for the hourly load data with 720 observations was undertaken. Autocorrelations of the data are characterized by a period of 24 and a failure to damp out, suggesting that the series is non-stationary, thus indicating the need for periodic differencing in this case also. The autocorrelations of periodic differenced series damp out. After testing many acceptable models, the following model was selected.

$$(1-\phi_1 B^1 - \phi_2 B^2) \nabla_{24} Z = (1-\theta_2 B^2 - \theta_{13} B^{13} - \theta_{24} B^{24}) a_t \quad (4.5)$$

Table VII lists the estimated values of the parameters.

The residuals of the process are randomly distributed (see autocorrelations of the residuals in Figure A6). The calculated $\chi^2 = 64.984$ is less than χ^2 with 67 degrees of freedom and 5% significance level from table. Therefore, there is no ground to reject the model.

The model (Equation 4.5) was then used to forecast the hourly load data.

At this stage, the PV output was calculated from the forecasted values of insolation, ambient temperature, and wind speed data by using algorithm "PVTSALGO" discussed in Chapter III.

TABLE VI
SUMMARY OF THE ESTIMATED PARAMETER VALUES
MODEL OF EQUATION 4.4

Parameter type	Estimated value	95% Confidence	
		Lower limit	Upper limit
μ	3.6677	3.0493	4.2860
ϕ_1	0.65681	0.57094	0.74267
θ_{24}	-0.18195	-0.29915	-0.064755

TABLE VII
 SUMMARY OF THE ESTIMATED PARAMETER VALUES
 FOR MODEL OF EQUATION 4.5

Parameter type	Estimated value	95% Confidence	
		Lower limits	Upper limits
ϕ_1	1.2961	1.1784	1.4137
ϕ_2	-0.33170	-0.44925	-0.21415
θ_2	-0.12340	-0.20440	-0.042393
θ_{13}	-0.086106	-0.16714	-0.0050755
θ_{24}	0.76228	0.68035	0.84421

Finally the net-demand forecast values were calculated by subtracting the PV system output from the forecasted load. The forecast, actual, and 95% confidence intervals values for the last day of June, 1975 are shown graphically in Figure 11. The forecast, and 95% confidence limits for the first day of July 1975 are shown in Figure 12.

The absolute value of the relative error between actual and forecasted values of net demand varies from 0.3% to 18.69% for time periods extending up to 24 hours. As expected, forecasting further and further into the future results in increasing errors.

4.2.1b Two-axis Tracking Concentrator

PV Systems

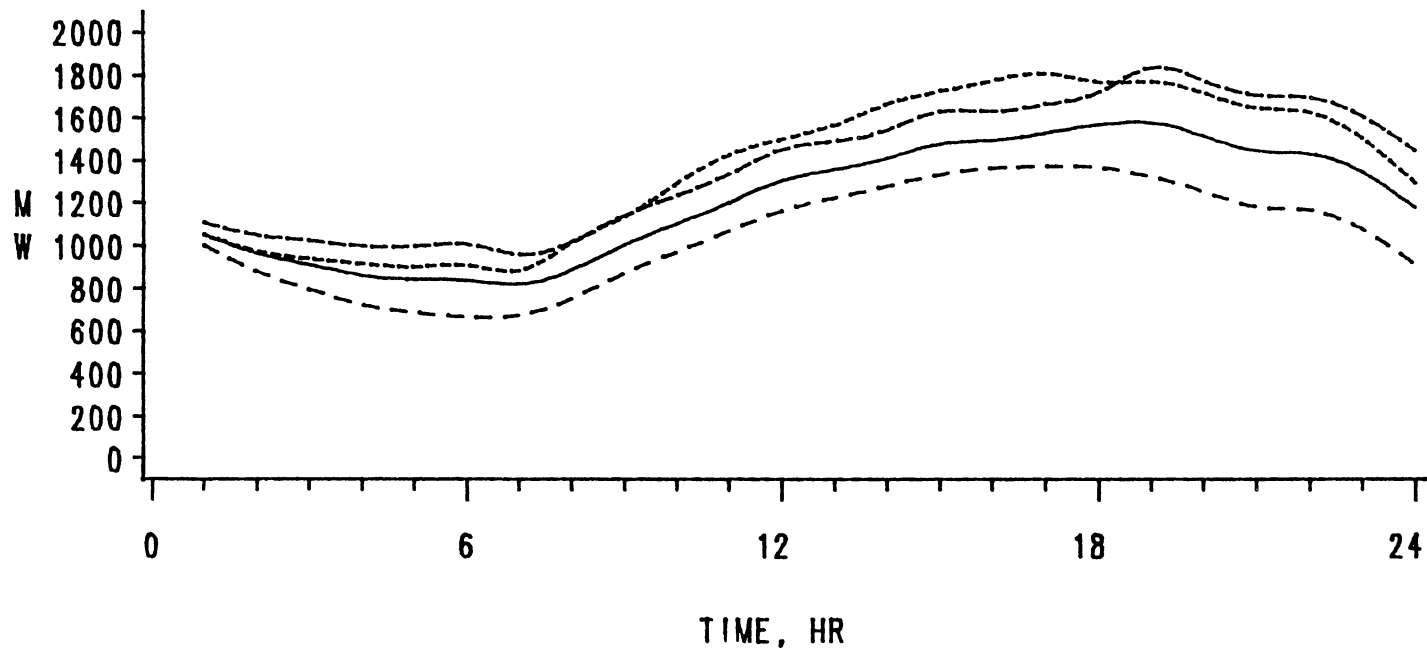
All of the data and developments which were undertaken in the case of flat-plate PV systems are applicable for the concentrator PV systems also, except the insolation data. For concentrator systems, only direct insolation data were used.

Identification, estimation, and diagnostic checking processes for the hourly direct insolation data with 360 observations were undertaken respectively. After testing many alternative models the following model, which satisfies all the statistical tests, was selected.

$$(1 - \phi_1 B^1 - \phi_2 B^2 - \phi_3 B^3 - \phi_4 B^4) \nabla_1 \nabla_{12} Z_t = (1 - \theta_{12} B^{12}) a_t \quad (4.6)$$

Table VIII lists the estimated values of the parameters.

The autocorrelations of the residuals indicate that the residuals of the process are randomly distributed (see Figure A7). Furthermore, the calculated $\chi^2 = 67.859$ is less than χ^2 with 55 degrees of freedom



LEGEND - - - - LOWER - - - - FORECAST
 - - - - UPPER - - - - ACTUAL
 95% Confidence

Figure 11 Forecasts of hourly net demand (MW) in the presence of two-axis tracking flat-plate PV systems with 5% penetration for June 30, 1975 (Approach A)

TABLE VIII
 SUMMARY OF THE ESTIMATED PARAMETER VALUES
 FOR MODEL OF EQUATION 4.6

Parameter type	Estimated value	95% Confidence	
		Lower limits	Upper limits
ϕ_1	-0.25630	-0.36460	-0.14800
ϕ_2	-0.21963	-0.33041	-0.10885
ϕ_3	-0.20767	-0.31848	-0.096858
ϕ_4	-0.15658	-0.26695	-0.046206
θ_{12}	0.80429	0.73766	0.87092

and 5% significance level from table. Consequently, this model could not be rejected, and was used to forecast the insolation (direct) data.

As in the case of flat-plate systems, the PV output was calculated from the forecasted values of direct insolation, ambient temperature, and wind speed data by using the algorithm "PVTSALGO" discussed in Chapter III. The net-demand forecast values were also calculated. Figure 13 illustrates the forecast, actual, and 95% confidence limit values for the last day of June, 1975. In addition, the forecast, and 95% confidence limits for the first day of July 1975 are shown in Figure 14.

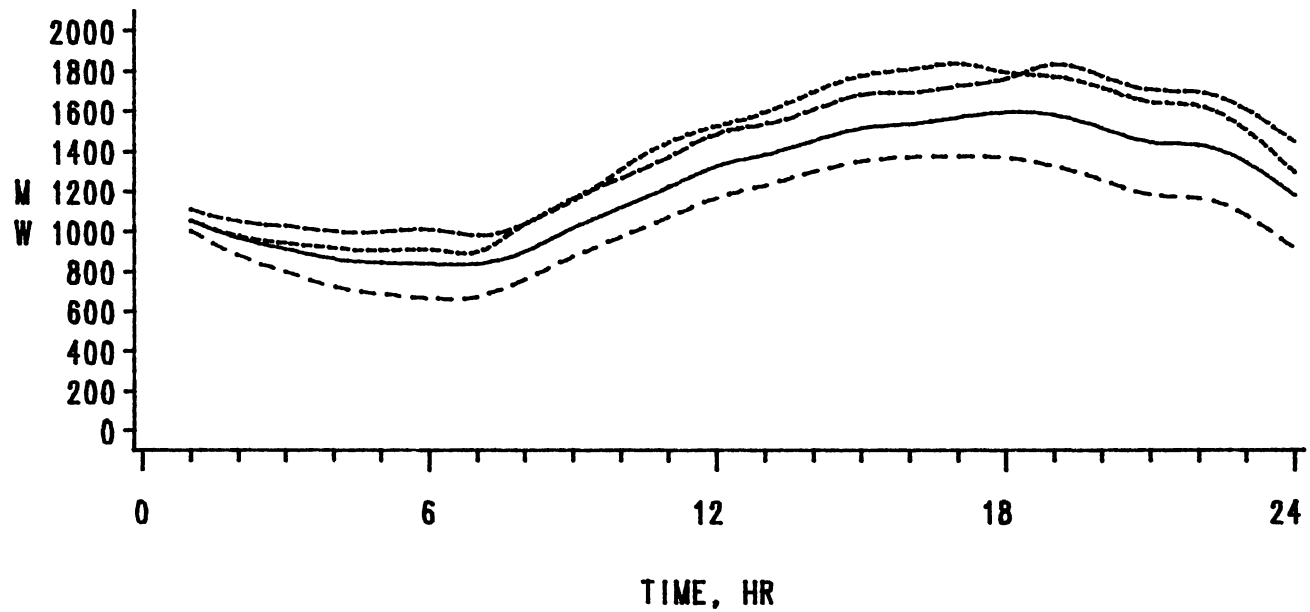
The absolute value of the relative error between actual and forecasted values of net demand varies from 0.3% to 18.15% for time periods extending up to 24 hours.

4.2.2 Net-demand Forecasting in the Presence of PV (Approach B)

The major steps involved in an alternative approach to net-demand forecasting in the presence of PV is shown in Figure 15 for both flat-plate and concentrator systems. In this case a time series model is developed for the PV systems output and it is used in one forecasting step to forecast future values of PV systems output.

4.2.2a Two-axis Tracking Flat-plate PV Systems

The output of the flat-plate PV system is calculated first from raw historical hourly data (total direct and diffuse insolation, ambient temperature, and wind speed) by using "PVTSALGO". Then a model is developed for this time series as before. All the steps for the



LEGEND - - - - LOWER ——— FORECAST
 - · - · - UPPER ····· ACTUAL
 95% Confidence

Figure 13 Forecasts of hourly net demand (MW) in the presence of two-axis tracking concentrator PV systems with 5% penetration for June 30, 1975 (Approach A)

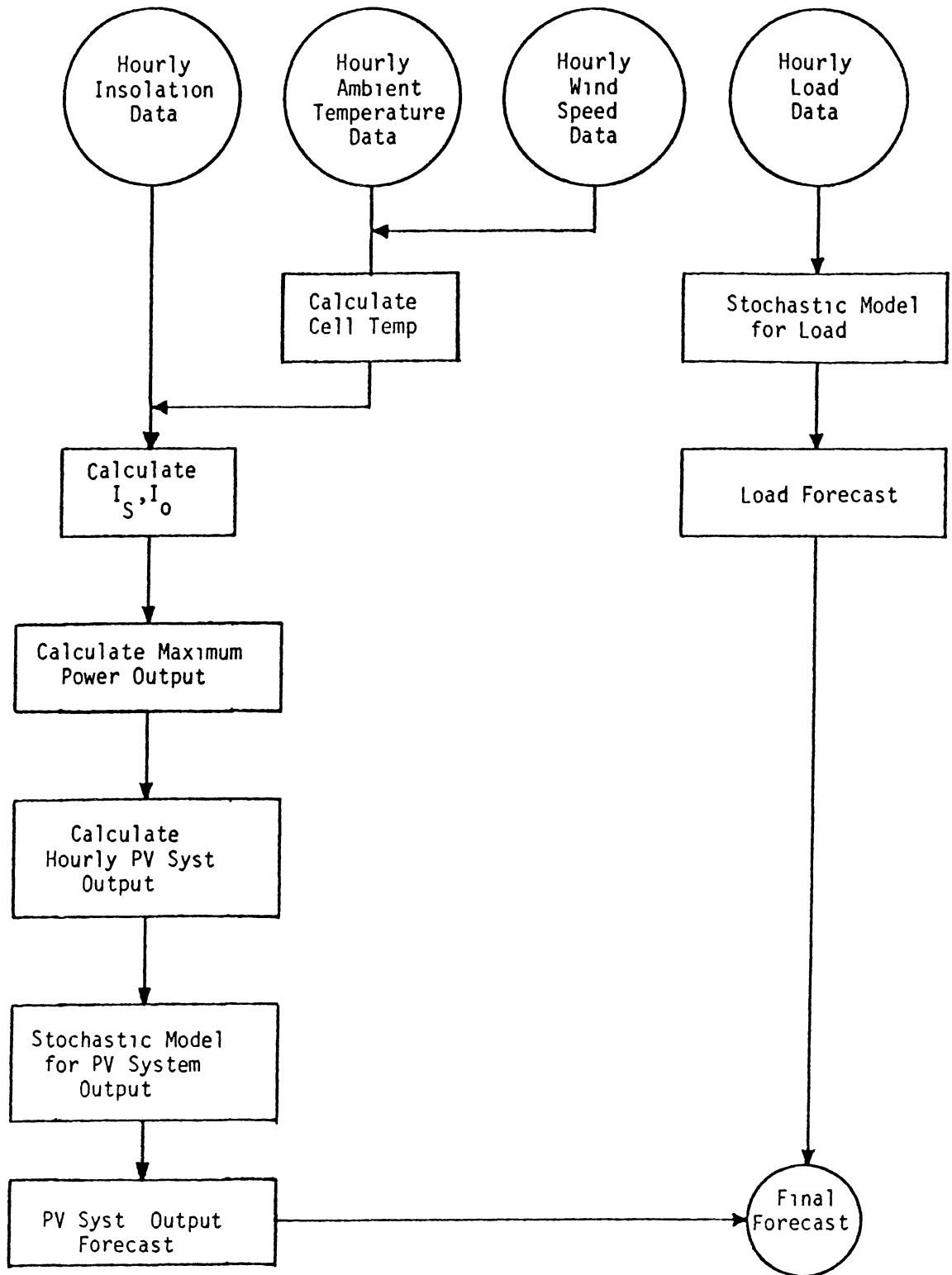


Figure 15 Forecast flowchart (Approach B)

development of a model for the hourly PV output data with 360 observations were undertaken. After testing many alternative models the following model was selected

$$(1-\phi_1 B^1) \nabla_{12} Z_t = (1-\theta_{12} B^{12}) a_t \quad (4.7)$$

Table IX lists the estimated values of the parameters.

All the statistical tests were satisfied by this model. The residuals are randomly distributed as can be seen from the residuals' autocorrelation functions which are shown in Figure A8. The calculated $\chi^2 = 54.134$ is less than χ^2 with 58 degrees of freedom and 5% significance level from table.

The model (Equation 4.7) then was used to forecast the PV output data. The net-demand forecast values were calculated by subtracting the forecasted PV output from the forecasted load data which were calculated earlier in subsection 4.2.1a. Figure 16 shows the net-demand forecast, actual, and 95% confidence limit values for the last day of June, 1975. Moreover, the forecast and 95% confidence limits for the first day of July 1975 are shown in Figure 17.

The absolute value of the relative error between actual and forecasted values of net demand varies from 0.3% to 19.18% for time periods extending up to 24 hours. The results of this method are compared with the results obtained by the previous approach at the end of this chapter.

TABLE IX
SUMMARY OF THE ESTIMATED PARAMETER VALUES
FOR MODEL OF EQUATION 4.7

Parameter type	Estimated value	95% Confidence intervals	
		Lower limit	Upper limit
ϕ_1	0.64489	0.56303	0.72674
ϕ_{12}	0.87028	0.81693	0.92363

4.2.2b Two-axis Tracking Concentrator

PV Systems

The steps which were followed for the case of flat-plate PV system were repeated for concentrator PV systems. Hourly direct insolation data were used in calculation of PV systems outputs. The resulting model for this case is given below.

$$(1-\phi_1 B^1)(1-\phi_{12} B^{12}) \nabla_{12} Z_t = (1-\theta_{24} B^{24}-\theta_{39} B^{39}) a_t \quad (4.8)$$

Parameters of the model were estimated, and listed in Table X.

Figure A9 shows that the residuals are randomly distributed. The calculated $\chi^2 = 58.373$ is less than χ^2 with 56 degrees of freedom and 5% significance level from table.

The PV output forecast values for the present system were calculated by using the model (Equation 4.8).

The forecast values of hourly net-demand were calculated next. The forecast, actual, and 95% confidence limit values for the last day of June, 1975 are shown in Figure 18. Forecast and 95% confidence limit values for the next day (1st day of July 1975) are given in Figure 19.

The absolute values of the relative error between actual and forecasted values of net demand varies from 0.3% to 19.16% for 24 hours.

4.2.3 Models For Net Demand With PV Present

(Approach C)

Since the goal is to forecast the "effective" or "net" demand which is equal to the total demand minus the PV power output, this "net" demand itself can be considered as a time series and used as final data

TABLE X
SUMMARY OF THE ESTIMATED PARAMETER VALUES
FOR MODEL OF EQUATION 4.8

Parameter type	Estimated value	95% Confidence limits	
		Lower	Upper
ϕ_1	0.64566	0.56153	0.72979
ϕ_{12}	-0.71760	-0.79808	-0.63713
θ_{24}	0.64626	0.54576	0.74676
θ_{39}	-0.096008	-0.18773	-0.0042828

to forecast the future "effective" hourly peak demand over the desired period of time. This approach is shown schematically in Figure 20.

4.2.3a Two-axis Tracking Flat-plate PV Systems

Identification process for the hourly net-demand (historical or raw data) with 720 observations was undertaken. Autocorrelations of the data are characterized by a period of 24 and a failure to damp out, suggesting that the series is non-stationary, thus indicating the need for periodic differencing. Nonstationarity was removed with the help of natural logarithm and periodic differencing. The resulting model is described by the following equation

$$(1-\phi_1 B^1-\phi_2 B^2) \nabla_{24} \ln Z = (1-\theta_2 B^2-\theta_{24} B^{24}) a_t \quad (4.9)$$

The parameters of the model were estimated and the values are listed in Table XI.

The residuals are randomly distributed. The randomness of the residuals can be seen from the residuals' autocorrelation functions which are shown in Figure A10. Furthermore, the calculated $\chi^2 = 59.771$ is less than χ^2 with 68 degrees of freedom and 5% significance level for table

This model was then used to forecast the future "effective" hourly demand

The forecasts, actual, and 95% confidence limits for the last day of June 1975 and the first day of July 1975 are shown graphically in Figures 21 and 22

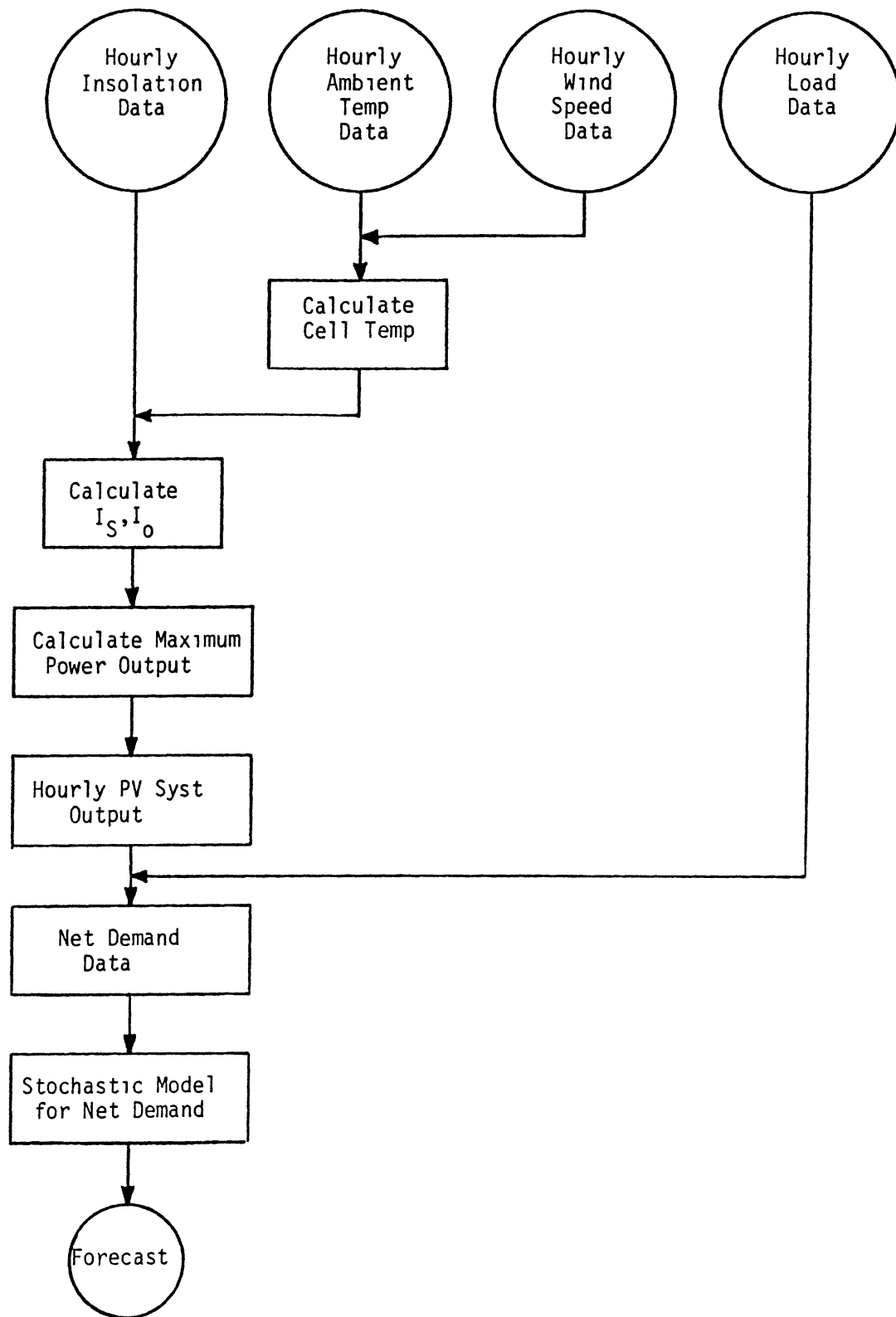


Figure 20 Forecast flowchart (Approach C)

TABLE XI
SUMMARY OF THE ESTIMATED PARAMETER FOR
MODEL OF EQUATION 4.9

Parameter type	Estimated value	95% Confidence limits	
		Lower	Upper
ϕ_1	1.1861	1.0672	1.3050
ϕ_2	-0.22480	-0.34374	-0.10587
θ_2	-0.12348	-0.20192	-0.045036
θ_{24}	0.77139	0.69278	0.85001

The absolute value of the relative error between actual and forecasted values of net-demand varies from 0.3% to 18.69% for forecast 24 hours ahead of the present.

As mentioned earlier, all of the results obtained from different approaches are discussed at the end of this chapter

4.2.3b Two-axis Tracking Concentrator PV Systems

All of the steps followed for the case of flat-plate systems were repeated in this case. The resulting model is described by the following equation

$$(1 - \phi_1 B^1 - \phi_2 B^2) \nabla_{24} \ln Z = (1 - \theta_2 B^2 - \theta_{24} B^{24}) a_t \quad (4.10)$$

The parameters of the model were estimated and the values are listed in Table XII.

This model satisfies all of the statistical tests. The residuals are randomly distributed (see Figure A11). The calculated $\chi^2 = 55.137$ is less than χ^2 with 68 degrees of freedom and 5% significance level from table

Equation 4.10 can now be used to forecast the future "effective" hourly demand. The forecasts, actual, and 95% confidence limits for the last day of June 1975, and the next day (first of June 1975), are shown graphically in Figures 23 and 24.

The absolute value of the relative error between actual and forecasted values of net demand varies from 15% to 26% for forecasts 24 hours ahead of the present.

TABLE XII
SUMMARY OF THE ESTIMATED PARAMETER
FOR MODEL OF EQUATION 4.10

Parameter type	Estimated value	95% Confidence limits	
		Lower	Upper
ϕ_1	1.1951	1.0763	1.3140
ϕ_2	-0.23487	-0.35366	-0.11609
θ_3	-0.10581	-0.18445	-.027176
θ_{24}	0.77988	0.70139	0.85837

4.2.4 Net Demand Forecasting in the Presence of PV and Wind Electric Systems (Approach D)

As mentioned in the previous chapter, both photovoltaic systems and MW-size wind farms connected to an utility grid are considered in this part of the research. For the purposes of this study, a 5% penetration of WECS is assumed. Meeting this level of penetration from WECS will require the employment of 50 units of NASA 2.5 MW MOD-2 units or equivalent. The specifications of the selected unit were introduced in the previous chapter.

All the steps taken in the previous approaches were repeated with the inclusion of wind electric systems as illustrated in the flowcharts of Figures 25 and 26 respectively.

4.2.4a Two-axis Tracking Flat-plate PV Systems

Earlier in this section, the forecasts of hourly wind data were calculated by using the model (Equation 4.4) which was derived from an analysis of the hourly wind speed data. The forecast values were used to calculate the wind-electric system output by using the power output characteristics of MOD-2 units.

These outputs along with the other forecasted data (PV output for tracking flat-plate PV systems and load) were used to calculate the net-demand (see Figure 25). The forecasts, actual, and 95% confidence limits of the net-demand for the last day of June 1975 and the first day of July 1975 are shown in Figures 27 and 28.

The absolute values of the relative error between actual and forecasted values of net demand varies from 0.3% to 18.62% for forecasts 24 hours ahead of the present.

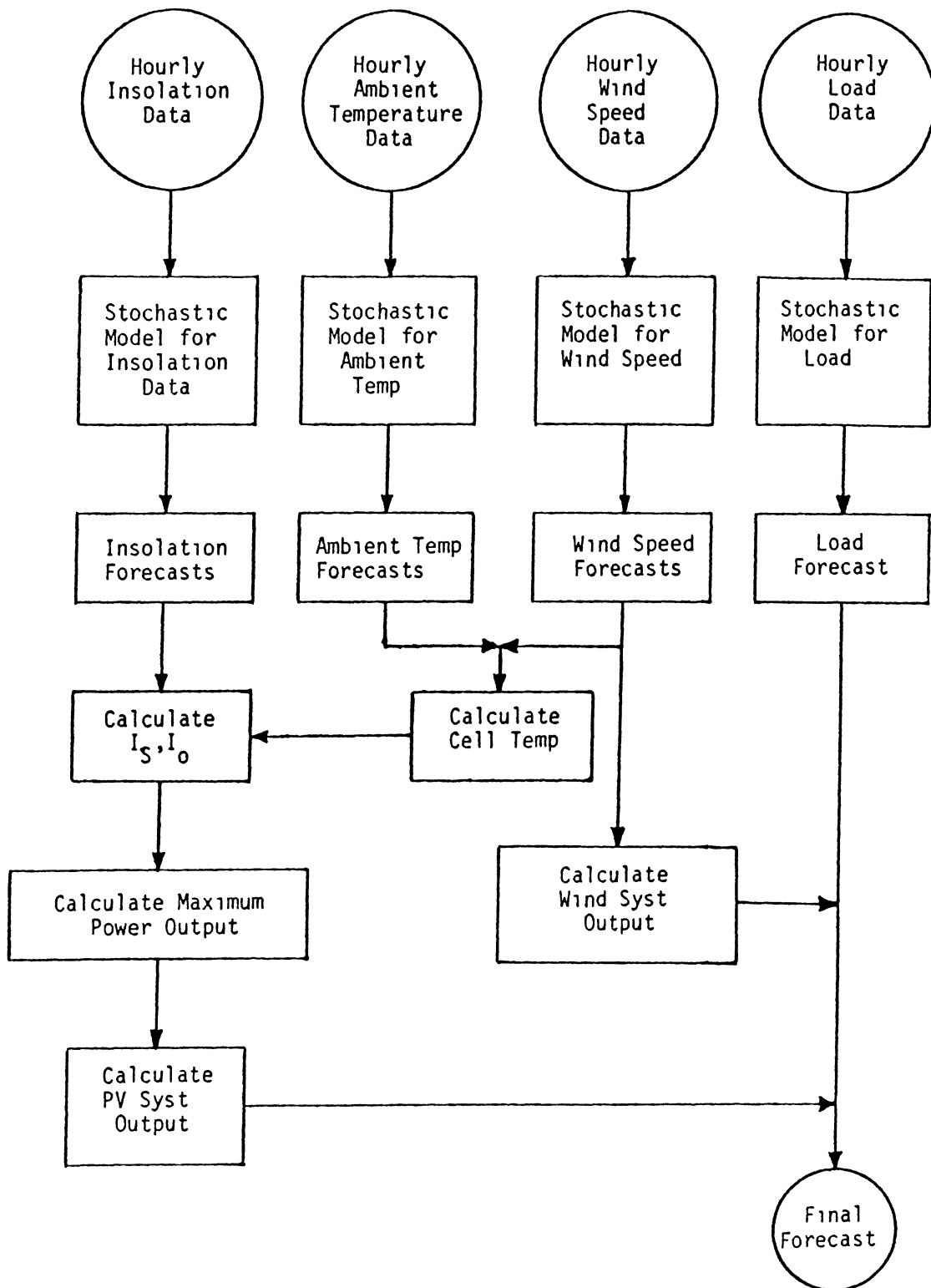


Figure 25 Forecast flowchart (Approach D corresponds to Approach A)

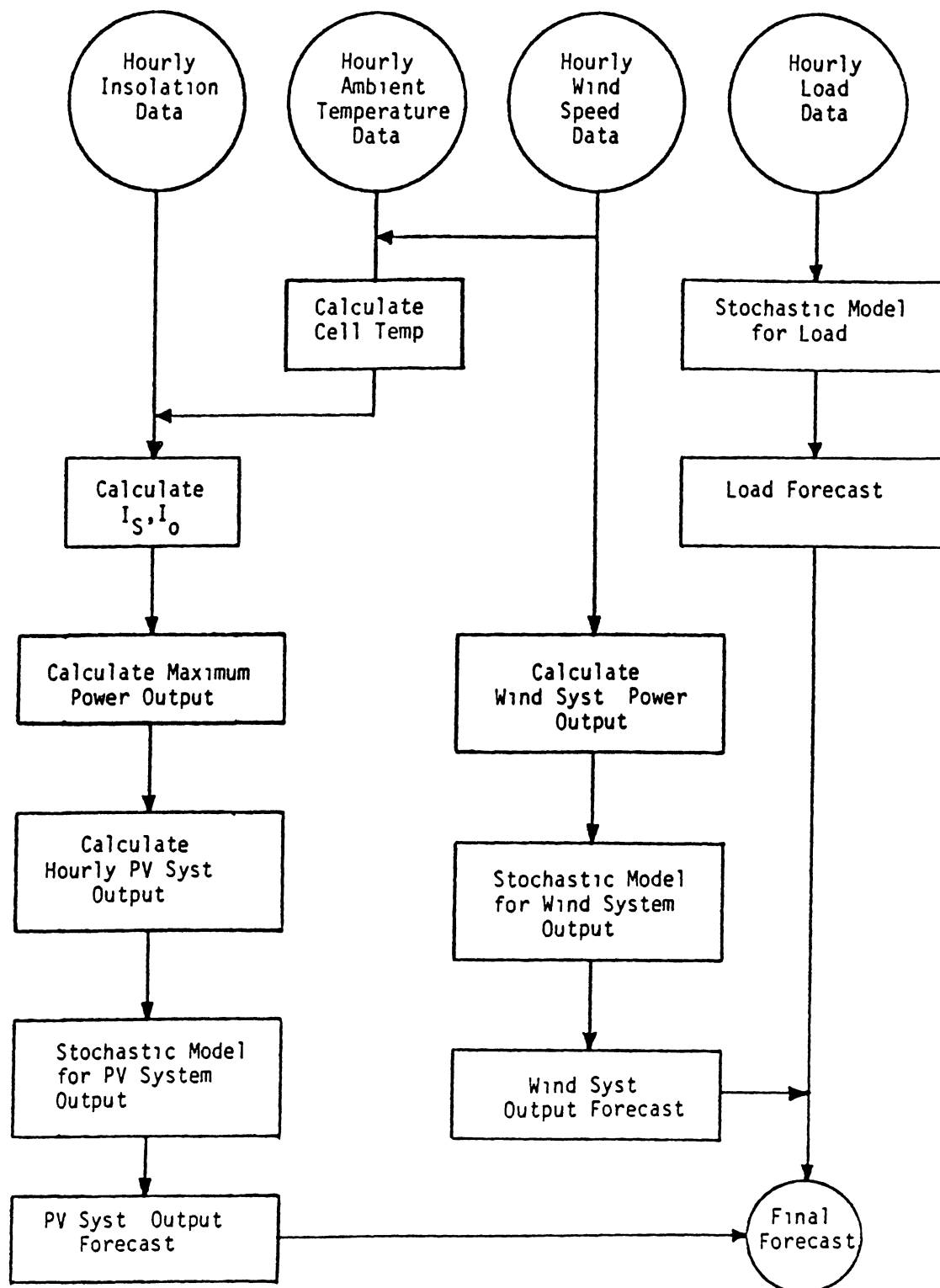


Figure 26 Forecast flowchart (Approach D corresponds to Approach B)

The approach B (see Figure 26) was employed next to forecast the net-demand in the presence of PV (flat-plate) and wind electric systems. For this, the wind system output was calculated first, then the output data were analyzed to develop a model and then to forecast values.

Identification process for the hourly wind-electric system output data with 312 observations was undertaken. Autocorrelations and partial autocorrelations of the data are characterized in such a way that the data can be modeled without using any kind of transformation. After testing many models even with the transformed (differenced) data, the following model was selected.

$$\phi_2(B) (Z-\mu) = (1-\theta_{24}B^{24})a_t \quad (4.11)$$

The parameters of the model were estimated and the values are listed in Table XIII.

The residuals are randomly distributed. The randomness of the residuals is indicated by the residuals' autocorrelation functions which are shown in Figure A12. Furthermore, the calculated $\chi^2 = 52.613$ is less than χ^2 with 68 degrees of freedom and 5% significance level from table.

The model (Equation 4.9) then was used to forecast the wind electric system output data. These data along with the other forecasted (PV output for flat-plate PV systems, and load) were used to calculate the net-demand (see Figure 20). The forecasts, actual, and 95% confidence limits of the net-demand for the last day of June 1975 and the first day of July 1975 are shown graphically in Figures 29 and 30.

TABLE XIII
 SUMMARY OF THE ESTIMATED PARAMETER VALUES
 FOR MODEL OF EQUATION 4.11

Parameter type	Estimated value	95% Confidence limits	
		Lower	Upper
μ	13.676	6.3271	21.025
ϕ_1	0.75864	0.64486	0.87242
ϕ_2	-0.11678	-0.23049	-0.0030745
θ_{24}	-0.12874	-0.24360	-0.013886

The absolute values of the relative error between actual and forecasted values of net-demand varies from 0.3% to 20.28% for forecasts of 24 hours into the future.

The results are compared with the results of the other approaches at the end of this chapter.

4.2.4b Two-axis Tracking Concentrator PV Systems

For this part of the study, all of the necessary data and forecasts are available from the previous parts of this section. Consequently, the net-demand for both approaches could be calculated easily just by subtracting the forecasts of the PV (concentrator systems), and wind system outputs from the forecasted values of the load. Figures 31 and 32 show the forecasts, actual, and 95% confidence limits of the net-demand for the last day of June 1975 and the first day of July 1975 respectively.

The absolute value of the relative error between actual and forecasted values of net demand varies from .3% to 18.15% for time periods extending up to 24 hours. Corresponding forecasts made using the approachB, are shown plotted Figures 33 and 34.

The absolute value of the relative error between actual and forecasted values of net demand varies from 0.3% to 19.86% for forecasts of 24 hours into the future.

4.2.5 Models For Net Demand With PV and WECS Present (Approach D Continued)

All the steps taken in the part 4.2.3 were repeated with the inclusion of wind electric systems output as illustrated in the flow chart shown in Figure 35.

4.2.5a Two-axis Tracking Flat-plate PV Systems

As mentioned earlier, all of the steps were repeated with 300 observations. The procedure is similar to the one followed in the case of PV present, except that now WECS is also included. After testing several models the following model was selected

$$(1-\phi_1 B^1 - \phi_2 B^2) \nabla_{24} \ln Z = (1-\theta_{13} B^{13} - \theta_{21} B^{21} - \theta_{24} B^{24}) a_t \quad (4.12)$$

The parameters of the model were estimated and the values are listed in Table XIV.

This model satisfies all of the statistical tests. The residuals are randomly distributed (see Figure A13). The calculated $\chi^2 = 52.021$ is less than χ^2 with 67 degrees of freedom and 5% significance level from table.

The equation 3.12 was then used to forecast the future "effective" hourly demand. The forecasts, actual, and 95% confidence limits for the last day of June 1975 and the next (first day of July 1975) are shown graphically in Figures 36 and 37.

The absolute value of the relative error between actual and forecasted values of net demand varies from 0.51% to 23.88% for time periods extending up to 24 hours

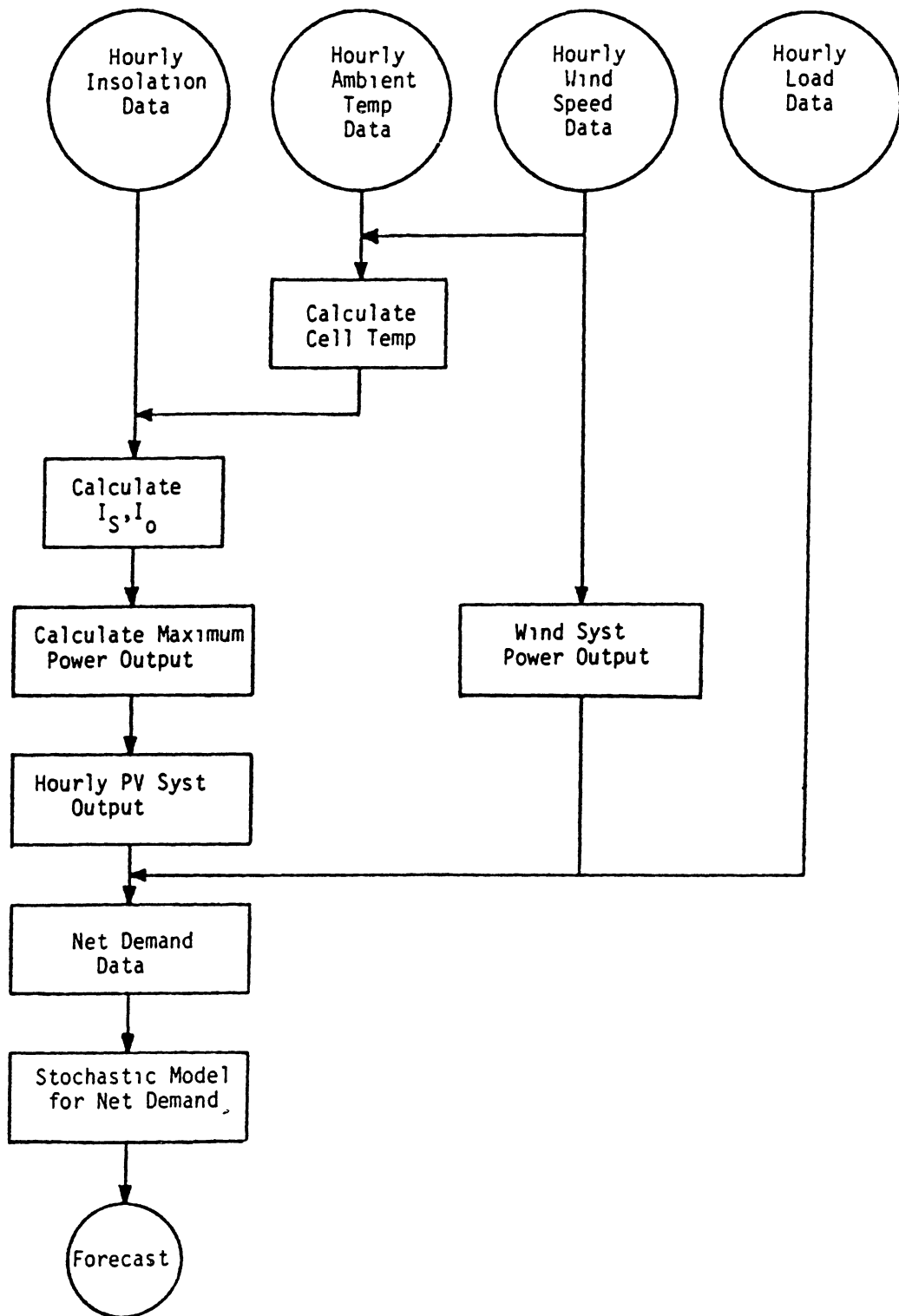


Figure 35 Forecast flowchart (Approach D corresponds to Approach C)

TABLE XIV
 SUMMARY OF THE ESTIMATED PARAMETER VALUES
 FOR MODEL OF EQUATION 4.12

Parameter type	Estimated values	95% Confidence limits	
		Lower	Upper
ϕ_1	1.0369	0.91408	1.1596
ϕ_2	-0.092049	-0.21519	0.031089
θ_{13}	-0.08524	-0.19932	0.026274
θ_{21}	0.10667	-0.0060178	0.21936
θ_{24}	0.42472	0.31282	0.53662

4.2.5b Two-axis Tracking Concentrator PV Systems

Once again all the steps which were followed in former case was repeated for the present case.

The resulting model which satisfies all of the statistical tests is given below.

$$(1-\phi_1B^1-\phi_2B^2) \nabla_{24} \ln Z = (1-\theta_{13}B^{13}-\theta_{22}B^{22}-\theta_{24}B^{24}) \quad (4.13)$$

The parameters of the model were estimated and listed in Table XV.

The residuals are randomly distributed (see Figure A14). The calculated $\chi^2 = 45.785$ is less than χ^2 with 67 degrees of freedom and 5% significance level from table.

Equation 4.13 was then used to forecast the future "effective" hourly demand. The forecasts, actual, and 95% confidence limits for the last day of June 1975 and first day of July 1975 are shown graphically in Figures 38 and 39.

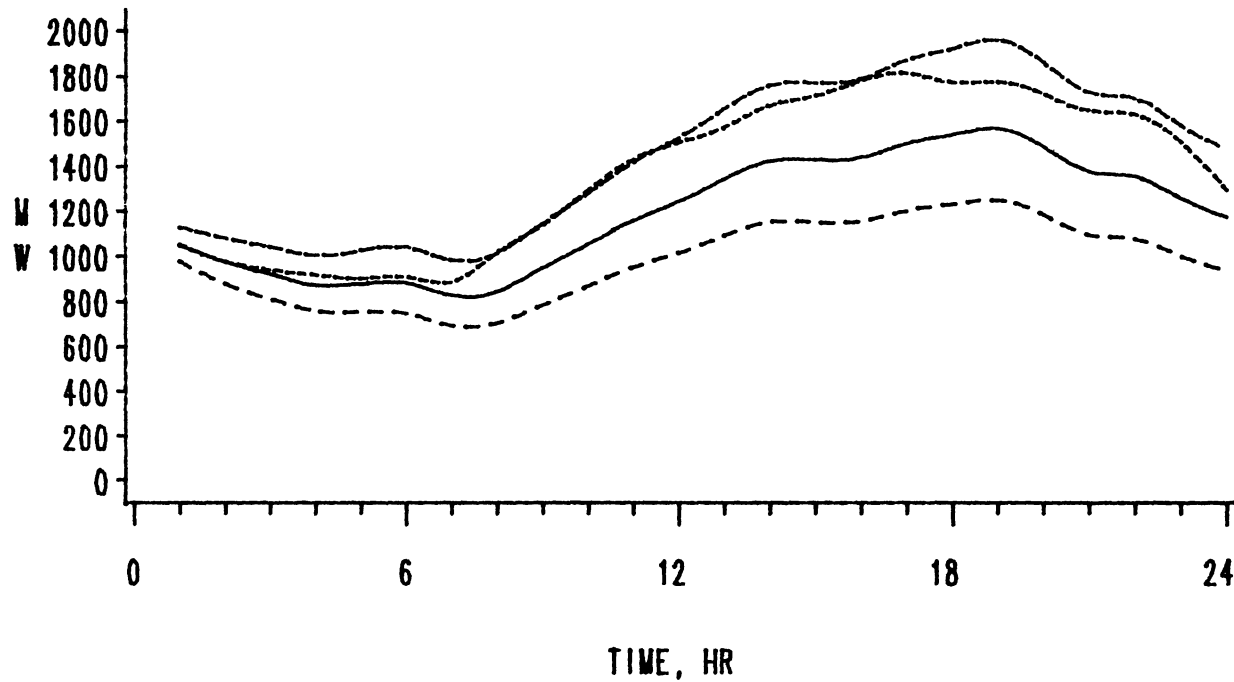
The absolute value of the relative error between actual and forecasted values of net demand varies from 09% to 23.61% for forecasts 24 hours into the future.

4 3 Multiple Time Series Analyses

The impact of temperature on load and its effect on forecasting are considered in this section. To handle this problem, transfer function methodology was employed. This approach expresses the interrelationships or dynamic relationships between two or more time series. The process of identification, estimation, and checking is done iteratively until an acceptable model is evolved. This procedure is comparable to

TABLE XV
 SUMMARY OF THE ESTIMATED PARAMETER VALUES
 FOR MODEL OF EQUATION 4.13

Parameter type	Estimated value	95% Confidence limits	
		Lower	Upper
ϕ_1	1.0351	0.91183	1.1583
ϕ_2	-0.089857	-0.21363	0.033920
θ_{13}	-0.080127	-0.18974	0.029486
θ_{22}	0.11514	0.0031454	0.22714
θ_{24}	0.43885	0.32811	0.54960



LEGEND - - - - LOWER ——— FORECAST
 - - - - UPPER - - - - ACTUAL
 95% Confidence

Figure 38 Forecasts of hourly net demand (MW) in the presence of two-axis tracking concentrator PV and WECS with 5% penetration each for June 30, 1975 (Approach D continued)

the procedure for the development of an ARIMA model for a univariate time series.

A very general form of the transfer function model for a bivariate time series such as load (output Y_t) and temperature (input X_t) can be written as in the form of a discrete linear process (see reference 46).

$$\begin{aligned} Y_t &= \nu_0 X_t + \nu_1 X_{t-1} + \nu_2 X_{t-2} + \nu_3 X_{t-3} + \dots + N_t \\ &= (\nu_0 + \nu_1 B^1 + \nu_2 B^2 + \nu_3 B^3 + \dots) X_t + N_t \\ &= \nu(B) X_t + N_t \end{aligned} \quad (4.14)$$

where, N_t is the combined effects of all other factors influencing Y_t and it is called "noise". The weights $\nu_0, \nu_1, \nu_2, \dots$ are called the impulse response function of the system which would be used in the identification process to determine the order (nature) of the system.

To identify a tentative model for the bivariate (X_t, Y_t) process. It may be simpler to find the prewhitened values for input, output, and noise data. Consequently, equation 4.14 can be modified as follows

$$\beta_t = \nu(B) \alpha_t + \epsilon_t \quad (4.15)$$

where, $\alpha_t = \phi_p(B) \theta_q^{-1}(B) x_t$, prewhitened value of X_t ,

$\beta_t = \phi_p(B) \theta_q^{-1}(B) y_t$, prewhitened value of y_t ,

$\epsilon_t = \phi_{p_n}(B) \theta_{q_n}^{-1}(B) n_t$, prewhitened value of N_t ,

n_t, x_t and y_t = the transformed and differenced values of N_t , X_t , and y_t .

The prewhitened α_t and β_t will be used in the bivariate stochastic process to identify the shape of the transfer function (the specific values of b, n, s and p_n, q_n) which maps α values into β values. It

should be noted that x_t , y_t and even a_t do not have to be white noise series

In order to have a parsimonious form, it is preferable to write the transfer function model in the following form.

$$\begin{aligned} y_t &= \nu(B) x_{t-b} + n_t \\ &= \frac{\omega(B)}{\delta(B)} x_{t-b} + \frac{\theta(B)}{\phi(B)} a_t \end{aligned} \quad (4.16)$$

or

$$\delta_r(B)\phi_{p_n}(B)y_t = \phi_{p_n}(B)\omega_s(B) x_{t-b} + \delta_r(B)\theta_{q_n}(B) a_t \quad (4.17)$$

where, a_t = a random noise values,

$$\delta(B) = 1 - \delta_1 B - \dots - \delta_r B^r,$$

$$\omega(B) = \omega_0 - \delta_1 B - \dots - \delta_s B^s,$$

and b, p_n, q_n, r and s are constants

The subscript $(t-b)$ for x indicates that there is a delay of b periods before x begins to influence y . The cross-correlation functions between the input and output or between the prewhitened input x_t and the filtered output β_t , $(r_{\alpha\beta})$, are used as guides in the identification process. The impulse response functions are directly proportional to the cross-correlation functions. Once the $r_{\alpha\beta}(K)$'s are estimated, the \hat{v}_k 's can be calculated and used in tentatively identifying the order of the parameters of the transfer function. Furthermore, the \hat{v}_k 's could also be used to estimate the initial values of the parameters. Further information on this topic available in Reference 46.

After the estimation process, a model needs to be checked for adequacy. The residual autocorrelations $r_{\hat{a}\hat{a}}$ and the cross-correlation function $r_{\alpha\hat{a}}$ between α_t and \hat{a}_t can be used to check the adequacy of the

model. The $\hat{r}_{\hat{a}\hat{a}}$ would have some patterns if the noise model is incorrect. When the transfer function model is not adequate the $\hat{r}_{\hat{a}\hat{a}}$ and $\hat{r}_{\hat{a}\hat{a}}$ show some patterns, in other words $\hat{r}_{\hat{a}\hat{a}}$ are correlated and so are $\hat{r}_{\hat{a}\hat{a}}$. Then the model is rejected or modified for further testing.

The load model (equation 4.5) was developed based on the past history of the load. The forecast values are shown graphically in Figures 40-41. The absolute value of the relative error between actual and forecasted values of net demand varies from 0.3% to 17% for time periods extending up to 24 hours.

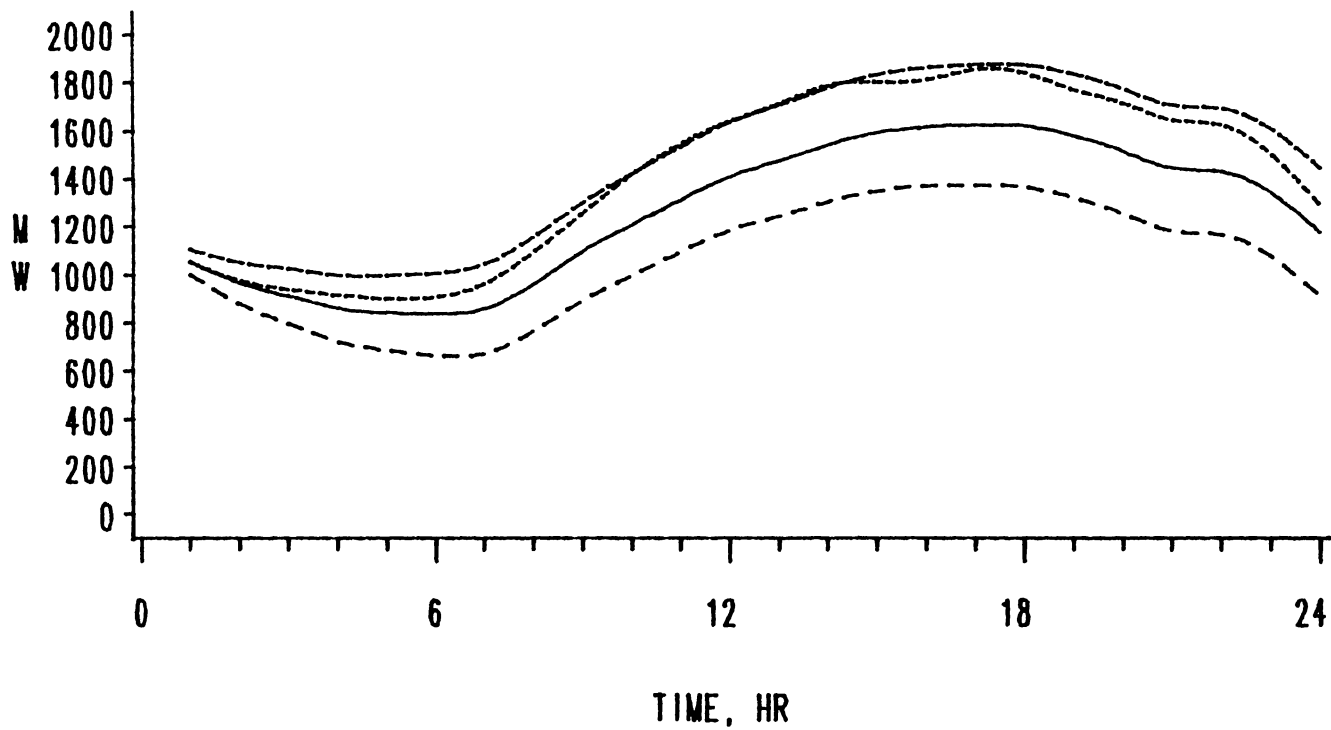
In this section a transfer function model which includes not only the past demand history, but also information on the associated temperature data is derived. It should be mentioned that this temperature data are different from the previous temperature data which were used in the calculation of the PV system output. The present temperature data were provided by the Public Service Company of Oklahoma (PSO) for their main service area.

The iterative process involving identification, estimation and diagnostic checking stages were undertaken for 720 hourly temperature data. After testing many models the following model, which satisfies all the statistical tests, was selected:

$$\nabla_1 \nabla_{24} X_t = (1 - \theta_{24} B^{24}) \alpha_t \quad (4.18)$$

The parameter of the model was calculated and listed in Table XVI.

The autocorrelations of the residuals indicate that the residuals of the process are randomly distributed (see Figure A15). Furthermore, the calculated $\chi^2 = 72.897$ is less than χ^2 with 55 degrees of freedom.



LEGEND - - - - LOWER ——— FORECAST
 - - - - UPPER - - - - ACTUAL
 95% Confidence

Figure 40 Forecasts of hourly load (MW) for June 30, 1975 (Univariate Time Series Process)

TABLE XVI
SUMMARY OF THE ESTIMATED PARAMETER VALUES
FOR MODEL OF EQUATION 4.18

Parameter type	Estimated value	95% Confidence limits	
		Lower	Upper
θ_{24}	0.86742	0.83033	0.90452

and 5% significance level from table. Consequently, the prewhitened input can be written as follows

$$\nabla_1 \nabla_{24} (1 - \theta_{24} B^{24})^{-1} x_t = \alpha_t \quad (4.19)$$

With the same transformation on Y_t and noise N_t , the following prewhitened models were derived (see reference 46)

$$\nabla_1 \nabla_{24} (1 - \theta_{24} B^{24})^{-1} Y_t = \beta_t \quad (4.20)$$

$$\nabla_1 \nabla_{24} (1 - \theta_{24} B^{24})^{-1} N_t = \epsilon_t \quad (4.21)$$

The impulse response weights were calculated and shown graphically in Figure B16. In addition, the autocorrelation functions of the noise series were calculated and they are shown graphically in Figure A17. Finally, after checking several models the following model was derived.

$$Y_t = \frac{\omega_0}{1 - \delta_1 B^1} x_t + \frac{(1 - \theta_5 B^5 - \theta_{11} B^{11} - \theta_{24} B^{24})}{(1 - \phi_1 B^1 - \phi_2 B^2)} a_t \quad (4.22)$$

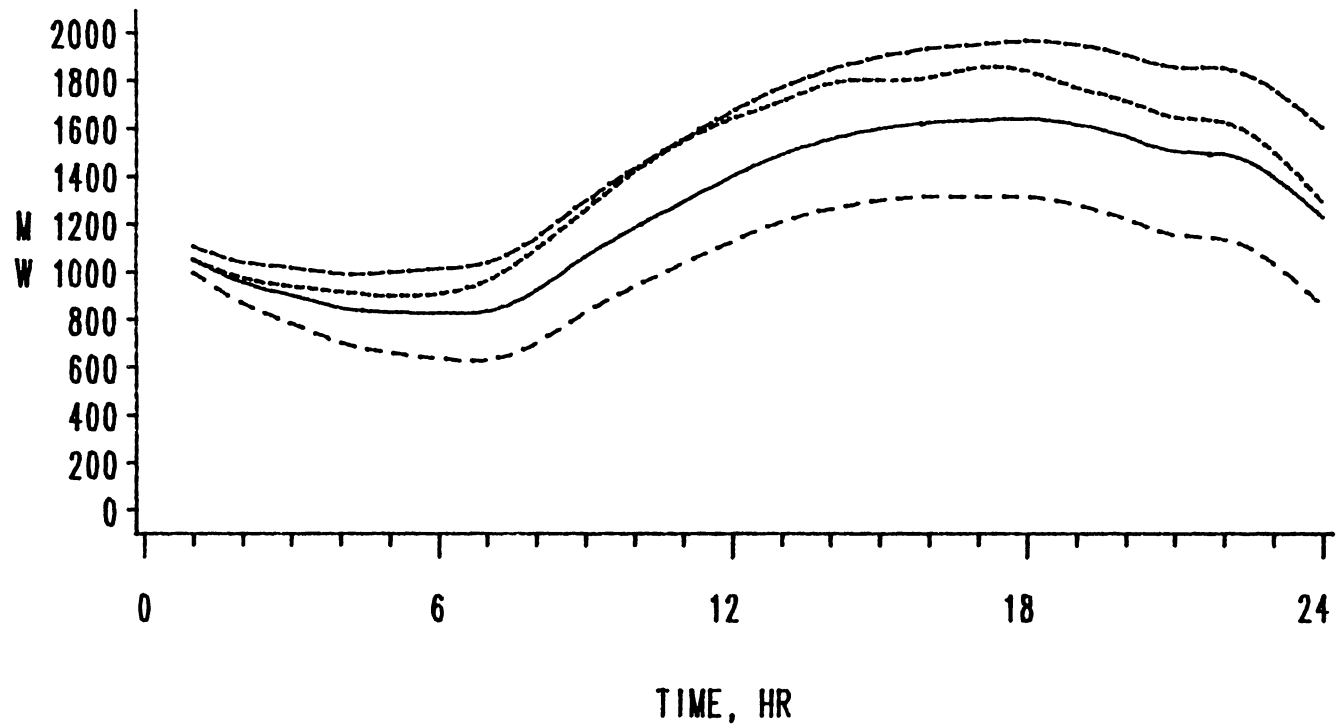
The parameters of the model were estimated using least square approach iteratively. The iterative process was terminated when the relative change in the residual sum of squares was less than 1.0×10^{-4} . The estimated parameters with their 95% confidence limits are listed in Table XVII.

The residuals are randomly distributed (see Figure A18). The calculated $\chi^2 = 66.943$ is less than χ^2 with 69 degrees of freedom and 5% significance level from table.

The model was then used to forecast the hourly load data (see Figures 42 and 43).

TABLE XVII
 SUMMARY OF THE ESTIMATED PARAMETER VALUES
 FOR MODEL OF EQUATION 4. 22

Parameter type	Estimated value	95% Confidence limits	
		Lower	Upper
δ_1	0.66264	0.30840	1.0169
ω_0	4.64429	2.1412	7.1447
ϕ_1	0.22713	0.034788	0.41948
ϕ_2	0.12804	-0.062182	0.31826
θ_5	0.19473	0.04617	0.34328
θ_{11}	0.11920	-0.033919	0.27232
θ_{24}	0.60366	0.44219	0.76512



LEGEND - - - - LOWER ——— FORECAST
 - - - - UPPER - - - - ACTUAL
 95% Confidence

Figure 42 Forecasts of hourly load (MW) for June 30, 1975 (Bivariate Time Series Process)

The absolute values of the relative error value between actual and forecasted values of net demand varies from 0.09% to 18% for 24 hours ahead. The results are compared in the next section.

4.4 Discussion of Results

The net demand on a power system was forecasted by applying different approaches in the presence of PV alone, and PV in conjunction with WECS. The forecast values were compared with actual values wherever possible and the ranges of error were computed. The approaches studied are summarized below.

A. The algorithm "PVTALGO" developed in Chapter III is used in conjunction with univariate time series analyses for insolation, wind speed, and ambient temperature to forecast PV system output for both two-axis tracking flat-plate and concentrator systems. The final forecasts of "net" demand are obtained by subtracting the calculated PV system output from the load forecast.

B. PV system output for both two-axis tracking flat-plate and concentrator systems are calculated from raw historical data first. These values are considered as a set of time series and future values are forecasted by using suitable models. Once again, forecasts of the final "net" demand are obtained by subtracting the calculated PV output from the load forecast.

C. The historical "net" demand, which is equal to the actual demand minus the PV output, is calculated and used as final data to forecast the future "effective" demand.

D. The steps outlined in A through C are repeated for the case of grid-connected PV and WECS to forecast final "effective" demand on the utility.

E. The impact of temperature on load and its effect on forecasting and modeling procedures is studied by using multiple time series analyses.

A study of forecast values and error ranges indicate that Approach A is preferable to the other approaches. This is because in A each of the raw (original) data set is analyzed, modeled and forecasted individually. Since each raw data set is subject to detailed analysis, the resulting models represent more truly the nature of the data sets -- insolation, wind speed, ambient temperature, and load -- considered in the identification process. Consequently, the resulting forecasts are more accurate than others. The output of a PV system is not solely dependent on insolation data, it is calculated through a step-by-step procedure and it is strongly dependent on the operating cell temperature (see Equation 3.4) and, in turn, on the ambient temperature and wind speed. As such, the time series of PV output data has substantially different characteristics from the time series of insolation data. This point is brought out clearly by comparing the models of Equations 4.2 and 4.7, and also by comparing Equation 4.6 with Equation 4.8 for flat-plate and concentrator systems respectively.

Similar discussion and comparisons can be made for wind speed and wind system output also. However, ambient temperature has very little effect on WECS output. In short, PV and WECS outputs are second hand data and some of the characteristics of the key inputs (insolation,

wind speed and ambient temperature) become obscure by not considering individual models.

The nonstationarity of the insolation data for both flat-plate (total) and concentrator (direct) systems can almost be removed by applying the periodic (seasonal differencing for the seasonal data) with the order of 12, $\nabla_{12} = (1-B^{12})$ and regular first order differencing, $\nabla_1 = (1-B)$ (see Equations 4.2 and 4.6). But this process takes on a different form for the PV output data (see Equations 4.7 and 4.8).

Stationarity is achieved for the data in Approach C by applying natural logarithm to get more homogeneous data and a 24 order differencing, $\nabla_{24} = (1-B^{24})$ to remove the daily periodic nonstationarity (similar to 12 that is expected in the monthly seasonal data).

Figures 16 and 18 reveal that Approach B has a smaller error than Approach C. This can be attributed to the fact that some more naturalness is lost in the data transformation.

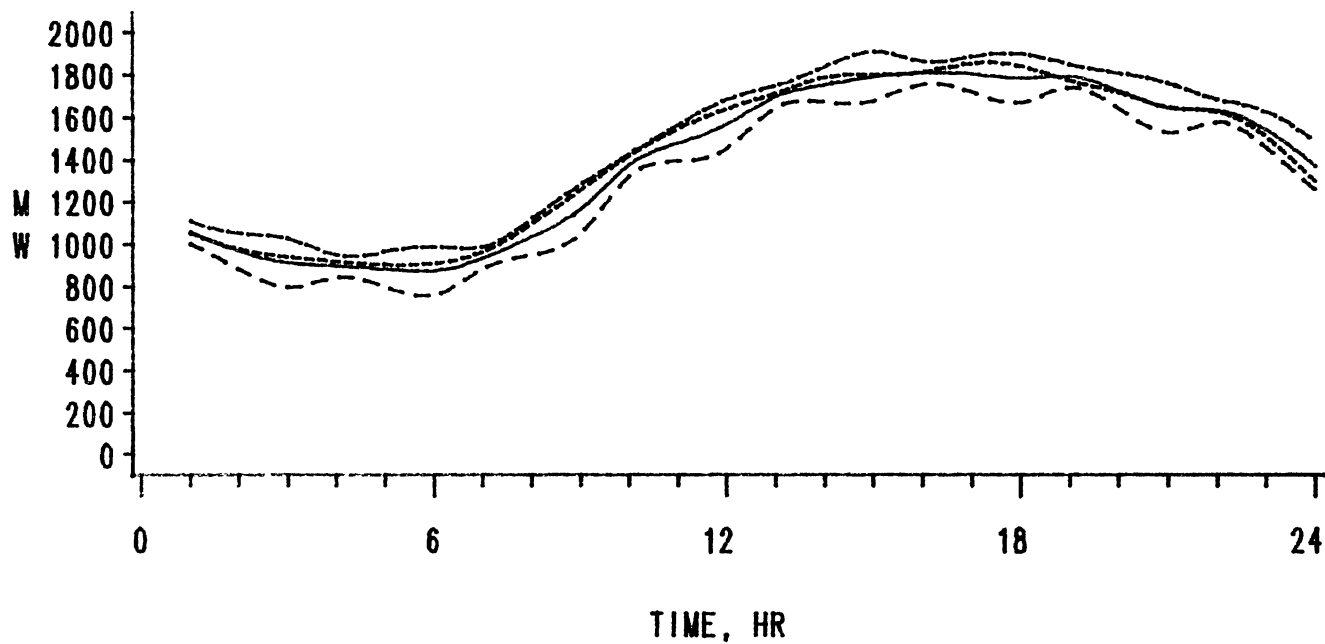
It should be mentioned that for the first few steps of the forecasts, Approach C gives much better results. For example, the error for the first hour net demand forecast value is only 0.15% for the flat-plate case, which is only one half of the 0.3% obtained with the first two approaches. Also 0.18% for concentrator system is again smaller than 0.3%.

Considering all these results Approach A is more accurate and preferable. However, it involves more calculations. This is true in the case of both flat-plate and concentrator PV systems. Both are assumed to have two-axis tracking although it is absolutely necessary only for latter.

Once again, in the case of the presence of PV and wind systems, Approach A has smaller error range and average error. With Approach C, forecasts of the very first few steps have smaller error as compared to the other approaches. As an example, 0.09% for the first step ahead forecast is an excellent improvement, but the overall range of error is larger and so is the average error with respect to the other approaches.

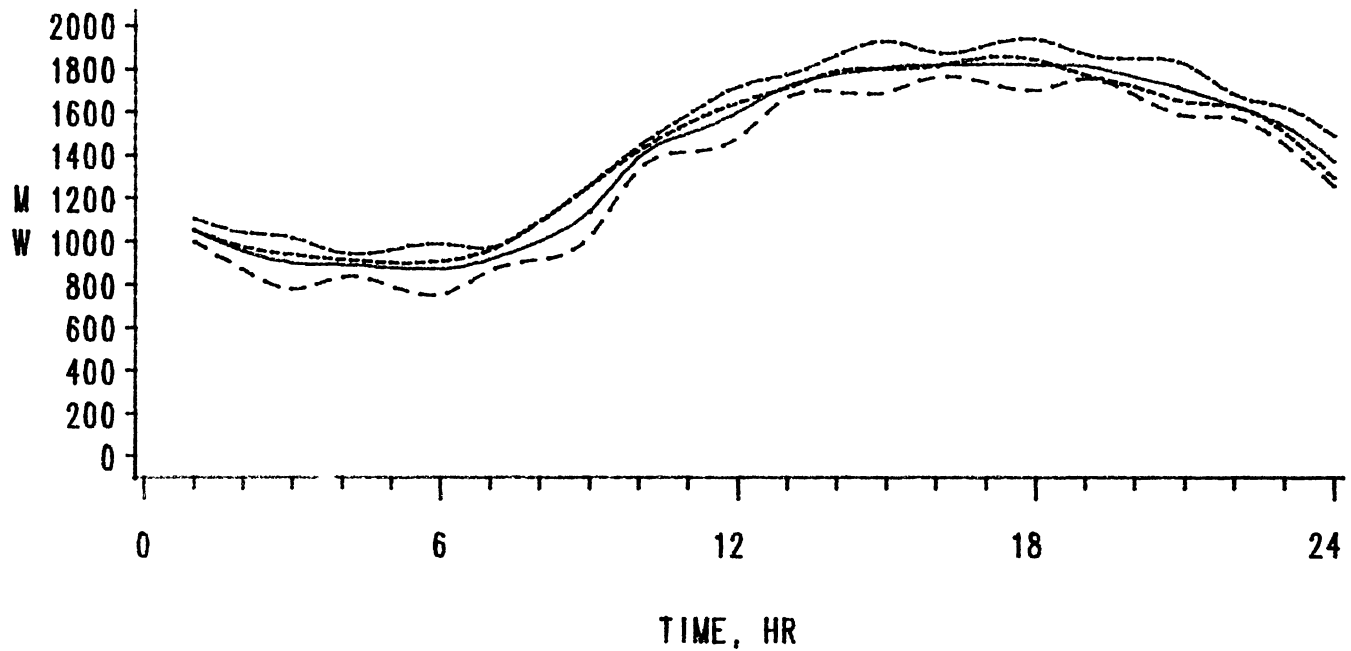
Comparing the graphics in Figures 40 and 42 (see section 4.3) it is noticeable that there are some improvements on load forecasting when the effect of temperature is included, specifically for the first few steps -- compare 0.09% with 0.3%. Also the average error is smaller than in the case of univariate time series (about 0.2%). Overall, the difference is not that significant.

Error in the hourly load forecasts is higher than monthly or weekly even daily forecasts because of the rapid variations of data. In other words, the variation of data obtained over a longer period of time is more static, therefore the error would be smaller. Smaller errors result if the forecasting process is done for a shorter time lead (a few hours) ahead rather than a day ahead. This process can then be repeated for the next few hours and so on. To illustrate this, forecasting of the load using univariate time series analysis has been repeated by considering a period of only three hours ahead at a time. The results are shown in Figure 44. The closeness of the forecast to the actual value is clearly evident. A similar procedure for the bivariate analysis results in the plots shown in Figure 45. Once again, the forecasts are much closer to the actual values. Such a procedure of forecasting over smaller period of time can be used to forecast insolation, wind speed, temperature, PV output, and WECS output with improved results.



LEGEND - - - - LOWER - - - - FORECAST
 - - - - UPPER - - - - ACTUAL
 95% Confidence

Figure 44 Forecasts of hourly load (MW) over each 3 hour period for June 30, 1975 (Univariate Time Series Process)



LEGEND - - - - LOWER - - - - FORECAST
 - - - - UPPER - - - - ACTUAL
 95% Confidence 95% Confidence

Figure 45 Forecasts of hourly load (MW) over each 3 hour period for June 30, 1975 (Bivariate Time Series Process)

The absolute value of the relative error for the results shown in Figure 44 for the univariate process varies from 0.18% to 7.7%, and for the bivariate process shown in Figure 45 from 0.06% to 10%. In general, the average error in the case of bivariate process is smaller than the univariate process as expected.

The results are not the same under different penetration. For instance, the numerical value of the difference between actual and forecasted PV and/or WECS output would be double or one-half under 10% or 2.5% penetrations respectively from the Approaches A and C, and the same thing is expected from Approach B too. However, the percentage differences would remain the same.

It should be realized that one cannot expect to use the same model during different seasons or even for different months in the same season -- Fall, Winter, Spring or Summer. Because of many reasons such as variation of weather, economy, different demands etc., different models would be necessary. Moreover, these models will be highly site-specific and utility-specific.

Comparing the results in the case of flat-plate and concentrator systems, slightly smaller error range and average error have been achieved in the case of concentrator systems. This can be attributed to the many factors that could influence total insolation as compared to only the direct portion of the insolation considered in the case of concentrator systems.

CHAPTER V

SUMMARY AND CONCLUSIONS

5.1 SUMMARY AND CONCLUDING REMARKS

Methodologies for forecasting power system loads involving conventional generation units are well developed and have been used for many years. These methods are firmly established in power utilities and the necessary requirements are well laid out not only for generation sector but also for transmission and distribution parts of the power system.

During the last few years, research and development around the world have laid the groundwork necessary for the design, development, and fabrication of large MW-size PV and WECS for the generation of electricity.

The world-wide accumulated production of PV approached the 100 MW level towards the end of 1985 and it is expected to soar to 10,000 MW sometime during the 1990-1995 time period.

The central-station PV projects in California have been quite successful and have boosted the confidence level of utilities considerably. The combination of high capacity factors during peak hours, low maintenance, unattended operation, modular design, no harmful emissions and no water requirements make PV a very attractive option in many parts of the world.

The experience of California utilities, SCE and PG & E in particular, which have MW-size windfarms in their service area has been very

positive and it has increased the confidence that wind could also be a good alternative source of electric power generation for utilities around the world.

The introduction of a new power generation technology such as photovoltaics or wind electric generation into an existing electric utility system requires the consideration and resolution of several issues. Planning issues are among those important issues and they include the study of load forecasting in the presence of there (new) alternative electric power generation technologies.

The reason for this focus is that the power generated by these two new generation technologies is highly variable and could adversely affect utility planning based on load forecasting, under high penetrations. In contrast, the outputs of cogeneration plants utilizing biomass and other resources are "schedulable".

Load forecasting in the presence of new (alternative) generation technologies provides information useful in several aspects of power system planning and operation -- generation planning, system operation, revenue forecasting, unit commitment and economic dispatch, and system security assessment.

Available hourly data such as insolation, wind speed, ambient temperature, and load were used to forecast the net demand on the utility.

Chapter II discussed the impacts of alternative electric generation on the utility system, brought about by the significant differences between conventional and unconventional technologies. Major differences from conventional technologies are present in the following aspects scale, intermittent output, correlation of generation with demand,

ownership, economic dispatch, quality of power, and load shifting. Utility-related issues, impacts and concerns as well as barriers to load modeling and load forecasting were also discussed.

Chapter III presented an approach and developed an algorithm to calculate PV system output under variable insolation, temperature, and wind speed conditions in the form of a time series, designated as "PVTALGO". This algorithm has been tested and used to calculate the PV output for different sets of selected data. Table II lists the calculated values of output power for the selected PV module using New Mexico data for one day. These values and the corresponding insolation data are shown graphically in Figures 6 and 7 respectively.

Table II and Figure 6 show that the algorithm works well and can be used to calculate the power output of large PV systems. The output and efficiency of a PV system strongly depend on cell operating temperature and insolation. The wind speed has less effect on cell temperature and consequently on the PV output. Calculation of the power output of a wind electric conversion system is also discussed in this chapter.

Chapter IV discusses the impact of grid-connect PV and WECS from the load forecasting point of view. Several approaches were investigated to forecast the net load on a utility in the presence of new power generation technologies. They are summarized below.

A. The algorithm "PVTALGO" developed in Chapter III is used in conjunction with univariate time series analyses for insolation, wind speed, and ambient temperature to forecast PV system output for both two-axis tracking flat-plate and concentrator systems. The final forecasts of "net" demand are obtained by subtracting the calculated PV system output from the load forecast.

B. PV system output for both two-axis tracking flat-plate and concentrator systems are calculated from raw historical data first. These values are considered as a set of time series and future values are forecasted by using suitable models. Once again, forecasts of the final "net" demand are obtained by subtracting the calculated PV output from the load forecast.

C. The historical "effective" demand, which is equal to the actual demand minus the PV output, is calculated and used as final data to forecast the future "net" demand.

D. The steps outlined in A through C are repeated for the case of grid-connected PV and WECS to forecast final "net" demand on the utility.

E. The impact of temperature on load and its effect on forecasting and modeling procedures is studied by using multiple time series analyses.

A study of forecast values and error ranges indicate that Approach A is preferable to the other approaches. This is because in A each of the raw (original) data set is analyzed, modeled and forecasted individually. Since each raw data set is subject to detailed analysis, the resulting models represent more truly the nature of the data sets -- insolation, wind speed, ambient temperature, and load -- considered in the identification process. Consequently, the resulting forecasts are more accurate than others. The output of a PV system is not solely dependent on insolation data, it is calculated through a step-by-step procedure and it is strongly dependent on the operating cell temperature (see Equation 3.4) and, in turn, on the ambient temperature and wind speed. As such, the time series of PV output data has substantially different characteristics from the time series of insolation data. This

point is brought out clearly by comparing the models of Equations 4.2 and 4.7, and also by comparing Equation 4.6 with Equation 4.8 for flat-plate and concentrator systems respectively.

Similar discussion and comparisons can be made for wind speed and wind system output also. However, ambient temperature has very little effect on WECS output. In short, PV and WECS outputs are second hand data and some of the characteristics of the key inputs (insolation, wind speed and ambient temperature) become obscure by not considering individual models.

The nonstationarity of the insolation data for both flat-plate (total) and concentrator (direct) systems can almost be removed by applying periodic differencing (seasonal differencing for the seasonal data) with the order of 12, $\nabla_{12} = (1-B^{12})$ and regular first order differencing, $\nabla_1 = (1-B)$ (see Equations 4.2 and 4.6). But this process takes on a different form for the PV output data (see Equations 4.7 and 4.8).

Stationarity is achieved for the data in Approach C by applying natural logarithm to get a more homogeneous data and a 24 order differencing, $\nabla_{24} = (1-B^{24})$ to remove the daily periodic nonstationarity (similar to 12 that is expected in the monthly seasonal data).

Figures 16 and 18 reveal that Approach B has a smaller error than Approach C. This can be attributed to the fact that some more naturality is lost in the data transformation.

It should be mentioned that for the first few steps of the forecasts, Approach C gives much better results. For example, the error for the first hour net demand forecast value is only 0.15% for the flat-plate case, which is only one half of the 0.3% obtained with the first

two approaches. Also 0.18% for concentrator system is again smaller than 0.3%.

Considering all these results, Approach A is more accurate and preferable. However, it involves more calculations. This is true in the case of both flat-plate and concentrator PV systems. Both are assumed to have two-axis tracking although it is absolutely necessary only for the latter.

Once again, in the case of the presence of PV and wind systems, Approach A has smaller error range and average error. With Approach C, forecasts of the very first few steps have smaller error as compared to the other approaches. As an example, 0.09% for the first step ahead forecast is an excellent improvement, but the overall range of error is larger and so is the average error with respect to the other approaches.

Comparing the graphs in Figures 40 and 42 (see section 4.3) it is noticeable that there are some improvements on load forecasting when the effect of temperature is included, specifically for the first few steps -- compare 0.09% with 0.3%. Also the average error is smaller than in the case of univariate time series (about 0.2%). Overall, the difference is not that significant. As expected error in hourly load forecasts is higher than in monthly or weekly even daily forecasts because of the rapid variations of data. In other words, the variation of data obtained over a longer period of time is more static, therefore the error would be smaller. Smaller errors result if the forecasting process is done for a shorter time lead (a few hours) ahead rather than a day ahead. This process can then be repeated for the next few hours and so on. To illustrate this, forecasting of the load using univariate time series analysis has been repeated by considering a period of only

three hours ahead at a time. The results are shown in Figure 44. The closeness of the forecast to the actual value is clearly evident. A similar procedure for the bivariate analysis results in the plots shown in Figure 45. Once again, the forecasts are much closer to the actual values. Such a procedure of forecasting over smaller period of time can be used to forecast insolation, wind speed, temperature, PV output, and WECS output with improved results.

The absolute value of the relative error for the results shown in Figure 44 for the univariate process varies from 0.18% to 7.7%, and for the bivariate process shown in Figure 45 from 0.06% to 10%. In general, the average error in the case of bivariate process is smaller than the univariate process as expected.

The results are not the same under different penetrations. For instance, the numerical value of the difference between actual and forecasted PV and/or WECS output would be double or one-half under 10% or 2.5% penetrations respectively from the Approaches A and C, and the same thing is expected from Approach B too. However, the percentage differences would remain the same.

It should be realized that one cannot expect to use the same model during different seasons or even for different months in the same season -- Fall, Winter, Spring or Summer. Because of many reasons such as variation of weather, economy, different demands etc., different models would be necessary. Moreover, the models will be highly site-specific and utility-specific.

Comparing the results in the case of flat-plate and concentrator systems, slightly smaller error range and average error have been achieved in the case of concentrator systems. This can be attributed to

the many factors that could influence total insolation as compared to only the direct portion of the insolation considered in the case of concentrator systems.

The studies pursued in this research have practical importance. The process developed is general and is applicable to any utility system in the presence of PV and WECS. The results presented and discussed have laid the necessary groundwork for better understanding of the forecasting aspects of alternative (PV and WECS) power generation technologies assisting conventional generators, supplying a common load. The results and discussion presented should be helpful for further studies in this area.

5.2 Scope for Suggested Further Work

Integration of new (alternative) generation technologies with present-day power systems is a multi-step iterative process involving economics, institutional issues, environmental issues, customer acceptance, and hardware development. Appropriate load forecasting can provide some of the information and impetus needed for the characterization, design, evaluation, and demonstration of new generation technologies.

Future work on forecasting the net demand on PV and WECS - assisted utility systems appears necessary in many areas and some of the important ones are outlined below.

1. Decompose the load and outputs of new generation technologies on the basis of distinctly identifiable service regions. Develop models for each part individually and obtain net forecasts in terms of these individual forecasts.

2. Improve the models for insolation, wind speed, load, ambient temperature, PV output, and WECS output.

3. Develop ways to include the diversity and/or the complementary nature of solar and wind resources in the study and forecasting.

4. Study different mixes of PV and WECS depending on the availability of the resources.

5. Consider the possibility of including other energy technologies such as heat pumps and solar heating and cooling which could have an impact on the net load experienced by the utility.

6. Include other new electric power generation technologies such as solar-thermal-electric, solar ponds, and geothermal in the forecasting process.

7. Study different seasons and the different models necessary. Find ways and means to arrive at simpler models useful for longer range forecasting.

The paragraphs that follow discuss some of these points in more detail.

The studies documented in this thesis consider total system hourly loads and central station PV and windfarms outputs. Utility load can be broken down into different sectors -- agricultural, commercial, industrial, and residential. The loads contributed by each of these sectors depend on certain variables. Such as population, economy, and weather. Identification of these variables and their relationship to sector loads and in turn to total system demand will improve the forecasting process considerably. Moreover, each region in the utility service area will have distinct insolation and wind characteristics. Consequently, it will be better to develop separate models of the outputs of PV and WECS, depending on their geographic locations.

Although the models developed in Chapter IV are reasonably accurate for a first-cut study, improvements are certainly possible and they could come from employing different types of data transformations and by considering specifically seasonal, weekly, and shorter-term (less than hour) variations.

Data concerning new (alternative) energy resources, say for example insolation, usually takes the form of consecutive hourly or daily averages values of the available resource. Typically they are highly correlated. Consequently, further study is strongly warranted to develop new and improved forecasting methodologies to handle the continuous and dependent data.

Due to the basic nature of solar and wind resources, short-term (hourly) load forecasting approach is employed to consider the presence of new generation technologies for one site. Any generalization of the findings of this document will require the study and evaluation of many more sites within the utility service area with different insolation patterns and wind regimes and longer periods of time, especially in the case of larger penetrations. Based on the availability of insolation and wind speeds, different penetration mixes for PV and WECS should also be studied.

It would be worth while to include other new technologies such as solar-thermal electrical generation, solar heating and cooling, heat pumps, solar pond electric generation, and geothermal units in the forecasting of future net demand.

It is desirable to include as many of the environmental factors such as cloud cover, humidity, etc. as possible in the modeling of the resources and the outputs of new generation technologies. However, one

should also be careful not to make the models too complicated to be of much use as far as forecasting is concerned.

Since large scale arrays of PV and WECS are expected to be located in remote areas served by the utility, it is clear that transmission and even distribution lines constitute an integral part of a PV and WECS - assisted utility system. Therefore, the inclusion of transmission and distribution in forecasting opens up another area for future research.

Finally, PV modules and WECS with different operating characteristics should be studied in detail. As an example, WECS could be a constant-speed type or a variable-speed type and its output as a function of wind speed strongly depends on this point. PV modules could be made of single-crystal semiconductor or amorphous silicon, to mention just one point. Their outputs as functions of insolation depends on factors such as these. All such factors will have an impact on the models and methods used in forecasting the net demand on an electric utility.

REFERENCES

1. Moore, T., "Pioneering the Solid-State Power Plant," EPRJ Journal, Vol. 10, No. 10, December 1985.
2. Ramakumar, R., "Photovoltaic and Electric Utilities -- Promises and Prospects," paper presented at the Energy Information Dissemination Program, Engineering Energy Laboratory, Oklahoma State University, Stillwater, Oklahoma, Report No. 17, Jan. 1986.
3. Ramakumar, R., "An Update on the Technical and Economic Status of Photovoltaics with Special Reference to Utility Applications," paper presented at the Energy Information Dissemination Program, Engineering Energy Laboratory, Oklahoma State University, Stillwater, Oklahoma, Report No. 14, pp. 40-85, July 1984.
4. Patapoff Jr., N. W. and Mattijetz, D. R., "Utility Interconnection Experience with an Operating Central Station MW-Sized Photovoltaic Plant," IEEE Transactions on Power Apparatus and Systems, Vol. PAS-104, No. 8, pp. 2020-2024, August 1985.
5. Rosen, D. J., et al., "Design, Construction, and Startup of the SMUDPV1 1-MW Photovoltaic Central Station Power Plant," IEEE Paper No. 85 WM 098-9, presented at the 1985 IEEE Winter Power Meeting, New York, NY, February 1985.
6. Hoff, T. and Jennings, C., "Match Between PG&E's Peak Demand Period and Insolation Availability," paper presented at the 18th IEEE Photovoltaic Specialists Conference, Las Vegas, Nevada, October 1985.
7. Taylor, R., et al., "Photovoltaics Generation - Recent Technology Advancements," a panel discussion, IEEE Transactions on Power Apparatus and Systems, Vol. PAS-104, No. 11, pp. 2962-2967, November 1985.
8. O'Neill, M. J., "Measured Performance for the First Three Years of Operation of the DFW Airport 27 kW (Electric) 120 kW (Thermal) Linear Fresnel Lens Photovoltaic & Thermal (PVT) Concentrator System," paper presented at the 18th IEEE Photovoltaic Specialists Conference, Las Vegas, Nevada, October 1985.
9. Grassi, G., "Two-Year Experience of the EC Photovoltaic Pilot Projects," paper presented at the 18th IEEE Photovoltaic Specialists Conference, Las Vegas, Nevada, October 1985.

10. Fischetti, M. A. and Zorpette, G., "Technology '86 - Power and Energy," IEEE Spectrum, Vol. 23, No. 1, pp. 65-68, January 1986.
11. Leonard, S. L., "Photovoltaic Power Generation for Utilities The Implications of Some Recent Projects and Design Studies," IEEE Paper No. 85 WM 100-3, presented at the 1985 IEEE Winter Power Meeting, New York, NY, February 1985.
12. Chinery, G. T., and Wood, J. M., "TVA's Photovoltaic Activities," IEEE Transactions on Power Apparatus and Systems, Vol. PAS-104, No. 8, pp. 1998-2005, August 1985.
13. Fan, J. C. C., "Single-Cell Concepts for Obtaining Photovoltaic Conversion Efficiencies over 30%," paper presented at the 18th IEEE Photovoltaic Specialists Conference, Las Vegas, Nevada, October 1985.
14. Ramakumar, R., "Wind Electric Conversion and Utilization," paper presented in the Arab School of Science and Technology, Kuwait, January 1982.
15. Deshmukh, R. G., "A Probabilistic Study of Wind-Electric Conversion Systems for the Point of View of Reliability," Ph.D. thesis, Oklahoma State University, Stillwater, Oklahoma, USA, May 1979.
16. Fisher, J., "Past and Future of Energy in Denmark," Proceedings, Second Workshop on Wind Energy Conversion Systems, Washington, D.C., June, 1975.
17. Bonafille, Rene. "French Contribution to Wind Power Development by EDF - 1966," Proceedings, Workshop on Advanced Energy Systems, Stockholm, Sweden, Vol. 1, August 1975.
18. Golding, E.E., Generation of Electricity by Wind Power London E and F. N. Spon, Ltd., 1955.
19. Stodhart, A. H., "Review of the U.K. Wind Power Programme 1948-1960." Proceedings, Workshop on Advanced Energy Systems, Stockholm, Sweden, Vol. 1, August, 1974.
20. Hutter, U., "Influence of Wind Frequency on Rotational Speed Adjustments of Windmill Generators." NASA Technical Translation, NASA-TT-F 15184, November, 1973.
21. Hutter, U. "The Aerodynamic Layout of Wind Blades of Wind Turbines with High Tip - Speed Ratio." Proceedings, United Nations Conference on New Sources of Energy, Vol. VII, Rome, Italy, August, 1961.
22. Putnam, P. C. Power From the Wind. New York D. Van Nostrand Company, Inc., 1948.

23. Savino, J. M., "A Brief Summary of the Attempts to Develop Large Wind-Electric Generating Systems in the U.S. Proceedings, Workshop on Advanced Wind Energy Systems, Stockholm, Sweden, August, 1974.
24. "Going With the Wind," EPRI Journal, March, 1980.
25. "Dimensions in Wind," EPRI Journal, May, 1984.
26. Marier, D., "Windfarm Update," ASE No. 72, March/April, 1985.
27. Marier, D., "Windfarm Update," ASE No. 79, March, 1986.
28. Papper, J. C., "Wind Farm Economics Utility Perspective," ASE, No. 79, March, 1986.
29. Kuliasha, M. A. and Reddoch, T. W. Editors. "Research Needs for the Effective Integration of New Technologies into the Electric Utility," Oak Ridge National Laboratory, Report No. CONF-820772, July 1982.
30. Sachdev, M. S. and Billington, R. "A Review of the Technologies for Forecasting Power and Energy Demands," Transactions of the Canadian Electrical Association, Paper No. 76-SP-141, Vol. 15, Part 2, 1976.
31. Stevenson, W. D. Jr., Elements of Power System Analysis, McGraw-Hill Book Company, New York, pp. 193-223, 1982.
32. Anderson, P. M. and Fauad, A. A. Power System Control and Stability, The Iowa State University Press, Ames, Iowa, 1977.
33. Gupta, P. C., "A Stochastic Approach to Peak Power-Demand Forecasting in Electrical Utility Systems," IEEE Transactions on PAS, Vol. PAS-90, No. 2, March-April 1971.
34. Sullivan, R. L., Power System Planning, McGraw-Hill Book Company, New York, 1977.
35. Hagan, M. and Klein, R., "On-Line Maximum Likelihood Estimation for Load Forecasting," IEEE Transactions on SMC, Vol. 8, No. 9, September 1978.
36. Saidian, A., A Study of Electrical Load Forecasting Using Box-Jenkins Technique, M.S. Thesis, Department of Electrical Engineering and Computer Science, The University of Oklahoma, 1980.
37. Comerford, R. B. and Gellings, C. W., "The Application of Classical Forecasting Techniques to Load Management," IEEE Transactions on PAS, Vol. 101, No. 12, December 1982, pp. 4656-4664.

38. Makridakis, S., Wheelwright, S. C. and McGee, V. E., Forecasting Methods and Applications, John Wiley & Sons, Inc., New York, 1978.
39. Makridakis, S. and Wheelwright, S. C., Interactive Forecasting, Holden-Day, Inc., San Francisco, 1978.
40. Sachdev, M. S., and Billington, R., "Representative Bibliography on Load Forecasting," IEEE Trans. on PAS, Vol. PAS-96, No. 2, March/April 1977, pp. 697-700.
41. Christiaanse, W. R., "Short Term Load Forecasting Using General Exponential Smoothing." IEEE Transactions on PAS, Vol. 90, No. 2, March/April 1971, pp. 900-910.
42. Keyhani, A., Daniels, H., "Real Time Load Modeling Technique. An Application to Short Term Load Prediction," presented at the Control of Power Systems 1976 Conference and Exposition, pp. 132-136.
43. Vemuri, S., Liang W., and Nelson D. J., "On Line Algorithms for Forecasting Hourly Loads of an Electric Utility." IEEE Transaction on PAS, Vol. 100, No. 8, August 1981, pp. 3775-3784.
44. Meslier, F., "New Advances in Short Term Load Forecasting Using Box and Jenkins Approach," Paper No. A 78 051-5, IEEE PAS Winter Meeting, New York, N.Y., January 29 - February 3, 1978.
45. Mabert, V., "An Introduction to Short Term Forecasting Using the Box-Jenkins Methodology, Publication #2 in the Monograph Series, Production Planning and Control Division, American Institute of Industrial Engineers, Inc., 1975.
46. Box, G. E. P. and Jenkins, G. M., Time Series Analysis, Forecasting and Control, Holden-Day, Inc., San Francisco, 1970.
47. Thompson, R. P., "Weather Sensitive Electric Demand and Energy Analysis on a Large Geographically Diverse Power System. Application to Short Term Hourly Electric Demand Forecasting," IEEE Transactions on PAS, Vol. 9, No. 1, January/February 1976, pp. 385-393.
48. Kayhani, A. and Miri, S. M., "On-Line Weather and Industrial Group Bus Load Forecasting for Microprocessor-Based Applications," IEEE Transaction on PAS, Vol. 102, No. 12, December 1983, pp. 3868-3876.
49. Willis, H. L., "Load Forecasting for Distribution Planning-Error and Impact on Design," IEEE Transaction on PAS, Vol. 102, No. 3, March 1983, pp. 675-686.
50. Willis, H. L., Schauer, A. E., and Northcote-Green J. E. D., "Forecasting Distribution System Loads Using Curve Shape

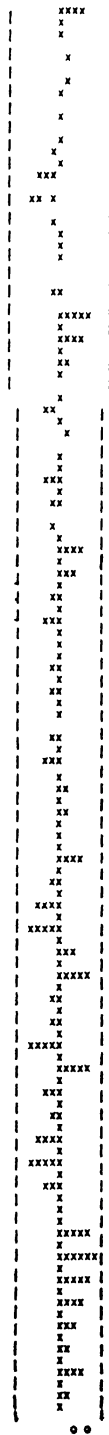
- Clustering," IEEE Transactions on PAS, Vol. 102, No. 4, April 1983, pp. 893-901.
51. Willis, H. L., "A Cluster Based V.A.E. Method for Distribution Load Forecasting," IEEE Transaction on PAS, Vol. 102, No. 8, August 1983, pp. 2677-2684.
 52. Willis, H. L. and Tram, H. N., "Load Forecasting for Transmission Planning," IEEE Transaction on PAS, Vol. 103, No. 3, March 1984, pp. 561-568.
 53. Fink, L. H. and Feero, W. E., "Effective Integration of New Technologies into Electric Energy Systems," IEEE Transaction on PAS, Vol. 101, No. 7, July 1982, pp. 1833-1842.
 54. Bose, A., and Anderson, P. M., "Impact of New Technologies on Generation Scheduling," IEEE Transacation PAS, Vol. 103, No. 1, January 1984, pp. 66-71.
 55. Chalmers, S. M., et al "The Effect of Photovoltaic Power Generation on Utility Operation," IEEE Transaction on PAS, Vol. 104, No. 3, March 1985, pp. 524-530.
 56. Mustacchi, C., et al "Stochastic Simulation of Hourly Global Radiation Sequences," Solar Energy, Vol. 23, pp. 47-51, 1979.
 57. Goh, T. N., and Ran, K. J., "Stochastic Modeling and Forecasting of Solar Radiation Data," Solar Energy, Vol. 19, pp. 755-757, 1977.
 58. Brown, B. G. et al, "Time Series Models on Simulate and Forecast Wind Speed and Wind Power," Journal of Climate and Applied Meteorology, Vol. 23, pp. 1184-1195, August 1984.
 59. Blanchard, M., and Desrochers, G., "Generation of Autocorrelated Wind Speeds for Wind Energy Conversion System Studies," Solar Energy, Vol. 33, No. 6, pp. 571-579, 1984.
 60. Lou, J. J., "Stochastic Analysis of Wind Stream and Turbine Power," Solar Energy, Vol. 35, No. 4, pp. 297-309, 1985.
 61. Solmet, "Hourly Solar Radiation - Surface Meteorological Observations," Vol. 1, User's Manual TD-9724, Reprinted Jan., 1982.
 62. Frior, K., "Rating PV Systems," paper presented at the 18th IEEE Photovoltaic Specialists Conference, Las Vegas, Nevada, October 1985.
 63. Hester, S. and Hoff T., "Long-Term PV Module Performance," paper presented at the 18th IEEE Photovoltaic Specialists Conference, Las Vegas, Nevada, October 1985.

64. Hock, S. and Flaim, T., "Wind Energy Systems for Electric Utilities A Synthesis of Value Studies," Sixth Biennial Energy Conference and Workshop, Minneapolis/St. Paul, Minnesota, June 1-3, 1983.
65. Angrist, S. W., Direct Energy Conversion, Allyn and Bacon, Inc., Boston, 1982.
66. Buresch, M., Photovoltaic Energy Systems, McGraw-Hill Book Company, New York, 1983.
67. Ambrosone, G., et al "Comparison Between Power and Energy Methods of Analyses of Photovoltaic Plants," Solar Energy, Vol. 34, No. 1, pp. 1-8, 1985.
68. Ramakumar, R. and Jewell, W., "Public Service Company of Oklahoma Guide to Utility Interactive Photovoltaic Systems," PSO Contract Agreement No. 9216, October 1984.
69. Singer, S., Rozenshtein, B. and Surazi, S., "Characterization of PV Array Output Using a Small Number of Measured Parameters," Solar Energy, Vol. 32, No. 5, pp. 603-607, 1984.
70. Jean, M. and Servant, M. "Calculation of the Cell Temperature for Photovoltaic Modules from Climate Data," paper presented at the Biennial International Solar Energy Congress INTERSOL 85, Montreal, Canada, June 1985.
71. Sharaf-Eldeen, Y. I., and Moretti, P. M., "Simulation of Electric Utility Systems with Wind Turbine Generators," paper for presentation at ASME International Computer in Engineering Conference and Exhibition, Chicago, Illinois, 1986.
72. Bowerman, B. L. and O'Connell, T. C., Forecasting and Time Series, Wadsworth, Inc., Belmont, California, 1979.
73. Nelson, Charles, R., Applied Time Series, for Managerial Forecasting, Holden-Day, Inc., San Francisco, 1973, pp. 30-32.
74. Mendenhall, W., Introduction to Probability and Statistics, Wadsworth, Inc., Belmont, California, 1979.
75. Pack, D. J., Documentation for a Computer Programs for the Analysis of Time Series Models Using the Box-Jenkins Philosophy, University of Wisconsin, Madison, Wisconsin, 1977.
76. SAS/Graph User's Guide Version 5 Edition, SAS Institute Inc., Cary, NC, USA, 1985.

APPENDIX A
PLOTS OF AUTOCORRELATION FUNCTIONS AND
IMPULSE RESPONSE WEIGHTS

VALUES

2377E 01
 58734E -01
 18280E -01
 40419E 01
 96408E 01
 72829E 01
 10544E +00
 7000E -01
 20 87E -02
 0 4140E 0
 0 8094E 01
 0 54087E 01
 0 1824E 01
 0 42817E 01
 0 42817E 01
 85905E 01
 0 7039 E 01
 0 2265E 01
 0 1022E 01
 8 47E 01
 326 8E 01
 0 8602E 01
 0 6308 E 01
 0 1644E 01
 54521E 01
 0 45929E 02
 2271 E 01
 29831E 01
 0 2223E 01
 0 141 0E 01
 7966E 02
 0 2866E 01
 0 4282 0
 0 98 53E 02
 0 4414E 0
 0 571E 01
 379 4E 01
 6880E 01
 0 152 2E 0
 0 32 7E 01
 0 4542E 01
 0 25679E 01
 2598 E 0
 0 5 569E 01
 0 1788E 01
 392E 0
 5264E 0
 7361E 0
 0 2 437E 0
 3928 E 0
 187 E 0
 0 4736E 01
 0 87 74E 01
 0 5262E 0
 0 2701E 0
 0 619E 0
 0 2866E 0
 2056 E 0
 66220E 0
 3 552E 02
 549 8E 01

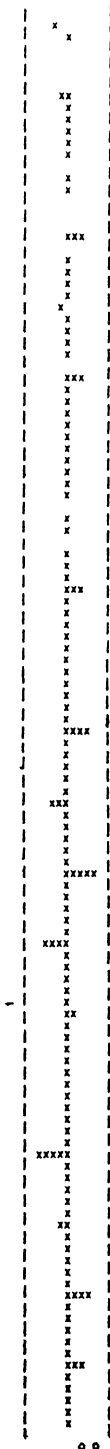


THE ESTIMATED RESIDUALS MODEL 1
 GRAPH OF OBSERVED SERIES AC
 GRAPH INTERVAL IS 0.200E-01
 1000E+01

1
2
3
4
5
6
7
8
9
10
11
12
13
14
15
16
17
18
19
20
21
22
23
24
25
26
27
28
29
30
31
32
33
34
35
36
37
38
39
40
41
42
43
44
45
46
47
48
49
50
51
52
53
54
55
56
57
58
59
60

Figure A3 Graph of Estimated Residuals' Autocorrelation Functions for Model of Equation 4.2

VALUES
 150791 02
 100306 02
 37324E 01
 10118E-02
 12089E-03
 54540E 01
 12186E 02
 16558E 02
 0 28025E 01
 16654E 02
 15697E 02
 0 86480E 01
 15784E 02
 18060E 02
 0 90858E 02
 18 56E 02
 21285E 02
 1698E 01
 21382E 02
 2 414E 02
 0 67696E 01
 24511E 02
 18383E 02
 705 7E 01
 18 80E 02
 2177E 02
 0 38865E 01
 21874E 02
 23489E 02
 6667E 01
 23586E 02
 25786E 02
 0 55632E 01
 2584E 02
 24826E 02
 46394E 01
 25023E 02
 2527E 02
 1729E 02
 25264E 02
 21890E 02
 0 31683E 02
 21987E 02
 21130E 02
 4146E 01
 21217E 02
 19748E 02
 0 37 2E 01
 98 E 02
 20591E 02
 32970E 01
 20688E 02
 20805E 02
 3 52E 0
 20902E 02
 92 8E 02
 0 27953E 01
 19315E 02
 1781E 02
 0 2 270E 0



1

MODEL
 GRAPH OF OBSERVED SERIES ACT
 GRAPH INTERVAL IS 0 2000E-01
 1000E+01

1
 2
 3
 4
 5
 6
 7
 8
 9
 10
 11
 12
 13
 14
 15
 16
 17
 18
 19
 20
 21
 22
 23
 24
 25
 26
 27
 28
 29
 30
 31
 32
 33
 34
 35
 36
 37
 38
 39
 40
 41
 42
 43
 44
 45
 46
 47
 48
 49
 50
 51
 52
 53
 54
 55
 56
 57
 58
 59
 60

Figure A4 Graph of Estimated Residuals' Autocorrelation Functions for Model of Equation 4.3

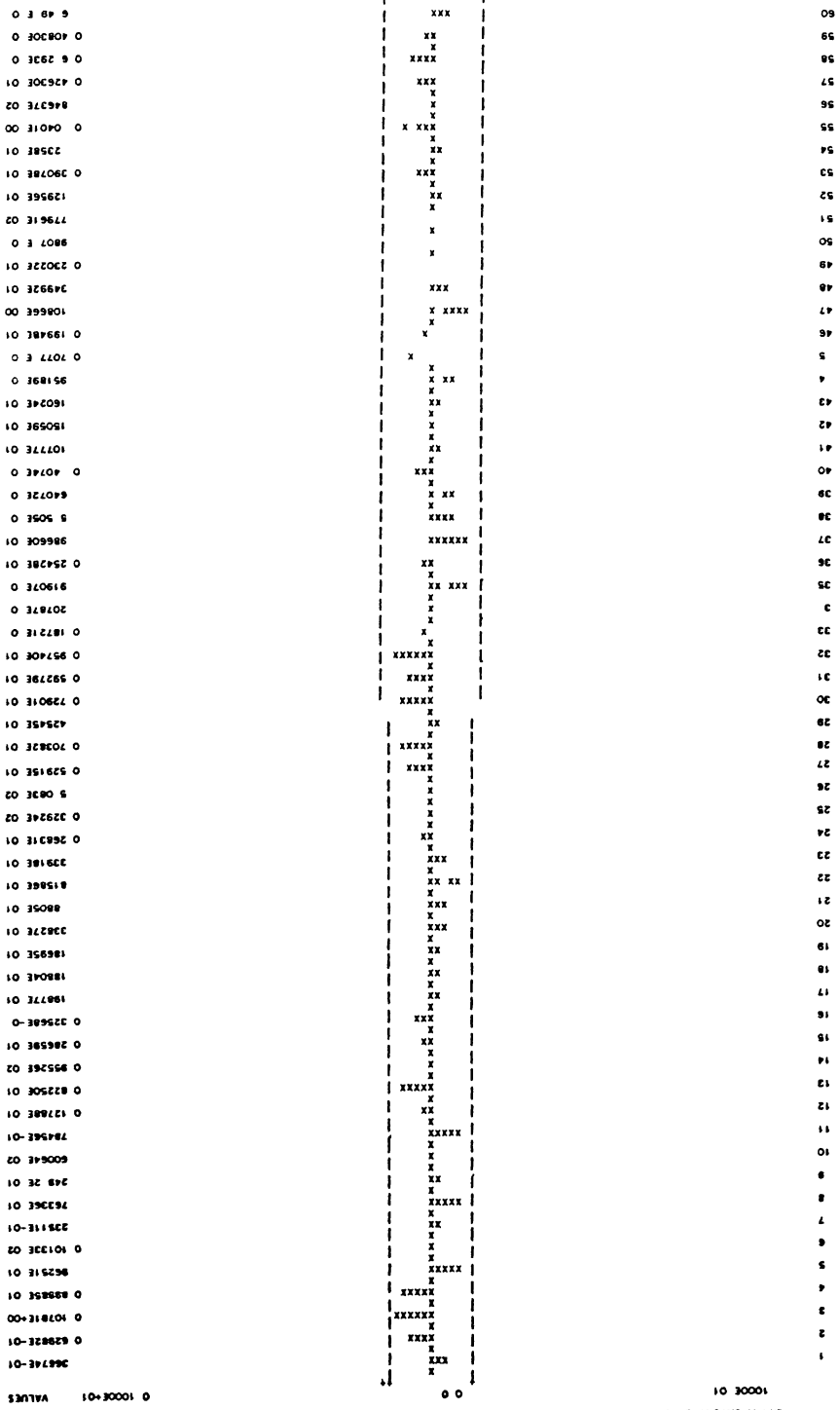


Figure A6 Graph of Estimated Residuals' Autocorrelation Functions for Model of Equation 4.5

THE ESTIMATED RESIDUALS MODEL 1
 GRAPH OF OBSERVED SERIES AC5
 GRAPH INTERVAL IS 0.2000E+01
 1000E+01

3 1083E 01
 35460E 01
 27669E 01
 45041E 0
 10 26E 00
 86593E 01
 0 2526E 01
 12 3E 00
 62728E 02
 78236E-01
 0 57771E 01
 0 31764E 01
 482 0E 01
 0 70 E 02
 0 3 808E 0
 0 293 8E 01
 0 52789E 0
 0 32378E 01
 48973E 01
 62054E 0
 0 50297E 01
 0 78 6E 0
 53001E 01
 52888E 0
 14395E 01
 03 6E 00
 32874E 0
 0 0453E 01
 3594E 02
 36 0E 01
 0 00 3E 00
 0 32 7E 02
 2 8E 01
 97E 0
 0 85 0E 02
 89 E 0
 47 5 E 02
 0 3 6 E 00
 0 0269E 00
 6 67 01
 0 68 0E 0
 0 897 E 0
 0 70 E 0
 8 8 E 01
 8 77E 0
 895 E 0
 25 E 0
 0 7 E 0
 0 3 072E 0
 4 8E 0
 0 26 2E 0
 0 2 0E 0
 0 2 07E 0
 0 1 E 01
 2 E 0
 12 87E 0

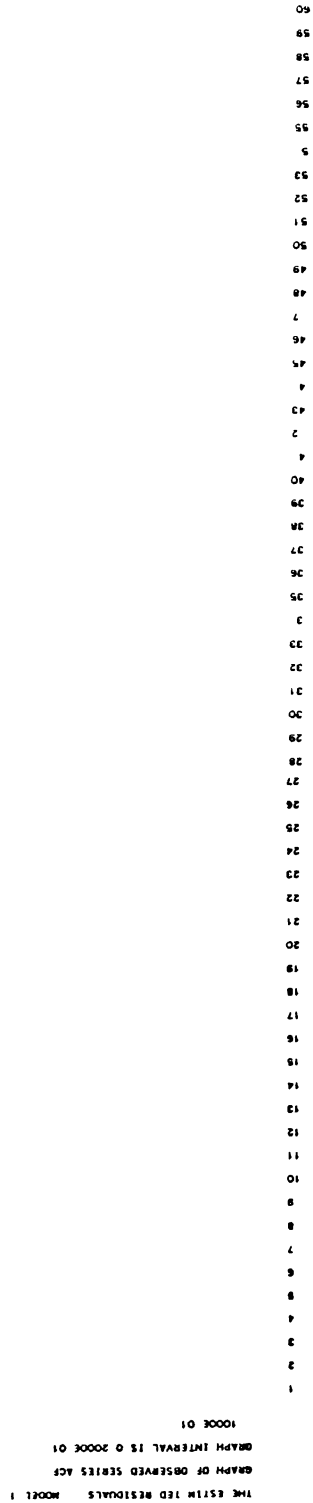
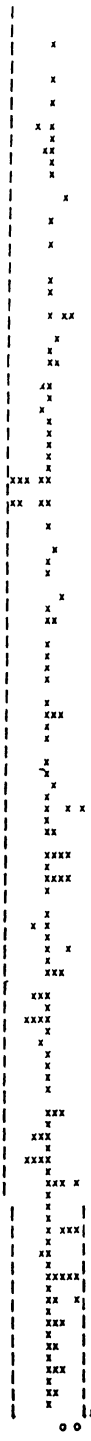
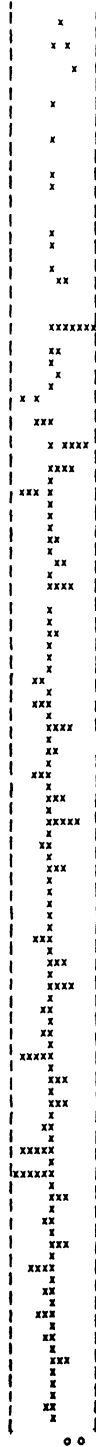


Figure A7 Graph of Estimated Residuals' Autocorrelation Functions for Model of Equation 4.6

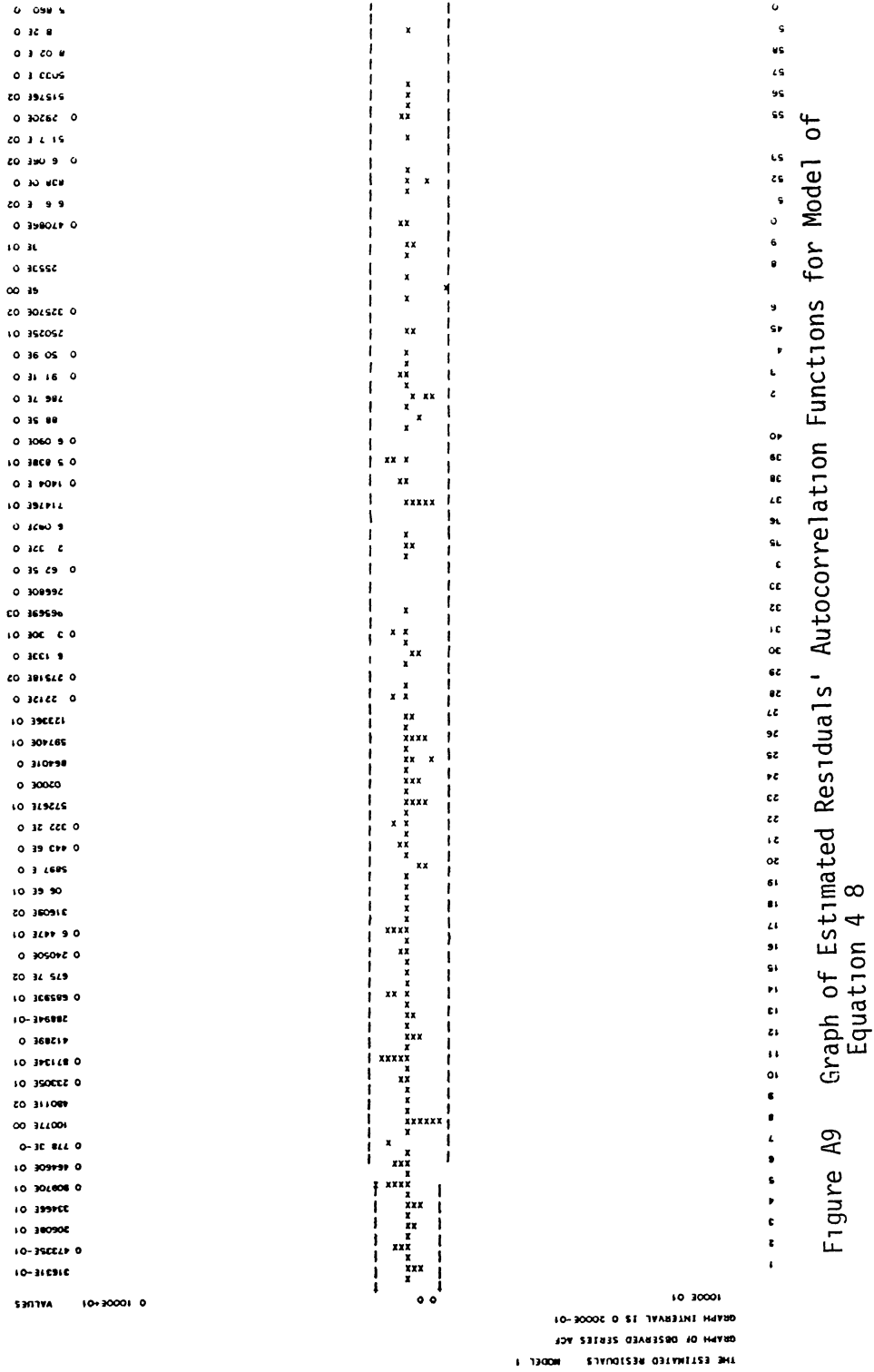
VALUES
 0 1000E+01
 0 20758E 01
 59800E 02
 44248E-0
 0 32035E 01
 0 42732E-01
 0 26252E-01
 0 56098E 01
 47161E-01
 0 1688E-01
 32122E 01
 0 10058E 00
 0 79570E 01
 0 14207E-01
 40029E 01
 3 867E 01
 0 85682E 0
 0 2295E 01
 0 16834E 0
 54824E 01
 41297E 01
 0 384 0E 01
 0 8322E 02
 44794E 02
 47020E 01
 0 11 04E 01
 88089E 01
 32659E 01
 0 50284E 0
 15075E 0
 58967E 01
 0 40623E 01
 0 3 820E 01
 0 2829 E 02
 32088E 0
 8 99 E 02
 53061E 01
 48182E 0
 2476E 01
 0 6901E 0
 0 78297E 0
 51255E 01
 92702E 0
 0 6795E 0
 0 7593 E 0
 369 0E 0
 0 7360E 0
 0 57317E 0
 0 85485E 02
 0 16554E 01
 883 2E 02
 0 37 90E 02
 0 9054E 0
 22529E 01
 98009E 0
 312 9E 0
 9 99E 0



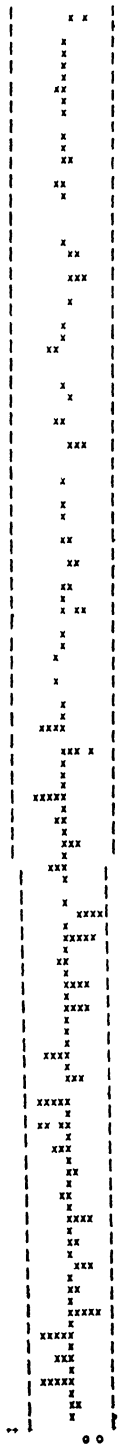
HE LS IMA ED 231DU 5 MOD L
 ON PM OF DBSE VED SERIES ACF
 GRAPH INTERVAL IS 0 2000E 01
 1000E+01

1
 2
 3
 4
 5
 6
 7
 8
 9
 10
 11
 12
 13
 14
 15
 16
 17
 18
 19
 20
 21
 22
 23
 24
 25
 26
 27
 28
 29
 30
 31
 32
 33
 34
 35
 36
 37
 38
 39
 40
 41
 42
 43
 44
 45
 46
 47
 48
 49
 50
 51
 52
 53
 54
 55
 56
 57
 58
 59
 60

Figure A8 Graph of Estimated Residuals' Autocorrelation Functions for Model of Equation 4.7



VALUES
 0 1000E+01
 21851E-01
 0 7048E-01
 0 4072E-01
 0 8528E-01
 78981E 0
 4519E 01
 539 2E 01
 2678E 01
 54734E-01
 0 22521E 01
 16595E 01
 0 2969E 0
 0 3965E 01
 0 85743E 01
 22609E 01
 0 63074E 01
 0 69935E 02
 55435E 01
 563 2E 01
 0 10256E 01
 83385E 01
 0487E 00
 12708E 01
 0 41777E 01
 309E E-01
 0 20387E 01
 0 86449E 01
 0 304 3E 0
 8 43E 0
 0 71286E 01
 0 94 6E 02
 0 20699E 0
 0 3 97E 01
 0 07 E 0
 82 8 E 01
 2905 E 01
 00E 01
 97 E 0
 10 00E 00
 0 20 1 E 0
 0 3 E 0
 45 E 0
 0 15833E 01
 4 94E 0
 0 0094E 0
 0 465 2E 01
 5 E 0
 35073E 0
 56 9 E 0
 584 E 0
 0 20 0E 0
 47 5E 0
 0 30267E 0
 2692 E 0
 0 3 0E 0
 0 120E 0
 0 360E 01
 0 4 9E 0
 0 4857E 0
 0 260E 01
 0 4 9E 0

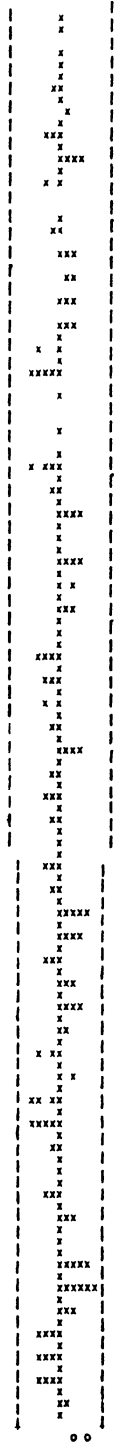


THE ESTIMATED RESIDUALS MODEL 1
 GRAPH OF OBSERVED SERIES ACT
 GRAPH INTERVAL IS 0 2000E 01
 1000E+01

1
 2
 3
 4
 5
 6
 7
 8
 9
 10
 11
 12
 13
 14
 15
 16
 17
 18
 19
 20
 21
 22
 23
 24
 25
 26
 27
 28
 29
 30
 31
 32
 33
 34
 35
 36
 37
 38
 39
 40
 41
 42
 43
 44
 45
 46
 47
 48
 49
 50

Figure A10 Graph of Estimated Residuals' Autocorrelation Functions for Model of Equation 4 9

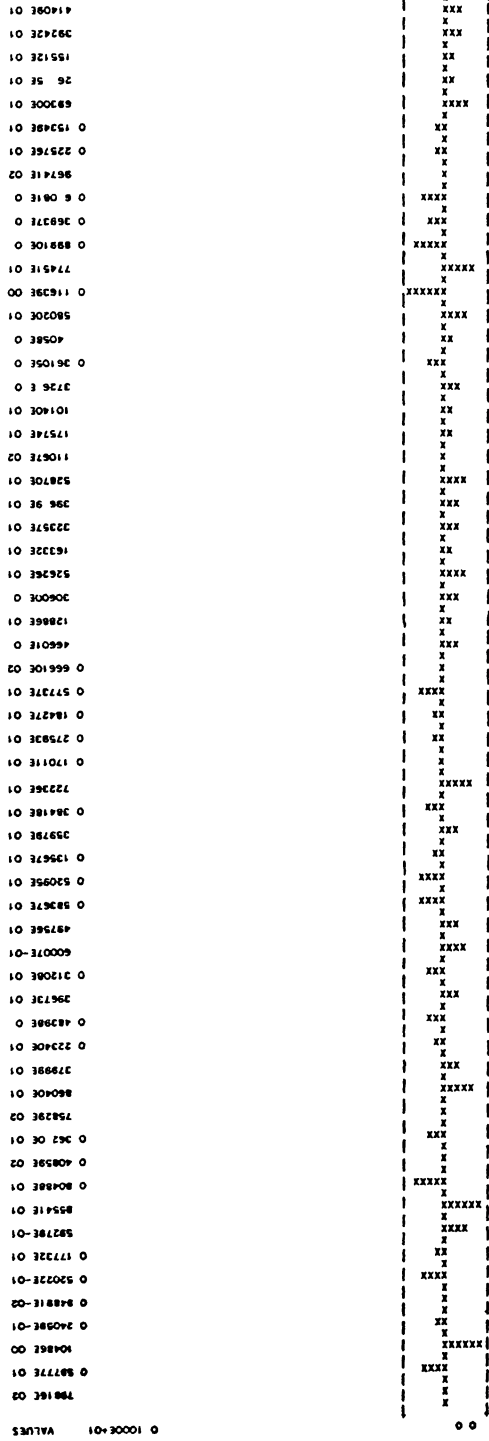
0 0000 01 VALUES
 21056E 01
 0 6488 E 01
 0 83318E-01
 0 66999E 01
 47695E 01
 92438E-01
 72223E 01
 0 949 7E 03
 47259E 0
 0 42876E 01
 11816E 02
 0 18203E 01
 0 84235E 01
 0 7 69E 0
 4 1E 01
 0 55 59E 0
 26796E 01
 69378E 01
 6787E 0
 0 3 001E 01
 58115E 0
 83440E 0
 0 14188E 01
 0 36 3E 01
 88 94E 02
 0 34504E 0
 0 2328E 01
 0 11752E 01
 0 19E 00
 0 2478E 0
 0 72E 0
 0 4 M AF 01
 0 664 E 01
 59266E 02
 37853E 01
 3 E 0
 67 53E 0
 0 5764E 02
 6817E 01
 0 82E 01
 0 4200 E 0
 270E 0
 AF 0
 0 9283 E 0
 0 5265E 0
 65 29E 0
 3508 E 0
 66412 01
 489 9E 0
 0 47403E 0
 0 2 50 E 01
 0 53 5 E 0
 19 E 0
 0 3569E 0
 45286E 0
 AF 0
 3007E 02
 0 35 43E 02
 4 72E 0



THE ESTIMATED RESIDUALS MODEL 1
 GRAPH OF OBSERVED SERIES PACT
 GRAPH INTERVAL IS 0 2000E 01
 1000E 01

1
 2
 3
 4
 5
 6
 7
 8
 9
 10
 11
 12
 13
 14
 15
 16
 17
 18
 19
 20
 21
 22
 23
 24
 25
 26
 27
 28
 29
 30
 31
 32
 33
 34
 35
 36
 37
 38
 39
 40
 41
 42
 43
 44
 45
 46
 47
 48
 49
 50
 51
 52
 53
 54
 55
 56
 57
 58
 59
 60

Figure A11 Graph of Estimated Residuals' Autocorrelation Functions for Model of Equation 4 10

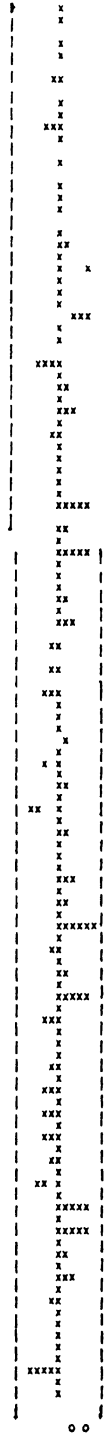


HE ESTIMATED ESTOU LS MOO
GRAPH OF OBSERVED SERIES ACF
GRAPH INTERVAL IS 0 2000E 01
1000E+01

60
59
58
57
56
55
54
53
52
51
50
49
48
47
46
45
44
43
42
41
40
39
38
37
36
35
34
33
32
31
30
29
28
27
26
25
24
23
22
21
20
19
18
17
16
15
14
13
12
11
10
9
8
7
6
5
4
3
2
1

Figure A12 Graph of Estimated Residuals' Autocorrelation Functions for Model of Equation 4.11

88074E-02
 0 80429E-01
 0 15069E-02
 0 25298E 0
 0 12269E 01
 20670E 01
 20783E 01
 76638E 01
 7 098E 01
 0 58802E 01
 0 17198E 01
 0 1083E 01
 0 38244E 01
 0 3 275E 0
 0 283 2E 0
 0 708 8E-02
 0 3238E 01
 81777E 01
 18646E 01
 0 5820E 01
 757E 00
 16298E 01
 3 885E 01
 0 97265E 02
 2778E 01
 0 74012E 01
 28454E 0
 0 3197E 0
 2533 E 0
 0 587 3E 02
 0 5 092E 0
 0 3392E 01
 0 25628E 01
 25538E 01
 15067E 0
 25528E 0
 8 2 E 0
 62 0E 0
 7722E 0
 0 0930E 02
 0 0890E 0
 0 2 67 E 0
 2 562E 0
 10 9E 01
 0 55065E 0
 0 182 0E 0
 75955E 0
 04 3E 0
 88890E 0
 2045 F 0
 0 2258E 0
 0 95052E 02
 26080F 0
 6034E 02
 0 6 45E 0
 0 27022E 02
 0 11227E 0
 0 150 1E 0
 29628E 0
 7 72F 0



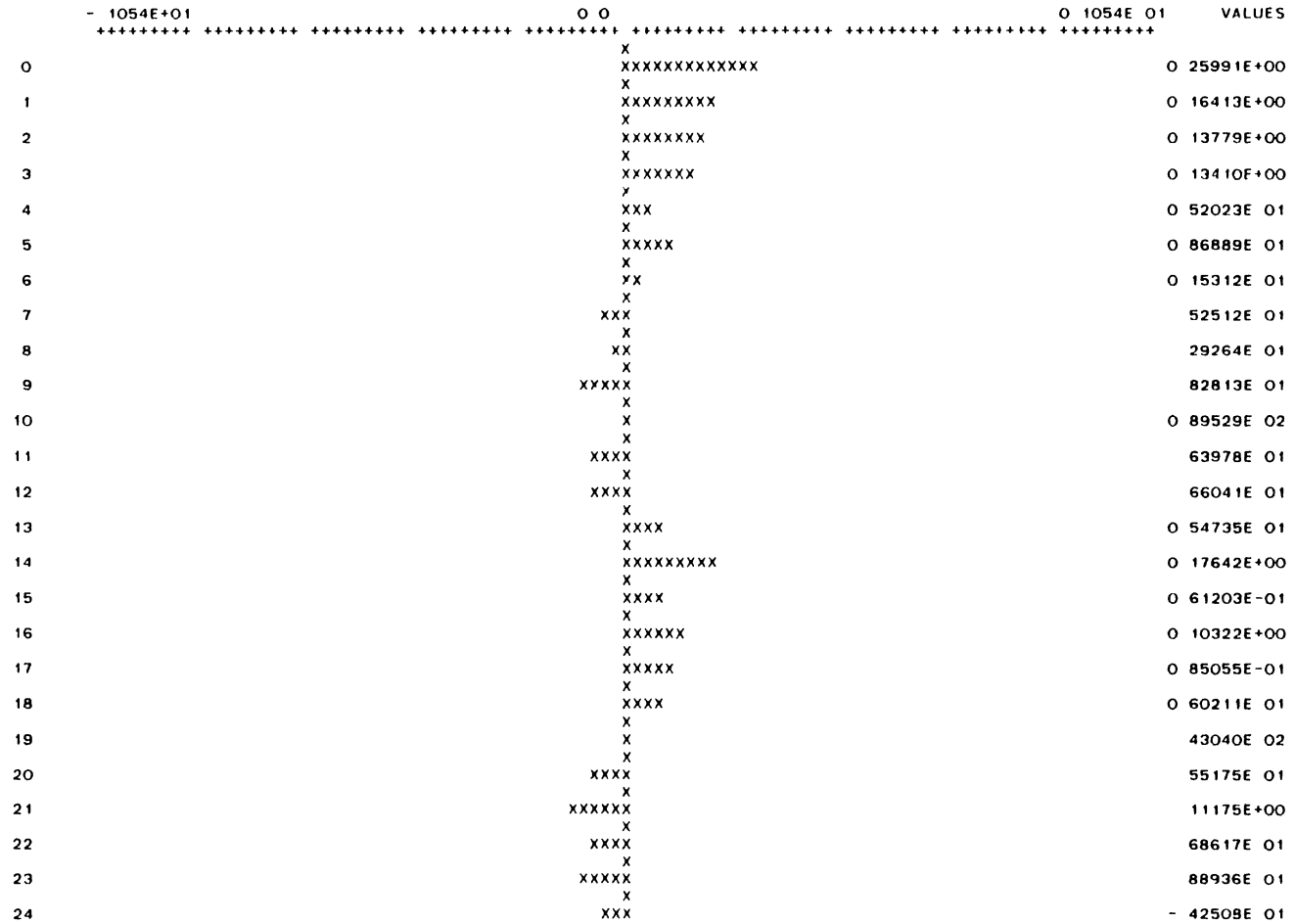
THE ESTIMATED RESIDUALS MODEL
 GRAPH OF OBSERVED SERIES ACT
 GRAPH INTERVAL IS 0.2000E 01
 1000E 01

1
 2
 3
 4
 5
 6
 7
 8
 9
 10
 11
 12
 13
 14
 15
 16
 17
 18
 19
 20
 21
 22
 23
 24
 25
 26
 27
 28
 29
 30
 31
 32
 33
 34
 35
 36
 37
 38
 39
 40
 41
 42
 43
 44
 45
 46
 47
 48
 49
 50
 51
 52
 53
 54
 55
 56
 57
 58
 59
 60

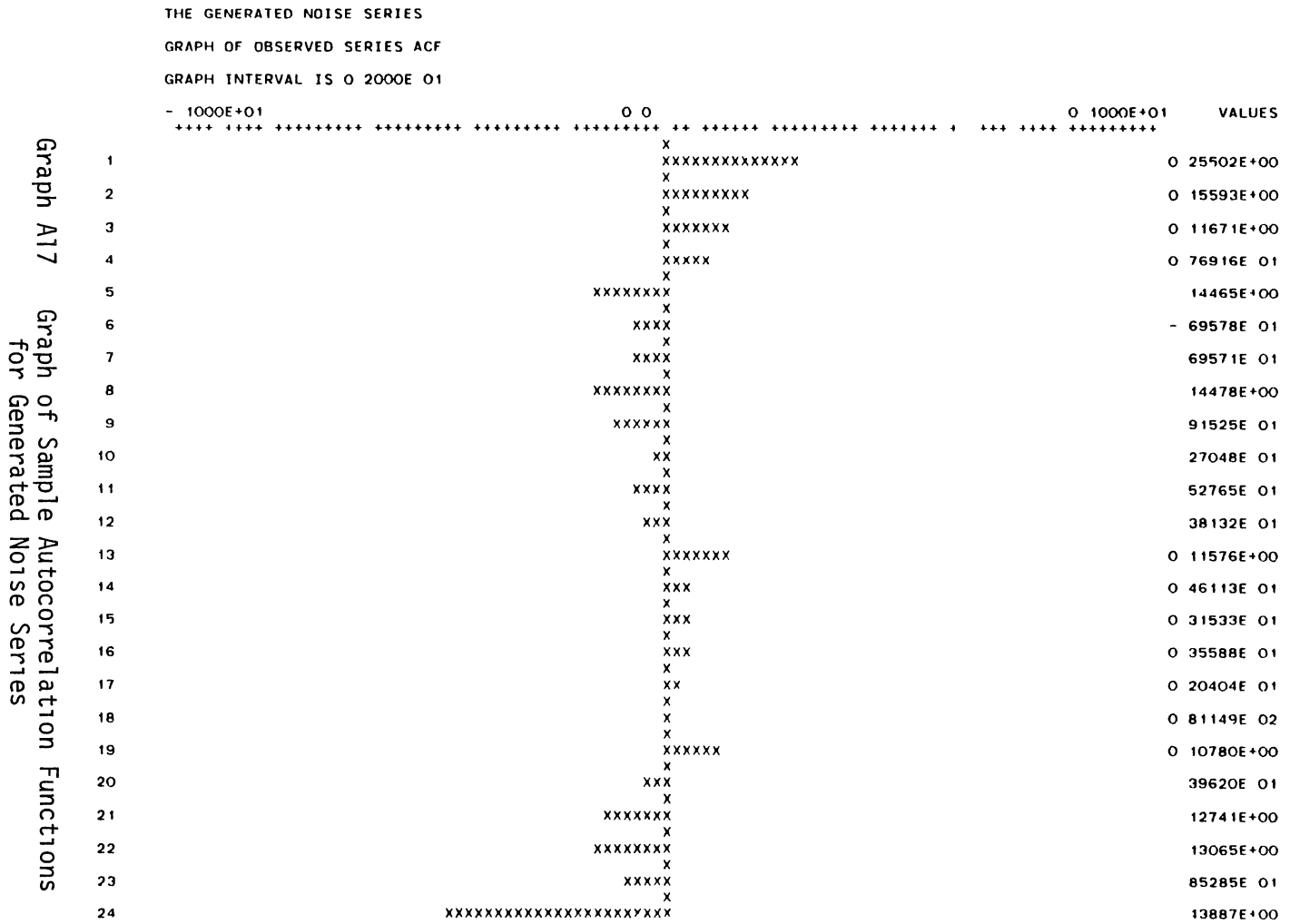
Figure A14 Graph of Estimated Residuals' Autocorrelation Functions for Model of Equation 4.13

GRAPH OF IMPULSE RESPONSE WEIGHTS

GRAPH INTERVAL IS 0 2108E 01



Graph A16 Impulse Response Weights, v_j



Graph A17 Graph of Sample Autocorrelation Functions
 for Generated Noise Series

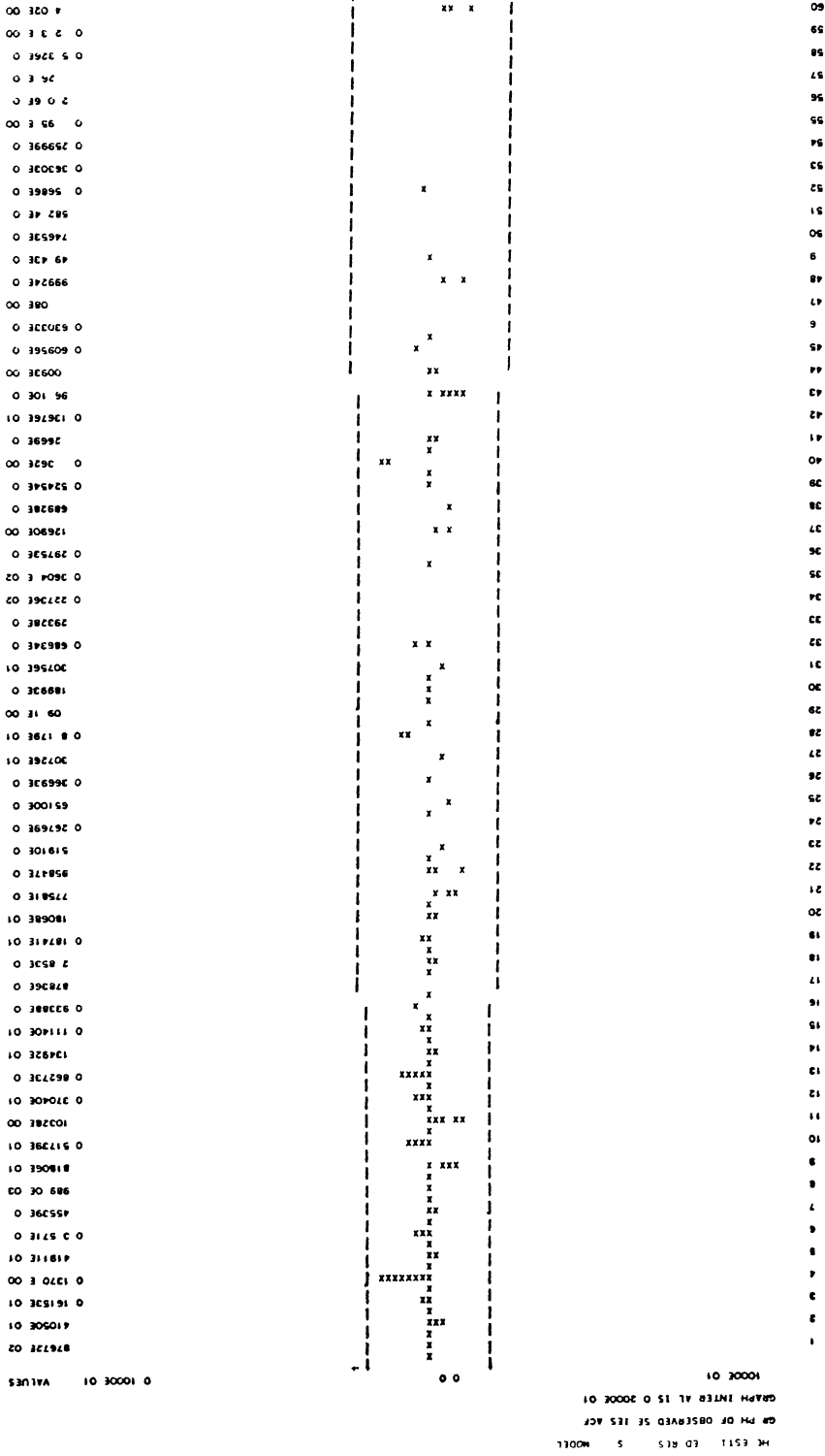


Figure A18 Graph of Sample Estimated Residuals' Autocorrelation Functions for Noise Model in Bivariate Process for Model of Equation 4 22

VITA

ALIRAHM SAIDIAN

Candidate for the Degree of

Doctor of Philosophy

Thesis NET ELECTRICAL LOAD FORECASTING IN THE PRESENCE OF NEW
GENERATION TECHNOLOGIES

Major Field Electrical Engineering

Biographical

Personal Data Born in Sadat Ramhormoz, Khozestan, Iran, on
December 23, 1946, the son of Mr. and Mrs Saidian

Education Graduated from primary school in Agajari, and secondary
school in Abadan, Iran, received the Bachelor of Science
degree in Physics Jundi Shapour University, Ahwaz, Iran, in
1971, received the Master of Science degree from Oklahoma
University, Norman, Oklahoma, August, 1980, with a Major in
Electrical Engineering, completed requirements for the Doctor
of Philosophy degree at Oklahoma State University with a Major
in Electrical Engineering, December, 1986.

Professional Experience Instructor in Physics Department, Jundi
Shapour University, Ahwaz, Iran, September 1971 to August 10,
1977, graduate teaching assistant, School of Electrical
Engineering, Oklahoma University, 1979-1983, and Oklahoma
State University, 1984-1986

Professional Organizations Member of the Institute of Electrical
and Electronics Engineers